

Auxin Transport During Early Pea (*Pisum sativum* L.) Fruit Development

by

Dilini Deshanee Adihetty

A thesis submitted in partial fulfillment of the requirements for the degree of

Master of Science

in

Plant Science

Department of Agricultural, Food and Nutritional Science
University of Alberta

© Dilini Deshanee Adihetty, 2018

Abstract

In pea (*Pisum sativum*), normal pericarp growth requires the presence of seeds and removal or abortion of seeds lead to reduced pericarp growth and subsequent abscission. Previous studies in pea showed that auxin levels are higher in seeds than the surrounding ovary (pericarp) tissues, suggesting that seeds are important to maintain the auxin pools and gradients in surrounding tissues to promote pericarp growth and development. However, further evidence for auxin transport from the seeds to the fruit and into the fruit attachment tissues (pedicel and peduncle) is required to confirm this hypothesis. To address this, we have investigated the spatial patterning of auxin activity in pericarps and associated fruit tissues using an auxin-inducible DR5:: β -Glucuronidase (GUS) reporter system in pea. We observed higher GUS staining and GUS enzyme activity in 4 days after anthesis (DAA) fruit and attached pedicel and peduncle tissues from seed-bearing fruits than those from deseeded fruits. The polar auxin transport inhibitor, *N*-1-naphthylphthalamic acid (NPA) applied to the peduncle attached to fruit with developing seeds increased GUS staining and GUS enzyme activity in the peduncle, pedicel and ovary (pericarp) tissues above the NPA application point. NPA application to the pericarp increased GUS staining and GUS enzyme activity within the pericarp and the seed/funiculus tissues of seeded fruits. NPA application to the peduncle, pericarp or simultaneously to the peduncle and pericarp did not induce deseeded pericarp growth. Pericarp growth was also not affected in pollinated fruits when NPA was applied at -2 DAA to either the peduncle or pedicel tissues. NPA application (at -2 DAA) to the peduncle or pedicel tissues attached to emasculated flowers, resulted in a minor increase in pericarp growth of the non-pollinated fruits, and pericarp tissue integrity was maintained up to 7 days after NPA treatment; however, the non-pollinated fruits abscised within

two weeks of NPA application. Overall, these data support that seeds act as a source of auxins for developing pea ovaries and fruit attachment tissues, and that auxin transport from the seeds to the fruit and attachment tissues is at least partially mediated through the polar auxin transport pathway.

Preface

All the experiments presented in this thesis were designed by Dr. Jocelyn A. Ozga (Plant BioSystem Group, Department of Agricultural, Food and Nutritional Science, University of Alberta). Dr. Dennis M. Reinecke created the DR5::GUS plants and prepared NPA and Tween 80 solutions, NPA plus lanolin mixtures, CFDA solutions, and hormonal solutions used for the thesis experiments. Dr. Rong-cai Yang completed the one-way and two way ANOVA analysis for the GUS enzyme activity data of intact and split pericarps, and growth data in the thesis. I performed all experiments, data collection, and performed the all other analysis for this thesis.

Dedication

To

my Guiding Star, Amara Rohini (mother)

and

my giant supportive pillars:

Samuel Adihetty (father),

Hasitha Adihetty (brother), and

Manoj Dilhara (husband)

Acknowledgment

This is a combined effort of many great people who have continuously supported and encouraged me throughout my graduate studies. First and foremost, my sincere gratitude and appreciation go to my supervisor, Dr. Jocelyn Ozga for her invaluable advice, guidance, and patience which lead me to completion of this research project. Above all and the most needed, she always provided me unflinching encouragement and support, whether it is a matter of science or life. I am also sincerely thankful to my supervisory committee member, Dr. Janice Cooke for her time, directions, and valuable inputs to my projects as well as for her continuous encouragement. My sincere gratefulness also goes to Dr. Dennis Reinecke for providing all solutions that I have used for plant applications and his expertise to troubleshoot my experiments. I should also thank Dr. Rong-cai Yang for his generous support for the statistical analysis.

I would also like to acknowledge the support given by all past and present members of the Ozga/Reinecke lab: Dinuka Waduthanthri, Dr. Charitha Jayasinghege, Dakshina Pahala Vithanage, Dhanuja Abeysingha, Dr. Harleen Kaur, and Lingchao Gao. A big thank goes to Dinuka for helping me to be familiarized with the university. As a newcomer it helped me a lot to stand on my own feet. My special gratitude goes to Dr. Charitha Jayasinghege for sharing his research experience with me and dedicating his valuable time to show me the path in the desert of experiments. Thank you Dakshina for making your time whenever I need an extra pair of hands, especially in the MUG assays. Dr. Harleen Kaur, thank you for sharing your expertise with me during this journey. Dhanuja and Lingchao, thank you for all your help and friendly smiles which made this journey easy. Thank you all my lab mates for your friendship, love and being cheerful companions.

All members in the Department of Agricultural, Food and Nutritional Science (AFNS) especially, Jody Forslund, Nikki-Karyssa Scott, and Dr. Urmila Basu thank you for your friendly support throughout my graduate life at AFNS.

There were many people outside the university who made my life in Edmonton happy and joyful. Ruwani & Gayan and Dakshina & Charitha, thank you for taking care of me and helping me to adapt the new life. I cannot forget the other crazy-nuts who always there for me with their supportive hands: Dhanuja & Nimesh, Kethmi & Dinuka, Gayesha & Lasantha,

Thushani & Wijaya, Anusha & Chandila, Chamila & Nandika, Nilusha & Chamila, Lalani & Chandana, Sureka & Viraj, Kanchan & Sumal, Shakila & Ravindra, Madhavi & Isuru, Kusuntha & Chathura, Ramya & Chaminda, Sachitha, Brasathe and Ranithri your supportiveness will always be remembered

I also gifted with a bunch of amazing and cheerful relations who knit together with love and affection. I truly appreciate your help, dedication, and love in all possible ways. With a heavy heart, I am grateful to my late mother for being my Guiding Star and for her unconditional love. Thank you, “Nanda” (Aunty) for taking care of us and your love and tremendous support after our great loss. Thank you “Ayya” (Brother) for your trust, love, and being the best brother in the universe. I am also thankful to Disna (Sister-in-law) and all other in-laws for their understanding. My father, my hero, you were the greatest strength behind me and words cannot express my gratitude towards your unreserved love and all your scarification. Finally, my heartfelt gratitude goes to my loving husband Dilhara for his true love, understanding, countless scarification, and patience. Your constant encouragement and trust have led me to where I am today and has shown me what happens when I never-give-up my goals and dreams.

Table of Contents

1. INTRODUCTION	1
1.1 Plant hormones.....	1
1.2 The class of hormones called auxins	1
1.3 Auxin regulation of plant reproductive development	4
1.4 Dynamics of auxin during early pea fruit development.....	6
1.5 Auxin transport in plants.....	9
1.5.1 <i>Auxin influx carriers</i>	11
1.5.2 <i>Auxin efflux carriers</i>	12
1.6 Auxin-sensitive promoter-gene reporter systems used to understand the auxin tissue dynamics in fruits.....	16
1.6.1 <i>DR5 promoter-reporter systems</i>	16
1.6.2 <i>AUX/IAA-based auxin sensors</i>	17
1.7 Auxin transport during fruit development	18
1.8 Thesis objectives.....	20
Objective 1	20
Objective 2.....	20
2. MATERIALS AND METHODS	22
2.1 Plant Materials and growth conditions	22
2.1.1 <i>Plant lines</i>	22
2.1.2 <i>Growth conditions</i>	22
2.2 Plant treatments.....	22
2.2.1 <i>Intact and split pericarp treatments</i>	22
2.2.2 <i>NPA treatments</i>	23
2.2.3 <i>5(6)-Carboxyfluorescein diacetate (CFDA) treatments</i>	25
2.3 Histochemical analysis of GUS activity	26
2.3.1 <i>Tissue dissection for GUS staining</i>	26
2.3.2 <i>GUS histological staining</i>	27
2.4 Fluorometric quantification of GUS enzyme activity.....	28
2.4.1 <i>Tissue dissection for GUS enzyme activity assays</i>	28

2.4.2	<i>Quantification of GUS enzyme activity</i>	29
2.5	Histochemical analysis of 5 (6)- carboxyfluorescein diacetate movement to identify phloem transport dynamics between the pedicel and the pericarp	31
2.6	Statistical analyses	31
3.	RESULTS	33
3.1	Pea inflorescence morphology and pedicel and peduncle anatomy.....	33
3.2	Morphology of the vasculature in the pea ovary	35
3.3	Vascular transport pathway from the pedicel to the fruit tissues as visualized using 5 (6)-carboxyfluorescein diacetate (CFDA) staining.....	36
3.4	DR5::GUS staining patterns in intact pea fruit and associated attachment tissues.....	38
3.5	DR5::GUS staining patterns in pedicels attach to pollinated or nonpollinated ovaries.....	39
3.6	GUS staining and enzyme activity in pea fruit and associate attachment tissues in response to pericarp splitting and seed removal	40
3.7	Effect of the polar auxin transport inhibitor NPA on GUS staining and enzyme activity in pea fruit and associate attachment tissues.....	44
3.7.1	<i>Effect of NPA application to the peduncle</i>	44
3.7.2	<i>Effect of NPA application to the pericarp</i>	49
3.7.3	<i>Effect of NPA application simultaneously to the peduncle and pericarp</i>	49
3.7.4	<i>Effect of NPA application on GUS enzyme activities in deseeded pericarps</i>	52
3.8	Effect of seeds and NPA application on pericarp growth.....	53
3.8.1	<i>Effect of seed on pericarp growth</i>	53
3.8.2	<i>Effect of NPA application on pericarp growth</i>	54
3.9	Effect of NPA on pea fruit set and pericarp growth	56
4.	DISCUSSION	59
4.1	Ovary and pedicel vasculature in <i>Pisum sativum</i>	59
4.2	Auxin and auxin activity in pea seeds.....	60
4.3	Auxin transport patterns in fruit and attachment tissues when seeds are present.....	61
4.3.1	<i>Funiculus</i>	61
4.3.2	<i>Pericarp</i>	61
4.3.3	<i>Pedicel and peduncle</i>	62
4.4	Auxin activity patterns in fruit and attachment tissues in the absence of seeds	64
4.5	Auxin activity patterns in fruit and attachment tissues after NPA treatments	65

4.5.1 <i>NPA application to the peduncle</i>	65
4.5.2 <i>NPA application to the pericarp</i>	66
4.5.3 <i>NPA application simultaneously to the peduncle and pericarp</i>	67
4.5.4 <i>NPA application to the deseeded fruits</i>	67
4.6 Effect of pericarp splitting, deseeding, and NPA applications on pericarp growth.....	68
4.6.1 <i>Pericarp splitting, and splitting and deseeding</i>	68
4.6.2 <i>NPA applications</i>	68
4.7 Effect of NPA applications on pollinated and non-pollinated ovary growth.....	69
5. CONCLUSION	71
5.1 Seeds serve as a source of auxins for the fruit and attachment tissues	71
5.2 Tissue-specific distribution of seed-derived auxins depends on the polar auxin transport	71
5.3 Future perspectives	73
Reference	75
Appendix A	
Supporting micrographs.....	88
Appendix B	
GUS micrographs from individual experiments.....	95
Appendix C	
Effect of NPA on IAA-, 4-Cl-IAA-, or GA ₃ -induced deseeded pericarp growth.....	124

List of Tables

Table		Page
3.1	Effect of pericarp splitting and splitting and deseeding at 2 DAA on pericarp growth and number of seed present at 4 DAA.....	54
3.2	The effect of NPA application to the pericarp, peduncle, or pericarp and peduncle on ovary growth and seed number 2 days after application.....	55
3.3	Effect of NPA applied to the inner pericarp wall of 2 DAA split or split and deseeded pericarps on pericarp growth, seed number and size, and abscission 7 days after application.....	56

List of Figures

Figure		Page
1.1	Chemical structures of four naturally occurring auxins and two common synthetic auxins.....	2
1.2	An approximately 8 DAA pea (<i>Pisum sativum</i> L.) fruit. Seeds are attached to the ventral suture of the pericarp through the funiculus.....	8
1.3	A schematic representation of polar auxin transport.....	15
2.1	Illustration of lanolin or lanolin plus NPA application to the peduncle tissue.....	25
2.2	The application of 5 (6)- carboxyfluorescein diacetate (CFDA) to the pedicel.....	26
2.3	A diagram of the fresh-tissue cross-sectioning for GUS staining.....	27
2.4	A diagram of tissue collected for determining GUS enzyme activity in DR5::GUS lines.....	29
3.1	Illustrations of the inflorescence, and pedicel and peduncle cross-sectional anatomy of pea (<i>Pisum sativum</i> L.)	34
3.2	Representative micrographs showing the vascular arrangement in the pericarps of ~ approximately 20 DAA ovaries of <i>Pisum sativum</i> (Sugar snap pea)	35
3.3	Representative micrographs of 5 (6)-carboxyfluorescein diacetate (CFDA) fluorescence (green color) patterns in the pedicels and pericarps of 4-6 DAA pea inflorescence.....	37
3.4	Representative micrographs of the GUS staining patterns observed in cross-sections of intact ovaries (pericarp + seeds) of 4 DAA fruits and the attached pedicel, proximal and distal peduncle tissues from DR5::GUS expressing pea plants.....	39
3.5	Representative micrographs of the cross-section of pedicels attached to pollinated and nonpollinated ovaries at -2, 0, 2, and 3 DAA from DR5::GUS expressing pea plants.....	40

3.6	The effect of pericarp splitting on the GUS enzyme activity in fruit and attachment tissues of DR5::GUS expressing pea plants.....	41
3.7	The effect of seed removal on DR5-GUS staining patterns and GUS enzyme activity in 4 DAA fruit and attachment tissues of DR5::GUS expressing pea plants.....	43
3.8	The effect of NPA (polar auxin transport inhibitor) applied to the peduncle on DR5-GUS staining patterns and GUS enzyme activity in 4 DAA intact fruit and attachment tissues of DR5::GUS expressing pea plants.....	45
3.9	Representative micrographs showing the effect of NPA application to the peduncle or inner pericarp wall of 4 DAA split pericarps on GUS staining patterns in the ovary, pedicel, and proximal and distal peduncle tissues of DR5::GUS expressing pea plants.....	47
3.10	The effect of NPA application to the peduncle or inner pericarp wall of 4 DAA split pericarps on GUS enzyme activity in the ovary and attachment tissues of DR5:: GUS expressing pea plants.....	48
3.11	Representative micrographs showing the effect of NPA applied simultaneously to the peduncle and inner pericarp wall of 4 DAA fruits split along the dorsal pericarp suture (SP) on GUS staining patterns and GUS enzyme activity in the ovary, pedicel, proximal and distal peduncle tissues from DR5::GUS expressing pea plants.....	50
3.12	The effect of NPA application to the pericarp, peduncle, or simultaneously to the pericarp and peduncle on GUS enzyme activity in 4 DAA split and deseeded fruit (SPNS) and attachment tissues of DR5::GUS expressing pea plants.....	52
3.13	Effect of NPA application to pedicels or peduncle of emasculated (non-pollinated) or pollinated fruits on the growth of fruits.....	57
5.1	Proposed model for the source and possible transport routes of auxins in developing pea fruits.....	72
A1	Representative micrographs of 5 (6)-carboxyfluorescein diacetate (CFDA) fluorescence (green color) patterns in the pedicels and pericarps of 4-6 DAA pea inflorescences.....	88

A2	Representative micrographs of pedicel cross-sections showing GUS staining in the cortical region, with more prominent GUS staining usually occurring in the cortical region proximal to the pericarp dorsal suture attachment site.....	89
A3	Representative micrographs showing GUS staining patterns in the ovaries of 4 DAA fruits, and the attached pedicel, and proximal and distal peduncle tissues from WT pea plants.....	90
A4	The effect of pericarp splitting on the GUS staining patterns observed in pea fruit and attachment tissues of DR5::GUS expressing pea plants.....	91
A5	Representative micrographs of pedicel cross-sections showing GUS staining in the primary xylem and the cambium/primary phloem as a result of NPA application to the peduncles of split pericarps.....	92
A6	Representative micrographs of pedicel cross-sections showing GUS staining in the primary xylem and the cambium/ primary phloem as result of NPA application to the inner pericarp wall of split pericarps.....	93
A7	Representative micrographs of pedicel cross-sections showing GUS staining in the primary xylem and the cambium/primary phloem as a result of NPA application to both peduncle and inner pericarp wall of split pericarps.....	94
B1	Representative micrographs showing the GUS staining patterns in intact ovaries from three individual experiments.....	100
B2	Representative micrographs showing the GUS staining patterns in pedicels attached to intact ovaries from four individual experiments.....	101
B3	Representative micrographs showing the GUS staining patterns in proximal peduncles attached to the intact ovaries from four individual experiments...	102
B4	Representative micrographs showing the GUS staining patterns in distal peduncles attached to the intact ovaries from four individual experiments...	103
B5	Representative micrographs showing the GUS staining patterns in intact ovaries treated with NPA to the peduncle from four individual experiments.	104

B6	Representative micrographs showing the GUS staining patterns in pedicels attached to the intact ovaries treated with NPA to the peduncle from four individual experiments.....	105
B7	Representative micrographs showing the GUS staining patterns in proximal peduncles attached to intact ovaries treated with NPA to the peduncle from four individual experiments.....	106
B8	Representative micrographs showing the GUS staining patterns in distal peduncles attached to the intact ovaries treated with NPA to the peduncle from four individual experiments.....	107
B9	Representative micrographs showing the GUS staining patterns in split pericarps from three individual experiments.....	108
B10	Representative micrographs showing the GUS staining patterns in pedicels attached to split pericarps from three individual experiments.....	109
B11	Representative micrographs showing the GUS staining patterns in proximal peduncles attached to split pericarps from three individual experiments.....	110
B12	Representative micrographs showing the GUS staining patterns in distal peduncles attached to split pericarps from three individual experiments.....	111
B13	Representative micrographs showing the GUS staining patterns in split pericarps treated with NPA to the peduncle from four individual experiments.....	112
B14	Representative micrographs showing the GUS staining patterns in pedicels attached to the split pericarps treated with NPA to the peduncle from four individual experiments.....	113
B15	Representative micrographs showing the GUS staining patterns in proximal peduncles attached to the split pericarps treated with NPA to the peduncle from four individual experiments.....	114
B16	Representative micrographs showing the GUS staining patterns in distal peduncles attached to the split pericarps treated with NPA to the peduncle from four individual experiments.....	115

B17	Representative micrographs showing the GUS staining patterns in split pericarps treated with NPA to the inner pericarp wall from four individual experiments.....	116
B18	Representative micrographs showing the GUS staining patterns in pedicels attached to the split pericarps treated with NPA to the inner pericarp wall from four individual experiments.....	117
B19	Representative micrographs showing the GUS staining patterns in proximal peduncles attached to the split pericarps treated with NPA to the inner pericarp wall from four individual experiments.....	118
B20	Representative micrographs showing the GUS staining patterns in distal peduncles attached to the split pericarps treated with NPA to the inner pericarp wall from four individual experiments.....	119
B21	Representative micrographs showing the GUS staining patterns in split pericarps treated with NPA to both peduncle and inner pericarp wall from four individual experiments.....	120
B22	Representative micrographs showing the GUS staining patterns in pedicels attached to the split pericarps treated with NPA to both peduncle and inner pericarp wall from four individual experiments.....	121
B23	Representative micrographs showing the GUS staining patterns in proximal peduncles attached to the split pericarps treated with NPA to both peduncle and inner pericarp wall from four individual experiments.....	122
B24	Representative micrographs showing the GUS staining patterns in distal peduncles attached to the split pericarps treated with NPA to both peduncle and inner pericarp wall from four individual experiments.....	123
C1	Effect of NPA pre-treatment on auxin and gibberellin-induced deseeded pericarp growth.....	125

List of Abbreviations

Abbriviation	Definition
2, 4-D	2,4-dichlorophenoxyacetic acid
4-Cl-IAA	4-chloroindole-3-acetic acid
4-MU	4-methylumbelliferone
ABA	Abscisic acid
ABCB	ATP BINDING CASSETTE TYPE B
ANOVA	Anaysis of varience
ARF	AUXIN RESPONSE FACTOR
Aux/IAA	AUXIN/INDOLE-3-ACETIC ACID
AUX/LAX	AUXIN/LIKE AUX1
AUX1	AUXIN RESISTANT 1
AuxRE	Auxin response element
BR	Brassinosteroids
CaMV	Cauliflower mosaic virus
CFDA	Carboxyfluorescein diacetate
CK	Cytokinin
C/PP	Cambium/primary phloem
Cpw	Central pericarp wall
DII	Domain II
DAA	Days after anthesis
DPA	Days post anthesis
Dpe	Distal peduncle
DS	Dorsal suture
F	Funiculus
GA	Gibberellin
GC-MS	Gas chromatography- Mass spectrometry
GFP	Green fluorescent protein
GH3	GRETCHEN HAGEN 3

GUS	β -glucuronidase
HFCA	2-Chloro-phydroxyfluorene-9-carboxylic acid
IAA	Indole-3-acetic acid
IBA	Indole-3-butyric acid
LAX	LIKE AUX 1
LSMEANS	Least squares means
MCPA	2-methyl-4-chlorophenoxyacetic acid
MDR/PGP	Multi-drug resistant/P-glycoprotein
Mg ²⁺	Magnesium ion
MUG	4-methylumbelliferyl glucuronide
NAA	1-naphthaleneacetic acid
ng gdw ⁻¹	Nanograms per gram dry weight
nmol gfw ⁻¹	Nanomoles per gram fresh weight
NPA	<i>N</i> -1-naphthylphthalamic acid
P	Pericarp
PAA	Phenylacetic acid
PAT	Polar auxin transport
PCR	Polymerase Chain Reaction
Pds	Pericarp dorsal suture
PGP	P-glycoprotein
Ph	Phloem
PIN 1	PIN-FORMED 1
Pl	Pedicel
Ppe	Proximal peduncle
Pvs	Pericarp ventral suture
Pwv	Pericarp wall vasculature
qPCR	Quantitative Real-Time Polymerase Chain Reaction
RFP	Red fluorescent protein
RNA	Ribonucleic acid
mRNA	Messenger RNA
S	Seed

SF	Seed plus funiculus
SP	Split pericarp with seeds
SPNS	Split pod no seeds
STS	Silver thiosulfate
TIBA	2,3,5-triiodobenzoic acid
TIR1	TRANSPORT INHIBITOR RESPONSE 1
TPL	TOPLESS
TPR	TPL-RELATED
VS	Ventral side
WT	Wild-type
X	Xylem
YFP	Yellow fluorescent protein

1. INTRODUCTION

1.1 Plant hormones

Plant hormones (or phytohormones) are naturally occurring chemical messengers in plants which allow communication among cells, tissues, and organs that make up the plant, and between the plant and the environment (Davies, 2010). These molecules have specific effects on plant growth and development at relatively low concentrations. Although in initial studies, phytohormones were defined as a substance that can be transported from one part of the plant to another to do their action, now it is clear that synthesis of phytohormones can be either near or distant from their site of action (Went and Thimann, 1937; Davies, 2010). The five “classical” groups of phytohormones are auxins, gibberellins (GAs), cytokinins (CKs), abscisic acid (ABA) and ethylene. With a greater understanding of plant biology, the list of phytohormones is growing and now generally includes brassinosteroids (BRs) and jasmonates. In addition to these compounds, salicylic acids, some peptide growth regulators such as phytosulfokines and the branching hormone strigolactone also are now considered as phytohormones (Chapman and Estelle, 2009; Wolters and Jürgens, 2009).

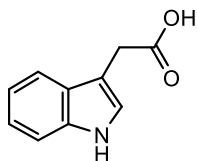
1.2 The class of hormones called auxins

The history of plant hormones goes back into the late 19th century, and the concept of phytohormones developed from the study of tropism (c.f. Went and Thimann, 1937). The work of Charles and Francis Darwin on the phototropism of seedlings postulated that the perception of light is done by the tip of the coleoptile and some “influence” is “transmitted” from tip to subapical growth zone to cause the unequal growth for bending (c.f. Went and Thimann, 1937). Another independent study in 1894, further supported Darwin’s observations and showed there is a separation between perception and reaction zones of the plant tissue (c.f. Went and Thimann, 1937). In 1926, Went was able to isolate this “influence” into an agar block and demonstrated that the growth of an *Avena sativa* (oat) coleoptile was dependent on the amount of substance in the agar block, and the coleoptile bending direction depends on the location of the agar block on the decapitated coleoptile (Went, 1926). This transmitting influence was originally named as “Wuchsstoff” by Went (c.f. Davies, 2010). However, after the structural identification of this

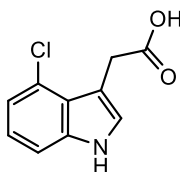
“influence” as indole-3-acetic acid (IAA), it was named “auxin”, meaning “to grow” (c.f. Went and Thimann, 1937; Abel and Theologis, 2010).

Auxins are defined as compounds with a spectrum of biological activities similar to IAA, but not necessarily structurally identical to IAA (Cleland, 1995). The types of biological assays used to assess auxin activity include induction of cell elongation in isolated coleoptile or stem sections, induction of cell division in callus tissues, and promotion of adventitious root formation in stem cuttings (Cleland, 1995). Chemically, many auxins have an aromatic ring system as a nucleus, and a carboxyl group separated from the ring by at least one carbon atom (see Fig. 1.1; Thimann, 1952; Katekar and Geissler, 1980; Ferro et al., 2010).

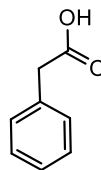
Natural auxins



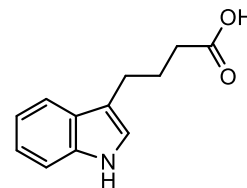
Indole-3-acetic acid
(IAA)



4-chloroindole-3-acetic acid
(4-Cl-IAA)

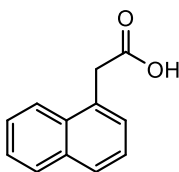


Phnylacetic acid
(PAA)

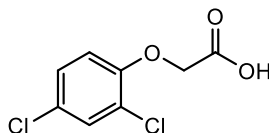


Indole-3-butyric acid
(IBA)

Synthetic auxins



1-naphthaleneacetic acid
(NAA)



2,4-dichlorophenoxyacetic acid
(2,4-D)

Figure 1.1. Chemical structures of four naturally occurring auxins and two common synthetic auxins

Auxin is known to mediate most aspects of plant growth and development (Sugawara et al., 2015) and IAA is the ubiquitous auxin found in higher plants, with higher concentrations of

IAA usually located in the meristematic regions and actively growing plant organs (Baker, 2000; Ljung et al., 2001; Noh et al., 2001; Blakeslee et al., 2005; Michniewicz et al., 2007). There are several other naturally occurring auxins in plants including 4-chloroindole-3-acetic acid (4-Cl-IAA), indole-3-butyric acid (IBA) and phenylacetic acid (PAA, a weak auxin) (Fig. 1.1; Davies, 2010). However, their roles in plant growth and development are less known compared to the IAA. The halogenated auxin, 4-Cl-IAA, is a highly active form of auxin, and in pea is thought to play a crucial role in early pericarp growth (Reinecke et al., 1995; Reinecke, 1999; Ozga et al., 2009). The natural occurrence of 4-Cl-IAA is reported to be limited to pea (*Pisum sativum*) and several other members of the Fabaceae family, with one exception, available in seeds of Scots pine (*Pinus sylvestris*; Ernstsén and Sandberg, 1986; reviewed by Reinecke, 1999). However, the occurrence of 4-Cl-IAA in Scots pine has been recently questioned by Lam et al. (2015). IBA more efficiently promotes rooting of plant parts than IAA and is commercially used in plant propagation procedures. The greater efficiency of IBA compared to IAA may be due to the stability of IBA against the catabolism and inactivation by conjugation within plant tissues compared to IAA (c.f. Davies, 2010). Studies showed that plants could convert IAA to IBA and also IBA to IAA in peroxisomes by a fatty acid β -oxidation-like process (Davies, 2010; Schlicht et al., 2013). Current evidence suggests that IBA is not active per se, but needs to be converted to IAA for auxin response in plant tissues (Schlicht et al., 2013). PAA has weak auxin activity and is the only phenyl-derivative among the natural auxins found in plants (Simon and Petrášek, 2011). The low biological activity, low abundance and unique distribution (non-polar transport and gradients are due to the local biosynthesis) of PAA in plants may suggest that PAA does not act strictly as auxin or it may have a specialized, yet unknown function in the plant kingdom (c.f. Davies, 2010). More recently, it has been shown that PAA transport is not active or directional like IAA, but PAA was observed to induce the same set of early IAA-responsive genes as IAA in *Arabidopsis* tissues (Sugawara et al., 2015).

After the isolation and chemical characterization of IAA, a number of chemical compounds mimicking the auxin activity were synthesized. These compounds are known as synthetic auxins or plant growth regulators, and they are widely used in the agricultural industry as bioregulators and herbicides due to their stability in plants compared to IAA (reviewed by Gianfagna, 1995; Grossmann, 2007). At low concentrations, these synthetic auxins stimulate growth and developmental processes, and therefore, are used in horticulture and agriculture

industry as a bioregulator (reviewed by Gianfagna, 1995; Grossmann, 2010; Do-Thanh et al., 2016). At high concentrations, some synthetic auxins are used as herbicides which cause growth disruption and lethal damage to plants by altering auxin-balance (Grossmann, 2010). After the discovery of the first growth regulators/herbicides, 2,4-dichlorophenoxyacetic acid (2, 4-D) and 2-methyl-4-chlorophenoxyacetic acid (MCPA), a wide variety of auxin herbicides with different types of weed spectra and selectivity have been synthesized (Cobb and Reade, 2010).

1.3 Auxin regulation of plant reproductive development

Angiosperms are unique among the plant kingdom as they enclose their seeds in a protective structure, the ovary. The fruit is the mature ovary, and the ovary wall (pericarp) can be fleshy or dry at maturity (McAtee et al., 2013). Fleshy fruits have a fleshy-consumable structure around the seed(s) to attract animals for dispersal purposes. Dry fruits use wind or mechanical force provided by the pericarp structure to split open the ovary for seed dispersal (Kumar et al., 2011; McAtee et al., 2013). According to evolutionary studies, dry fruits are ancestors of fleshy fruits, and both share a common mechanism of fruit development and ripening (McAtee et al., 2013). Despite the type of fruit, fruit development is divided into four steps; fruit set, growth, maturation, and ripening/senescence (Obroucheva, 2014). The transformation of the fertilized ovary into a mature fruit is a complex process which relies on the precise coordination at molecular, biochemical and structural levels. Work on plant reproductive development revealed that auxin mediates fruit development through an integrated process involving its biosynthesis, transport, and signaling, as well as its interaction with other hormonal pathways (Ozga and Reinecke, 2003; Sundberg and Østergaard, 2009).

Fruit set and initial fruit development are dependent on the successful pollination and fertilization of the ovules. The landing of mature pollen on a compatible stigma marks the beginning of pollination, and then the pollen will hydrate and germinate to make a pollen tube, which delivers the generative nuclei to the ovule to initiate the double fertilization process (Sundberg and Østergaard, 2009). A study in tobacco (*Nicotiana tabacum*) revealed that, after hydration and germination of the majority of pollen grains which have landed on the stigma, auxin (IAA) levels peak in the stigmatic tissues, then drop and start to increase in the style tissues (Chen and Zhao, 2008). Similarly, as the pollen tubes grow into the stylar tissue, higher

IAA levels were observed in style tissues where the pollen tube entered and, in contrast, dropped when the pollen tubes penetrated out that particular area (Chen and Zhao, 2008). Therefore, these authors postulated a correlation of pollen germination and pollen tube growth in the stigma/style tissue with auxin levels indicating that auxins are important in the coordination of these pollination events (Chen and Zhao, 2008).

The initial linkage between fruit set and plant hormones was established by Gustafson (1936) through the application of auxins to emasculated flowers of tomato, petunia, and *salpiglossus* (IAA, IBA or PAA in lanolin paste applied to the cut style after removal of stamens) which resulted in seedless (parthenocarpic) fruits (Gustafson, 1936; Gustafson, 1942). Application of auxin transport inhibitors such as *N*-1-naphthylphthalamic acid (NPA) and 2,3,5-triiodobenzoic acid (TIBA) to the emasculated fruits in *Arabidopsis* and tomato (Dorcey et al., 2009; Serrani et al., 2010), as well as to the unpollinated pistillate flowers of cucumber (Kim et al., 1992) can also induce parthenocarpic fruit development, indicating that elevated levels of endogenous auxins can mimic the fertilization process and stimulate the subsequent fruit growth (Kim et al., 1992; Dorcey et al., 2009; Serrani et al., 2010). Moreover, the modulation of the auxin signaling pathway in plants by down-regulation of genes encoding specific auxin response factors (ARFs) and/or Aux/IAAs, that are repressors of auxin signaling, also initiates parthenocarpic fruit development. For example, the loss-of-function mutation of the *AtARF8* gene in *Arabidopsis* (Goetz et al., 2007), and the Aux/IAA gene *IAA9* in tomato (Wang et al., 2005), produce parthenocarpic phenotypes in those fruits (Wang et al., 2005; Goetz et al., 2007; Serrani et al., 2008). Finally, overexpression of the tryptophan-dependent IAA-biosynthetic gene, *iaaM*, under the ovule specific *Deficiens Homolog 9* gene (*DefH9*) promoter, also induces parthenocarpy in cucumber and grape fruit (Yin et al., 2006; Costantini et al., 2007). Altogether, these observations establish that auxin can activate ovary growth and fruit set in the absence of ovule fertilization in these species.

Upon ovule fertilization, the developing fruit enters a stage in which ovary growth and maturation are tightly coordinated with seed development. It is now well established that fertilized ovules (seeds) are a rich source of hormones, particularly auxins and gibberellins (GA) which are involved in stimulating growth of surrounding tissues and even they are involved in determining the final size of the fruit (Eeuwens and Schwabe, 1975; Ozga et al., 1992; Ozga and Reinecke, 1999; Ozga et al., 2003; Dorcey et al., 2009). Consistent with this removal or

destruction of developing seeds result in the reduced pericarp growth and subsequent abscission (Ozga et al., 1992; Ozga and Reinecke, 1999; Ozga et al., 2003). A study by Dorcey et al. (2009) showed that there is a fertilization triggered increased auxin response in the ovules, which can be mimicked by either application of 2,4-D or blocking the outward transport of auxins. However, as they did not observe any modification in the localization of specific PIN auxin efflux carriers in the ovules and, they suggested the possibility of fertilization triggered auxin synthesis in the ovules (Dorcey et al., 2009). Supporting this, a more recent study by Larsson et al. (2017), showed that higher auxin response in the ovules, soon after the fertilization, is due to the *de novo* auxin synthesis together with the reduced auxin conjugation and auxin transport. Furthermore, It has been shown that the treatment of *Arabidopsis* ovaries with 2,4-D, led to changes in the GA biosynthesis gene expression in unfertilized ovules similar to that triggered by fertilization, pointing out the possibility of fertilization triggered auxin-dependent GA biosynthesis in developing *Arabidopsis* ovules (Dorcey et al., 2009). In tomato, application of NPA to unpollinated ovaries led to increased IAA accumulation, increased transcript abundance of GA biosynthetic genes (*SICPS*, *SIGA20ox1*, and *SIGA20ox2*), and GA₁ levels, and these changes were associated with parthenocarpic fruit development (Serrani et al., 2010). In addition, Lemaire-Chamley et al. (2005) observed that a gradient of expression of auxin biosynthetic, transport, signalling and response genes from the placenta and locular tissues towards the outer part of the tomato fruit tissues, reflects the possibility of auxin transport from seeds and or its surrounding tissues towards the outer layers of the fruit. It was first reported in pea that auxin stimulates GA biosynthesis in the ovary (van Huizen et al., 1995; van Huizen et al., 1997; Ngo et al., 2002; Ozga et al., 2002; Ozga et al., 2003). From work in pea (see section 1.4), it was suggested that auxin synthesized in seeds is transported to the pericarp where it induces GA biosynthesis promoting pericarp growth (Ngo et al., 2002; Ozga et al., 2009). In both scenarios, bioactive GA (synthesized in the seed or the pericarp) stimulates pericarp cell expansion (Ozga et al., 2002) and inhibits the negative regulators of the fruit development.

1.4 Dynamics of auxin during early pea fruit development

Pea (*Pisum sativum* L.) is a cool season annual crop which is used as a model system to understand hormonal interactions during fruit development as it produces moderately-sized fruits

allowing the accessibility to the seeds at a young developmental age (Ozga et al., 1992; Ozga et al., 2002; Ozga et al., 2003). Self-pollination in pea takes place approximately 24 to 36 h before flower opening (anthesis), and the ovules are fertilized by anthesis (Cooper, 1938). After successful pollination and fertilization, ovary development will take place to produce mature fruit. A pea fruit consists of a pericarp, with enclosed seeds attached to the ventral suture of the pericarp through the funiculus (Fig. 1.2; Cooper, 1938). The function of the pericarp is to protect developing seeds against mechanical damage, to stabilize the microenvironment during seed ontogeny, and as to act as a physiological buffer against fluctuations in the nutrient supply (Müntz et al., 1978). The pea pericarp has three distinct layers, the exocarp, mesocarp, and endocarp. With development, several structural changes are associated with these layers, especially in the endocarp layer. At anthesis (0 DAA; days after anthesis), the outermost exocarp consists of a single layer of epidermal cells; middle mesocarp contains approximately 15 layers of vacuolated parenchyma cells, and the inner-most endocarp is composed of several layers of undifferentiated parenchyma cells (Ozga et al., 2002). Cell division was observed from 0 to 2 DAA, where it evident by the increase in cell number of the exocarp, mesocarp, and the endocarp layers in the longitudinal plane (Ozga et al., 2002). From 2 to 4 DAA, the cell number was increased (observed in the longitudinal plane) only in the transition layer and inner epidermis of the endocarp (Ozga et al., 2002). From 4 to 7 DAA, cell division and differentiation mainly occurred in the middle parenchyma cells of endocarp and mesocarp vasculature (Ozga et al., 2002). The endocarp consisted with four cell layers at 7 days after anthesis (DAA); an inner epidermis, five to six layers of parenchyma cells, two to three layers of sclerenchyma cells near the mesocarp, and a transition cell layer separating the mesocarp and endocarp (Ozga et al., 2002). In parallel to the cell division, cell expansion occurred from 0-7 DAA as noted within the mesocarp cells. (Ozga et al., 2002). The effect of seed removal at the 2 DAA, was visible at 4 DAA. Although the three major pericarp cell layers were intact, minimal cell expansion was observed in the cell layers by 4 DAA in deseeded pericarps. Deseeded pericarps usually abscised after 6 DAA (Ozga et al., 2002), implying the importance of seeds for normal pericarp development. Application of GA₃ or 4-Cl-IAA reversed this effect in the deseeded pericarps. However, application of both hormones was required to obtained the normal cell size which observed in the intact fruits (Ozga et al., 2002).

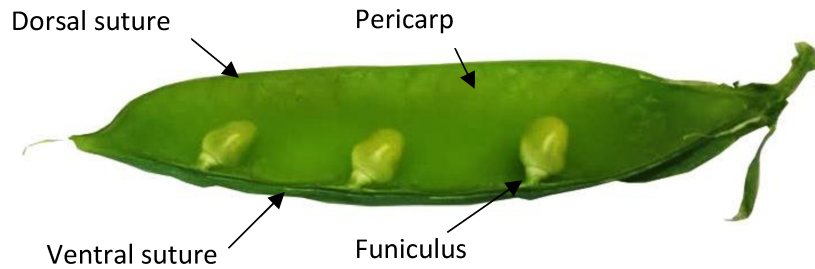


Figure 1.2. An approximately 8 DAA pea (*Pisum sativum* L.) fruit. Seeds are attached to the ventral suture of the pericarp through the funiculus.

In pea pericarps, the majority of GAs are synthesized via the early 13-hydroxylation pathway which converts GA₁₂ to bioactive GA₁ (Ozga et al., 2009). After pollination of the fruit and fertilization of the ovules, the pericarp (enclosing the developing seeds) is stimulated to grow. Increased mRNA levels of the pericarp GA biosynthetic genes *PsGA20ox1* (codes for GA 20-oxidase that converts GA₅₃ to GA₂₀), and *PsGA3ox1* (codes for GA 3-oxidase that converts GA₂₀ to bioactive GA₁), and reduced transcript abundance of GA catabolizing gene *PsGA2ox1* (codes for a GA 2-oxidase that converts GA₂₀ to GA₂₉ and bioactive GA₁ to inactive GA₈) is concomitant with this rapid pericarp growth (Ozga et al., 2009). Moreover, removal of seeds from pollinated pericarp greatly reduced the mRNA level of GA biosynthesis genes while increasing the GA catabolism genes (Ozga et al., 1992; Ozga et al., 2009). These results suggest that GA biosynthesis and catabolism gene expression and the bioactive GA levels are regulated by developing seeds in the young pea pericarps.

Developing pea fruits also contain the auxins, 4-Cl-IAA and IAA, with a higher concentration found in the young developing seeds than the pericarps (Magnus et al., 1997). However, only 4-Cl-IAA (not IAA) can mimic the presence of seeds and restore the deseeded pericarp growth (Reinecke et al., 1995). Furthermore, similar to the presence of seeds, 4-Cl-IAA can regulate GA biosynthesis and catabolism gene expression in deseeded pericarps by increasing transcript abundance of *PsGA20ox1* and *PsGA3ox1* and reduce the *PsGA2ox1* transcript abundance (Ozga et al., 2009). Therefore, it is hypothesized that seed-derived 4-Cl-IAA is transported to the pericarp, where it maintains the bioactive GA₁ levels in pericarps by

differentially regulating the GA biosynthesis and catabolism genes, leading to pericarp growth (Ozga et al., 2009).

Other than the ability to regulate bioactive GA₁ levels, 4-Cl-IAA can also minimize the pericarp growth inhibitory effect by ethylene (Johnstone et al., 2005). In growth assays, 4-Cl-IAA showed a dose-dependent induction of pericarp growth (from 1 to 100 μM), but IAA showed growth inhibitory effects when tested from 1 to 10 μM (Reinecke et al., 1995). The pre-treatment of deseeded pericarps with silver thiosulfate (STS; an ethylene action inhibitor) eliminates the IAA-induced pericarp growth inhibition, suggesting the possibility of IAA-induced ethylene as the factor for the growth inhibition by IAA (Johnstone et al., 2005). Johnstone et al., (2005) also found that the ethylene evolution profiles of both auxins in deseeded pea pericarps were similar, but 4-Cl-IAA was able to block ethylene action with respect to pericarp growth (Johnstone et al., 2005). Therefore, the authors concluded that IAA and 4-Cl-IAA regulate pericarp ethylene action in distinctly different manner. Furthermore, Jayasinghege (2017) showed that only 4-Cl-IAA treatment to the deseeded pericarps leads to higher transcript abundance of putative pea ethylene receptor genes *PsERS1* and *PsETR2* and the ethylene signaling *PsEBF1* and *PsEBF2* genes, which are known to act as negative regulators of ethylene signaling. In conclusion, the ability of 4-Cl-IAA, but not IAA, to modulate bioactive GA levels by regulating GA biosynthesis and catabolism together with its ability to regulate ethylene signaling and/or ethylene action, is believed to play an important role in 4-Cl-IAA-induced pericarp development in pea.

1.5 Auxin transport in plants

The temporal and spatial control of auxin distribution has a key role in regulating plant growth, and developmental processes (Pattison and Catalá, 2012) and therefore, the mechanism by which auxin is transported throughout the plant has been a great interest to plant biologists for years. Based on physiological, molecular and biochemical data, auxin distribution is considered to occur through at least two physiologically distinct and spatially separated transport pathways, a fast non-polar pathway through the phloem, and a slower cell-to-cell polar auxin transport (PAT) pathway mediated through auxin-influx and auxin-efflux carrier proteins (Morris et al., 2010).

Auxin (IAA) is a natural constituent of the phloem sap, and the first evidence for its existence in phloem transport was established by Hüber et al. (1937), through the exudates collected from the bark of *Fagus sylvatica*, *Robinia pseudoacacia*, and *Aesculus hippocastanum*, which could induce curvatures in the *Avena* coleoptiles (c.f. Hoad, 1995). Along with this observation, GC-MS quantitation of *Ricinus* phloem sap provided evidence for the phloem transport of free IAA (Allen and Baker, 1980). Moreover, radiolabelled IAA synthesized from the applied ^{14}C -tryptophan to the mature leaves of *Ricinus* was also detected in the phloem together with the endogenous IAA, further supporting the presence of IAA in phloem sap (Borkovec et al., 1994). The xylem does not seem to play an important role in the long-distance transport of auxin, for example, only trace amounts (less than 0.5 ng ml^{-1}) of endogenous IAA present in the xylem sap collected from 6 to 8 week old decapitated *Ricinus communis* L. plants stems (Allen et al., 1979). The interaction of phloem and PAT in relation to auxin transport was demonstrated by Cambridge and Morris (1996). They showed that efflux of radiolabelled IAA from internode segments was neither polar (can be detected in both above and below the (fed-leaf) nor NPA sensitive after 1hr of application of [$1\text{-}^{14}\text{C}$] IAA to the upper surface of the mature foliage leaf in pea. However, [$1\text{-}^{14}\text{C}$] IAA transport was polar (only in below internode segment to fed leaf; basipetal) and sensitive to NPA after 3.5-4hr of application (Cambridge and Morris, 1996). This observation pointed out that IAA is loaded into phloem in the mature leaf and subsequently it can be transferred to the PAT system after export from the leaf/ application point (Cambridge and Morris, 1996). Moreover, the decapitation of plants led to less recovery of radiolabel auxin in the internode sections, suggesting that radial transfer of auxin from phloem to PAT may be more efficient at the younger sink tissues of the shoot apex (Cambridge and Morris, 1996).

In contrast to phloem transport, PAT is specific for auxins, occurs in a cell-to-cell manner and has a strictly unidirectional character (reviewed by Morris et al., 2010). In the intact plants, the main polar flow of auxin can be seen in the shoot where auxin is transported basipetally towards the base of the plants and acropetally to root tip mainly via vascular cambium cells and adjacent, partially differentiated thin-walled living xylem elements (Michniewicz et al., 2007; Morris et al., 2010). Other than this downward movement, auxin was also detected in parenchyma cells of the xylem rays in the plant stem showing the lateral redistribution of auxins (Morris and Thomas, 1978). In roots, auxin transport towards the root tip and is redirected

toward the root elongation zone through the epidermis is also facilitated by PAT (Rashotte et al., 2000; reviewed by Morris et al., 2010).

Auxin transport assays revealed that PAT requires energy, is saturable and sensitive to protein synthesis inhibitors, suggesting the existence of specific auxin transport proteins (Morris et al., 2010). In the mid 1970s the chemiosmotic model for polar auxin transport was proposed (Rubery and Shelldrake, 1974; Raven, 1975). According to this model, in the acidic environment of the cell wall (pH 5.5; due to the proton-ATPase pumps), auxin (IAA) is present in both ionized (IAA^-) and protonated (IAAH) forms. Protonized, hydrophobic, IAAH passively diffuses into the cytoplasm through the plasma membrane. The alkalinity in the cytoplasm (~pH 7.0) facilitates the dissociation of IAAH and the resulting ionic IAA^- cannot passively move out of the cell because of its poor plasma membrane permeability. Therefore, carrier mediated auxin efflux was postulated, and their asymmetric localization within the plant cells dictates the polarity of the auxin movement in a particular tissue type. (Fig 1.3; Raven, 1975; Vieten et al., 2007).

1.5.1 Auxin influx carriers

The existence of auxin influx carriers was first proposed by the Rubery and Shelldrake in 1974 and supported by the later finding of Lomax et al. (1985), where they provide evidence for carrier-dependent uptake of IAA by zucchini (*Cucurbita pepo*) membrane vesicles, instead of passive diffusion, as the uptake of radiolabeled $[2\text{-}^{14}\text{C}]$ IAA was four times higher (depending on the calculations) than that expected from simple diffusion (Lomax et al., 1985). Moreover, as IAA uptake in zucchini membrane fractions was saturable (Rubery and Shelldrake, 1974) and independent of cations other than protons, it was later suggested that the uptake of auxin anions together with protons by a co-transport mechanism (Rubery, 1978). More recently, the auxin flux ratio between carrier mediated influx and diffusive influx was calculated using data derived from studies monitoring the uptake of radiolabeled auxin into *tobacco* suspension culture cells and intact tissues in *Vicia* root segments (Kramer and Bennett, 2006). These data showed that only a small portion of IAA is protonated in the acidic cell wall space, and the majority remains in the dissociated IAA^- form, which cannot diffuse passively into the cytoplasm (Kramer and Bennett, 2006), further supporting the involvement of carrier proteins for auxin influx.

The characterization of *Arabidopsis* agravitropic *auxin resistant 1 (aux1)* mutant led to the identification of the AUX1/LIKE AUX1 (AUX1/LAX) family of transmembrane, proton-driven transport proteins. *AtAUX1* encodes a polypeptide of 485 amino acids with sequence similarity to other known amino acid permeases in *Arabidopsis*, which can transport amino acids (Bennett et al., 1996). Structural similarity of IAA to the amino acid tryptophan suggests its ability to use AUX1 proteins as auxin influx carriers (Bennett et al., 1996). Further analysis of *aux1* mutants showed that this mutation could lead to root gravitropic defects which can be rescued by lipophilic membrane permeable NAA, but not auxins, 2,4-D or IAA, which need carriers for uptake (Yamamoto and Yamamoto, 1998). Evidence that AUX1 is a high affinity auxin transporter came with the experiments using *Xenopus laevis* oocytes, where AUX1 showed a saturable, pH-dependent IAA uptake (Yang et al., 2006), and a study that showed IAA binds to AUX1 in a pH-dependent manner with maximal binding taking place between pH 5 and 6 (60% to 95% of IAA in dissociated form at this pH; Carrier et al., 2008).

1.5.2 Auxin efflux carriers

IAA moves throughout the plant with the aid of efflux facilitators that are sensitive to synthetic inhibitors of auxin transport such as NPA, TIBA and 2-chloro-phydroxyfluorene-9-carboxylic acid (HFCA). Flavonoids are also suggested to act as natural auxin transport inhibitors in plants (Muday and DeLong, 2001; Michniewicz et al., 2007). Initially, it was thought that the NPA binding site and the actual auxin efflux catalytic site are two different domains residing in the same transmembrane transport protein (reviewed by Morris, 2000). However, later studies with auxin efflux inhibitors and protein synthesis inhibitors showed that the NPA binding site and auxin efflux catalyst site are located in two different polypeptides that are involved in making a multi-protein complex (Morris et al., 1991). This was first evident by the observation that pre-treatment with protein synthesis inhibitors could rapidly diminish the ability of NPA to block the IAA efflux without affecting (in short-term) the IAA efflux by itself or high affinity NPA binding to its receptor/NPA binding site. (Morris et al., 1991). To explain this, it was proposed that there is a specific NPA-binding protein which interacts with the efflux catalyst through a third, protein, which is relatively unstable (Fig. 1.3; Morris et al. 1991).

The localization of the NPA binding protein on the plasma membrane is peripheral, facing the cytoplasm (Fig. 1.3; Muday and DeLong, 2001; Morris et al., 2010). Several studies

have shown that there are different binding sites for different auxin efflux inhibitors, as TIBA does not compete with NPA for inhibition of auxin transport (Michniewicz et al., 2007; Morris et al., 2010). The other important component associated with the auxin efflux multi-subunit carrier system is the integral membrane transporter protein (efflux catalyst) encoded by the members of the *PIN* gene family, (Palme and Gälweiler, 1999). PIN proteins identified in *Arabidopsis* contain 10 transmembrane domains linked to a hydrophobic region, similar to other membrane transporters (Chen et al., 1998; Luschnig et al., 1998; Müller et al., 1998; Luschnig, 2001; Muday and DeLong, 2001; Křeček et al., 2009). Heterologous expression of *Arabidopsis PIN2* (*AtPIN2*) genes in yeast showed that these engineered cells retained less radiolabeled auxins, supporting the auxin efflux function of AtPIN2 (Chen et al., 1998). Moreover, *Atpin* mutants showing reduced polar auxin transport in stems (*Atpin1*) and roots (*Atpin2* or *eir1*) of *Arabidopsis* plants, supported its involvement in PAT (Okada et al., 1991; Rashotte et al., 2000). Also, as suggested by the polar auxin transport model, PIN proteins showed an asymmetric localization in the plasma membrane of the parenchymatous xylem cells of *Arabidopsis* inflorescence (Gälweiler et al., 1998) and *Arabidopsis* root cortical and epidermal cells in the meristematic zone (Müller et al., 1998). Eight *PIN* genes have been discovered to the date in *Arabidopsis* (Křeček et al., 2009), and this indicates the availability of multiple auxin efflux carriers with distinct expression patterns for more specific and efficient regulation of auxin-dependent development in plants (Palme and Gälweiler, 1999; Muday and DeLong, 2001).

Recently, another type of auxin transporter in plants has been identified. These transporters are called multi-drug resistant/P-glycoproteins (MDR/PGP), and they are part of the ATP-binding cassette (ABC) transporter superfamily (Martinoia et al., 2002). *MDR1* (also known as PGP19) and *PGP1* were originally identified as anion-channels in *Arabidopsis*, but later mutant analysis of these two genes (*atmdr1* and *atmdr1 atpgp1*) showed phenotypes with altered auxin response and/or auxin transport such as reduced apical dominance and reduced basipetal auxin transport in hypocotyls and inflorescences (Noh et al., 2001). Interestingly, these two PGP proteins together with three other family members (PGP 2, 4 and 10) also showing NPA binding ability *in vitro* as well as when expressed in yeast systems (Noh et al., 2001; Muday and Murphy, 2002) suggesting that these proteins could represent the so far molecularly uncharacterized NPA binding proteins.

PGP4, another member of MDR/PGP subfamily, showed auxin influx ability as

Arabidopsis pgp4-1 mutant plants exhibit reduced auxin uptake in root tips. Consistent with these results, increase auxin uptake was also observed in mammalian cells that heterologously express *AtPGP4* (Terasaka et al., 2005). Furthermore, when heterologously expressing *AtPGP4* in the Sf9 insect cells incubated with 8-azido-[α -³²P]ATP, in the presence of vanadate and Mg²⁺, showed a photoaffinity labeling, suggesting that *AtPGP4* having ATPase activity as other ABC family transporters (Terasaka et al., 2005). Together with these observations, it was hypothesized that PIN auxin efflux is distinct from PGP and thus PINs and PGPs code for two functionally distinct auxin efflux systems (Petrášek et al., 2006). Findings of Blakeslee et al. (2007) recently raised the possibility of functional interaction between these two systems as PGP1 and PGP19 co-localized with PIN1 and PIN1 and PIN2 in the *Arabidopsis* shoot apex and the root tissues, respectively. Yeast-two hybridization assays as well as co-immunoprecipitation assays further support PIN-PGP interactions (Blakeslee et al., 2007). Moreover, this interaction enhanced the auxin transport and substrate/inhibitor specifications than that of single proteins, when expressed in the HeLa and yeast heterologous systems (Blakeslee et al., 2007) which strengthens the prediction of possible interaction of these two proteins.

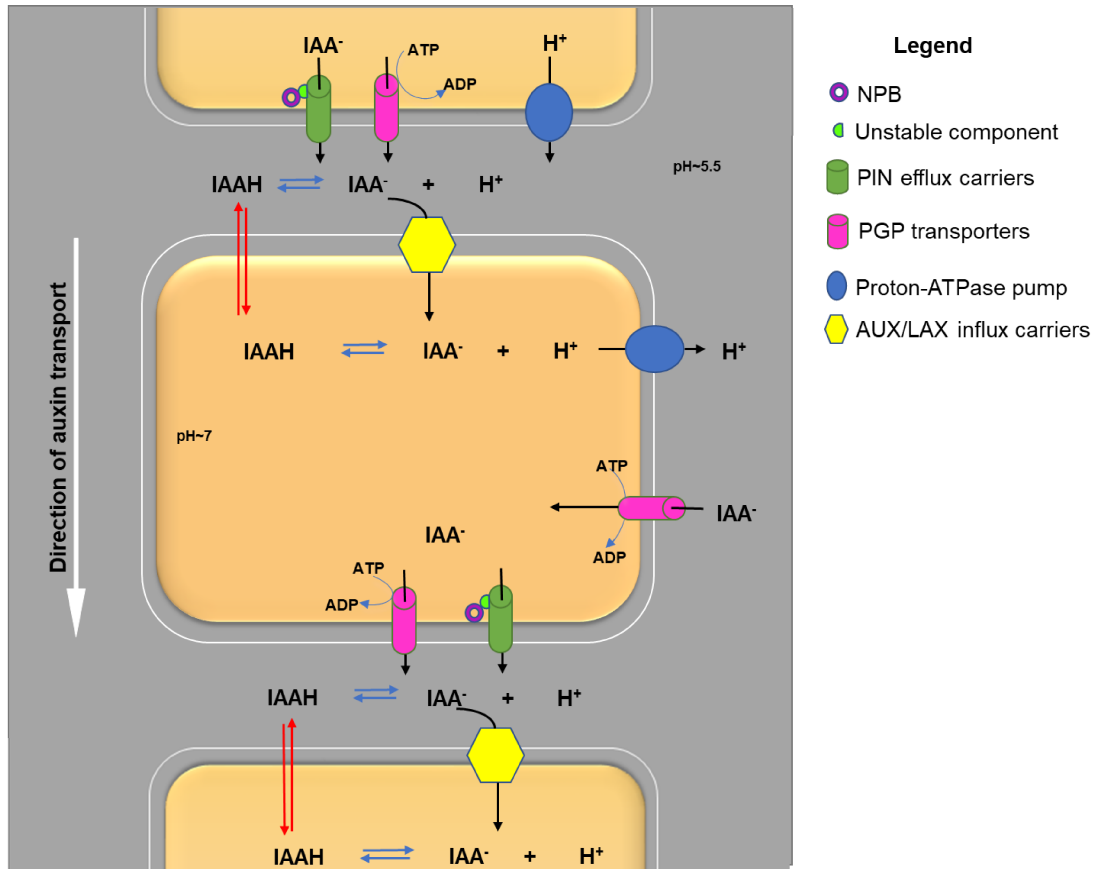


Figure 1.3. A schematic representation of polar auxin transport. Due to the relative acidity in the cell wall space, IAA can protonate (IAAH), and this IAAH can passively diffuse (Red arrows) across the plasma membrane. However, the majority of IAA present in the cell wall space is in the anionic form (IAA⁻) which requires influx carriers, AUX/LAX, to efficiently move it across the plasma membrane. In the alkaline cytoplasm, IAAH deprotonated to IAA⁻, and therefore, is trapped inside the cell. The trapped IAA⁻ requires efflux carriers to efficiently move it across the plasma membrane to the outside of the cell. The efflux carrier-multiprotein complex consists of an NPA binding protein (NPB), an efflux catalyst presumably encoded by the PIN family of genes, and a third unstable protein connecting NBP and efflux catalyst (light green color). The activity of PIN protein complex is facilitated by the proton-ATPase pump. ATP-binding cassette (ABC) subfamily P-glycoproteins (PGP) act as both auxin efflux and influx carriers, and it has its own ATPase ability. The figure was developed mainly on a representation of polar auxin transport from Michniewicz et al., 2007, with additions from Muday and DeLong (2001; NPA binding protein localization), Petrášek and Friml (2009; ABCB transporter localization), and Luschnig (2001; association of unstable protein to NPA binding protein and PIN efflux carrier).

1.6 Auxin-sensitive promoter-gene reporter systems used to understand the auxin tissue dynamics in fruits

1.6.1 DR5 promoter-reporter systems

DR5 promoter-reporter constructs have been used as a tool to visualize regions of local auxin maxima in plant tissues due to auxin responsive activation of the DR5 promoter (Ulmasov et al., 1995; Ulmasov et al., 1997; DeMason and Polowick, 2009; Pattison and Catalá, 2012). The DR5 promoter consists of seven direct tandem repeats taken from the AUXIN RESPONSIVE ELEMENT (AuxRE) of soybean *GRETCHEN-HEGEN 3 (GH3)* gene (Ulmasov et al., 1995; Ulmasov et al., 1997; DeMason and Polowick, 2009). These AuxREs are fused upstream of a CaMV 35S minimal promoter region which drives the expression of the reporter gene associated with the construct (Ulmasov et al., 1995; Ulmasov et al., 1997;). β -Glucuronidase (GUS; encoded by the *Escherichia coli urid A* gene) is one of the most common reporters associated with the DR5 promoter (DR5::GUS) for which standardized qualitative and quantitative assays are available (DeMason and Polowick, 2009). One limitation of this system is that the auxin-dependent expressed GUS enzyme need to be react with the externally supplied substrate (a glucuronide) to indicate the auxin responsiveness in the DR5::GUS expressing tissues, and therefore, the detection is dependent on the availability of substrate within the tissue producing the GUS enzyme (Jefferson, 1987). To minimize this issue, and increase the auxin sensitivity of promoter, the DR5rev::fluorescence construct (e.g. green fluorescent protein, GFP and red fluorescent protein, RFP), has been introduced. The DR5rev promoter consists of same AuxRE elements as in DR5 but in higher copy number (nine copies in reverse orientation) which increases the auxin sensitivity of the construct (Ulmasov et al., 1997; Friml et al., 2003)

However, DR5-based promoter systems do not necessarily reflect the auxin maxima present in tissues, as the transcriptional activation of the DR5 promoter depends on down stream signal transduction (Vernoux et al., 2011; Brunoud et al., 2012). The AuxREs of the DR5 promoter are recognized by the endogenous transcriptional activators called AUXIN RESPONSIVE FACTORS (ARFs). As generally described in the review by Wang and Estelle, (2014), at low auxin concentrations, AUXIN/INDOLE-3-ACETIC ACID (AUX/IAAs) block the expression of the downstream reporter gene (GUS or fluorescence) by binding with ARFs. Aux/IAA-ARF multimers recruit other co-repressors TOPLESS (TPL) and TPL-R, and repress

transcription of the target promoter (in this case DR5) through removing acetyls from local chromatin (Wang and Estelle, 2014). Aux/IAAs in these multimers may also block ARFs from effective binding to AuxREs in the DR5 promoter (Wang and Estelle, 2014). In the presence of auxin, the formation of a co-receptor complex between Aux/IAA and TRANSPORT INHIBITOR RESPONSE/AUXIN SIGNALING F-BOX (TIR1/AFB) auxin receptors occurs which results in targeting the Aux/IAA for degradation by the 26S proteasome complex (Wang and Estelle, 2014), thereby releasing the ARFs to activate downstream GUS-gene expression. Therefore, the auxin responsive activation of DR5 may not necessarily be a direct marker of auxin level, but it is a marker of auxin activity (Vernoux et al., 2011; Brunoud et al., 2012; Mir et al., 2017).

1.6.2 AUX/IAA-based auxin sensors

As auxin perception directly initiates Aux/IAA degradation, Aux/IAA degradation-related reporters have been introduced to detect auxin activity in plants (Brunoud et al., 2012). In this auxin reporter system, the reporter gene is fused to the auxin-interaction domain II (DII) of the Aux/IAAs and expressed under the CaMV 35S promoter (Brunoud et al., 2012). The most commonly used reporter gene for the DII construct is the VENUS fast maturing yellow fluorescent protein (YFP). As its signal maturation time is less than the Aux/IAA degradation rate, this system allows the real-time detection of the auxin response (Brunoud et al., 2012). As described earlier, in the presence of auxin, auxin receptors (TIR1/AFBs) and proteasome activity, Aux/IAAs are degraded, and therefore, the disappearance of the marker fluorescence is a reflection auxin availability. Because of this nature (disappearance-dependent detection) of the DII-VENUS system, auxin response should always be confirmed with another control line which expresses a mutated version of the DII gene (mDII-VENUS), where the expression of fluorescence protein is independent of the availability of auxin (Liao et al., 2015).

To minimize the limitations of the DII-VENUS auxin reporter system, recently a ratio-metric R2D2 sensor system was developed (Liao et al., 2015). This system is based on a single construct where the cell division-related RPS5A promoter drives the expression of both the auxin sensitive DII-linked nuclear targeted VENUS protein (DII::n3x-Venus; green) and auxin-resistant mutated DII (mDII)-linked nuclear targeted Tomato protein (mDII::ntdTomato; magenta; Liao et al., 2015). R2D2 measures the auxin response as a ratio between magenta and

green signal (mDII/DII). At low auxin levels, relatively equal amounts of green and magenta signal will accumulate in the cells while at the higher auxin levels auxin-resistant magenta signal will dominate in the cells (Liao et al., 2015).

1.7 Auxin transport during fruit development

Various lines of evidence support that auxin regulates the transition of the static ovary into a rapidly growing fruit (Ozga and Reinecke, 2003; Kumar et al., 2014; Obroucheva, 2014). Data obtained from tomato support that developing fruits act as a source of auxin, and there is a basipetal auxin transport from developing ovaries towards the peduncles to prevent fruit abscission (Serrani et al., 2010; Pattison and Catalá, 2012; Ito and Nakano, 2015). Furthermore, it was observed that there is an auxin gradient from seed to pericarp tissues, as auxin content in developing seeds are higher than that of surrounding fruit tissues in the ovaries of young developing fruit of pea (Magnus et al., 1997; Ozga and Reinecke, 2003) and in tomato (Pattison and Catalá, 2012). This raises the possibility that the seed is the main source of auxins in the ovary during early fruit development, and that auxins are transported to the surrounding fruit tissues to promote the cell division and expansion of the ovary. However, detailed information about auxin transport during the early stages of fruit development is remarkably lack compared to auxin transport in stems and root tissues.

In general, the possibility of involvement of PAT in fruit development was suggested as the phloem transport of auxin is non-directional and less regulated, which makes phloem a less likely a sole route for the transmission of auxins required for making local auxin gradients during growth and development (Petrášek and Friml, 2009; Morris et al., 2010). The ability of auxin transport inhibitors to induce parthenocarpic fruits in species such as *Arabidopsis*, tomato and cucumber (Kim et al., 1992; Dorcey et al., 2009; Serrani et al., 2010) implicated the involvement of PAT in fruit development. With the discovery of the PIN proteins, along with evidence that their auxin transporting function can be blocked by auxin transport inhibitors in vegetative tissues (Geldner et al., 2001), studies to understand the involvement of PIN protein in plant reproductive development were reported in the literature. In 2013, Ceccato et al. observed that *AtPIN1* is involved in female gametophyte development, whereas Sorefan et al. (2009) showed that *AtPIN3* is expressed during fruit development and data suggested that it is important for

regulation of local auxin levels in valve margins of *Arabidopsis* silique. In addition to PINs, the involvement of ABC transporters in fruit development has also been reported. It has been shown that *ABCB1* and *ABCB19* are expressed in developing *Arabidopsis* silique at a relatively high level during the early stages of silique development (Titapiwatanakun and Murphy, 2009).

A detailed study by Pattison and Catalá (2012) regarding PAT inhibitors and expression of the *PIN* and *AUX/LAX* genes during tomato fruit development provided evidence for the involvement of PAT in fruit development. Using the DR5::GUS reporter system to visualize local auxin activity patterns, they found at 9 DPA (days post anthesis), GUS staining was restricted to the funiculus within the ovary, and it became more prevalent by 16 DPA. GUS staining could also be observed in the vasculature of the placenta by 16 DPA, (Pattison and Catalá, 2012). Due to the lower sensitivity of the DR5::GUS reporter system to auxin activity in their studies, they also used the auxin responsive reporter system, DR5rev::mRFP_{er} and observed additional domains of auxin activity during pre-and-post anthesis fruit development. The red fluorescence of RFP reporter was restricted to the micropolar end of the embryo sack at 6 days before anthesis, and it spread to other ovule tissues, so by anthesis pronounced expression in embryo sack and ovule surface could be observed. After ovule fertilization, the red fluorescence could be observed all over the ovules, and by 2 DPA, the red fluorescence signal was strong in both seeds and funiculus tissues. Moreover, the outer layer of the placenta that surrounds the seeds also showing the RFP signal at 6 DPA stage (Pattison and Catalá, 2012). Overall, the pattern of GUS staining and fluorescence accumulation started in a developmental time frame from the seeds then extended to the placenta and pericarp tissues. Moreover, direct IAA quantitation in 21 DPA fruits supported that auxin is transported from the seeds to the surrounding fruit tissues (Pattison and Catalá, 2012). When auxin flow was blocked by supplying NPA containing water (every 2 days for a total of 6 days) to 2-months old plants, NPA caused a dose dependent increase of auxin accumulation in the placenta tissue by 9 DPA (Pattison and Catalá, 2012), pointing out the role of PAT in maintaining auxin flow across the placenta. PAT related genes, *PIN1*, *PIN4*, *PIN8*, and *LAX2* were primarily expressed in placental tissues from fruit set to the onset of ripening (Pattison and Catalá, 2012). This *PIN* and *LAX* gene expression profile suggested a complex but coordinated auxin distribution in the fruit tissues in the rapid period of growth (Pattison and Catalá, 2012).

In pea, studies have shown that auxin levels in young developing pea seeds are higher than that in the surrounding pericarp tissues, which led to the hypothesis that seeds are an auxin source for the developing pea fruits (Magnus et al., 1997). Along with these data, Jayasinghege (2017) observed a gradient (high to low) of IAA from seeds, to the ventral pericarp suture, to the pericarp wall in 8 DAA pea fruit. Furthermore, higher GUS staining was observed in the pea pericarp wall from -2 to 0 DAA, and it gradually declines to minimal intensity by 10 DAA (Jayasinghege, 2017), indicating that auxin activity in the pea ovary decrease over this developmental period. Altogether, these data indicate that seeds are a source of auxins for the surrounding fruit tissues, and that auxin concentration and activity vary in the ovary during early fruit development. However, details regarding the auxin accumulation patterns and mechanism(s) of its transport during pea fruit development are lacking.

1.8 Thesis objectives

The goal of my thesis research was to test the overall working hypothesis that seeds act as a source of auxins for the surrounding fruit and associated tissues (pedicels and peduncles) to coordinate normal seed and fruit development in pea. To test this hypothesis, the following specific objectives were addressed in my research.

Objective 1

To test if developing seeds are a source of auxins in pea fruits, pea (*Pisum sativum* L.) plants expressing DR5 promoter driven β -glucuronidase (*GUS*) reporter gene were used as a tool to assess the GUS localization patterns and GUS enzyme activity within the ovary and attached pedicel and peduncle tissues from seed-bearing fruits and those with the tissues from deseeded fruits.

Objective 2

To test if polar auxin transport is involved in auxin movement between the ovary/seeds and the attachment tissues, an auxin transport inhibitor, NPA, was added to inner pericarp wall

(as a solution) or peduncle (as a lanolin paste) or both inner pericarp wall and peduncle of ovaries, and the relative GUS localization patterns together with GUS enzyme activities were studied in ovary and attachment tissues (pedicels and peduncles) and compared those with respective controls.

2. MATERIALS AND METHODS

2.1 Plant Materials and growth conditions

2.1.1 Plant lines

The DR5::GUS construct in the pRD400 vector (DeMason and Polowick, 2009) was transformed into *Pisum sativum* L. cv. I₃ (Alaska-type) using the EHA105 *Agrobacterium* strain by Dennis M. Reinecke as described in Reinecke et al. (2013) and T3 or T4 plants homozygous for the transgene were used for histochemical and fluorometric analysis of GUS activity. The lines DR5P-R24A [7-3] [P-5] or [P-16] were used for these studies.

All the other experiments were carried out using *Pisum sativum* L. cv. I₃ (Alaska-type) wild-type plants.

2.1.2 Growth conditions

Dry, mature pea seeds were planted at the approximate depth of 2.5 cm in 3-L plastic pots containing a 4:1 (v/v) mixture of Sunshine No #4/ LA4 professional potting mix (Sun Gro Horticulture, Seba Beach, AB) and sand. In each pot, four seeds were planted, and when plants were about 15 cm tall, seedlings were thinned to three per pot. Plants were grown in a growth chamber with a 16 h photoperiod (16/8 h, 19/17°C light/dark) under cool-white fluorescent lights with an average photon flux density of $\sim 350 \mu\text{mol m}^{-2} \text{s}^{-2}$, measured with an LI-188 photometer (Li-Cor Biosciences, Lincoln, Nebraska). A slow-release fertilizer (13-13-13, N-P-K) was added to the potting medium when plants were about 30-50 cm tall. The terminal apical meristem remained intact throughout plant development and expanding lateral shoots were removed as they developed.

2.2 Plant treatments

2.2.1 Intact and split pericarp treatments

Two days after anthesis (2 DAA) pollinated ovaries (pericarps; 15-20 mm in length) on the 2nd to 5th flowering nodes of the main stems were either left intact (intact treatment), or split

down the dorsal suture and seeds were either left intact (split pericarp; SP treatment) or removed (split pericarp no seed; SPNS treatment) as described by Ozga et al. (1992). Surgically manipulated ovaries were covered with plastic bags to maintain high humidity, and the pericarps remained attached to the plant throughout the experiment until they were harvested. To determine the timing of tissue collection for GUS staining, the pericarps along with pedicels of SP and SPNS ovaries were harvested onto ice 24, 48 and 72 h after splitting or splitting and deseeding of the pericarps. Four to five biological replicates of each tissue were assessed at each time interval.

To determine the effect of seeds on GUS localization patterns and GUS enzyme activities in the developing pea fruit and associated tissues, of intact, SP and SPNS ovaries with their associated pedicels and peduncles were harvested onto ice 48 h after splitting or splitting and deseeding of the pericarps (the 48 h period was determined by the above experiment). Five to six biological replicates of each tissue type were assessed for each treatment type per experiment and the entire experiment was repeated twice over time.

2.2.2 NPA treatments

To determine the effect of altered polar auxin transport on GUS localization patterns and GUS enzyme activities in pea fruit and associated tissues, the polar auxin transport inhibitor NPA was applied to the peduncle of intact, SP and SPNS pericarps, or the pericarps of SP and SPNS ovaries, or simultaneously to both the peduncles and pericarps of SP and SPNS pericarps. For the pericarp treatment, the inner wall of SP and SPNS pericarps was treated with 30 μ L of NPA (10 μ M in 0.1% aqueous Tween 80), 12 h after splitting or splitting and deseeding of the pericarps. Thirty microliters of 0.1% aqueous Tween 80 solution was used for the pericarp control treatment. For the peduncle treatment, NPA in lanolin paste (approximately 25 μ L of 1.5 mg NPA per gram lanolin) or lanolin paste only (25 μ L) was placed on an aluminium foil strip (10 X 5 mm; Fig. 2.1 A). The aluminum foil strips were placed around the peduncle circumference, 20 mm away from the pedicel-peduncle junction (Fig. 2.1 B). The pericarps along with their associated pedicels and peduncles were harvested onto ice 48 h after NPA treatment. Five to six biological replicates per treatment were assessed per experiment. The entire experiment was repeated four times to assess the consistency of the DR5::GUS localization patterns.

To determine the effect of altered auxin transport on fruit-set in pea, one fruit per plant from the 2nd to the 5th flowering node was used, and all other flower buds and lateral shoots were removed as they emerged. Flowers were either emasculated at -2 DAA or allowed to self-pollinate. Pedicels (at the middle) or peduncles (20 mm away from the pedicle-peduncle junction) of emasculated or pollinated ovaries were treated with NPA in lanolin paste (approximately 25 μ L of 1.5 mg per gram lanolin), or lanolin paste only (control). All pericarps were covered with plastic bags after treatments for the duration of the experiment. Pericarp length and width, and the length and diameter of pedicels and peduncles were recorded daily from 0 to 5 DAA. Fruits were harvested at 5 DAA, seed number, and fresh weight of seeds, pericarp, and pedicels were recorded. Eight replicates per treatment type were assessed.

To study the effect of NPA on pea fruit growth, 2 DAA fruits from the 2nd to the 5th flowering nodes were split along the dorsal suture and seeds were either left intact (SP) or removed (SPNS). Twelve hours after splitting or splitting and deseeding, 30 μ L of NPA (10 μ M in 0.1% Tween 80) or 0.1% Tween 80 was applied to the inner pericarp wall of the fruit. Subsequently, 0.1% Tween 80 was applied to the inner pericarp wall of all split fruits approximately 24, 48, 72, and 96 h after the first solution application (30 μ L, 40 μ L, 40 μ L, and 40 μ L, respectively). Pericarps along with the pedicels were harvested two days after the final solution application (9 DAA). The pericarp length and width, pedicel and peduncle length and diameter were measured daily, and the pericarp and pedicel fresh weights were measured at harvesting. In the SPNS treatments, fruit abscission was also recorded. Eight individual pericarps were assessed for each treatment.

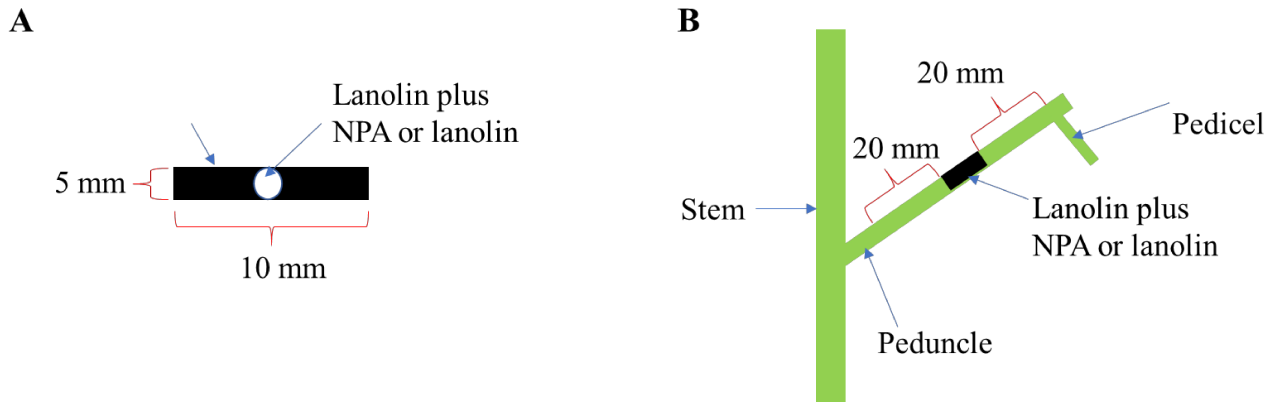


Figure 2.1: Illustration of lanolin or lanolin plus NPA application to the peduncle tissue. Preparation of aluminum foil (Al) strips containing 25 μ L of NPA in lanolin or lanolin only (A), and its application to the peduncle (B).

2.2.3 5(6)-Carboxyfluorescein diacetate (CFDA) treatments

Four to six days after anthesis fruits from the 2nd to the 5th flowering nodes of pea (*Pisum sativum* L. cv. I₃ (Alaska-type)) plants were used for this experiment. Pedicels were abraded mid-length using a fine sand paper either proximal to the pericarp ventral suture (Fig. 2.2 A) or proximal to the pericarp dorsal suture (Fig. 2.2 B), and 1 μ L of 5 (6)- carboxyfluorescein diacetate (CFDA dissolved in dimethyl sulfoxide; 5 mM) was applied to the abraded surface. Following application of CFDA, pericarps including the pedicels were covered with plastic bags to minimize solution evaporation. Pericarps together with the pedicels were collected onto ice, 2 or 3 hr after CFDA application to the pedicel area proximal to the pericarp ventral suture and 2 or 4 hr after CFDA application to the pedicel area proximal to the pericarp dorsal suture.

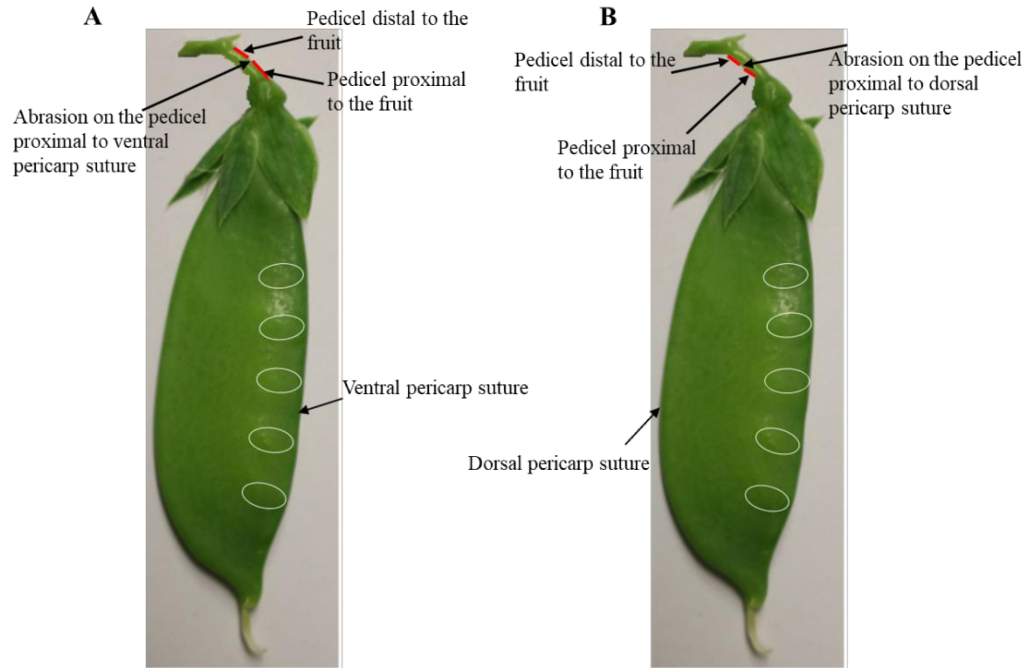


Figure 2.2. The application of 5 (6)- carboxyfluorescein diacetate (CFDA) to the pedicel. Pedicels were abraded either proximal to pericarp ventral suture (**A**) or proximal to pericarp dorsal suture (**B**), and 1 μ L of CFDA was applied to the abraded pedicel surface.

2.3 Histochemical analysis of GUS activity

2.3.1 Tissue dissection for GUS staining

Freshly harvested tissues were kept on ice until dissection for GUS staining. The ovaries were separated from the pedicel/peduncle tissue. Thin fresh-tissue cross-sections were hand-cut using a razor blade. Pericarps without seeds (SPNS) or pericarps with seeds (intact and SP) and pedicels were initially cut into two halves (length-wise), and from each half, two cross-sections were taken adjacent to the initial cut (Fig. 2.3 A and B). When the pericarp contained seeds (Intact and SP), cross-sections were taken to include the seed with the attached funiculus. When lanolin paste or lanolin paste plus NPA were applied to the peduncle, peduncle dissection occurred as follows. First, the section containing the lanolin paste was removed. Secondly, 20 mm peduncle sections above (referred to as the proximal peduncle section, Fig 2.3 C) and below the lanolin paste application site (referred to as the distal peduncle section, Fig. 2.3 C) were

excised and used for cross sectioning; tissue section was cut into two halves, and two cross-sections were taken near to the initial cut of each peduncle half (Fig 2.3 D). Proximal peduncle sections were dissected first followed by the distal peduncle sections.

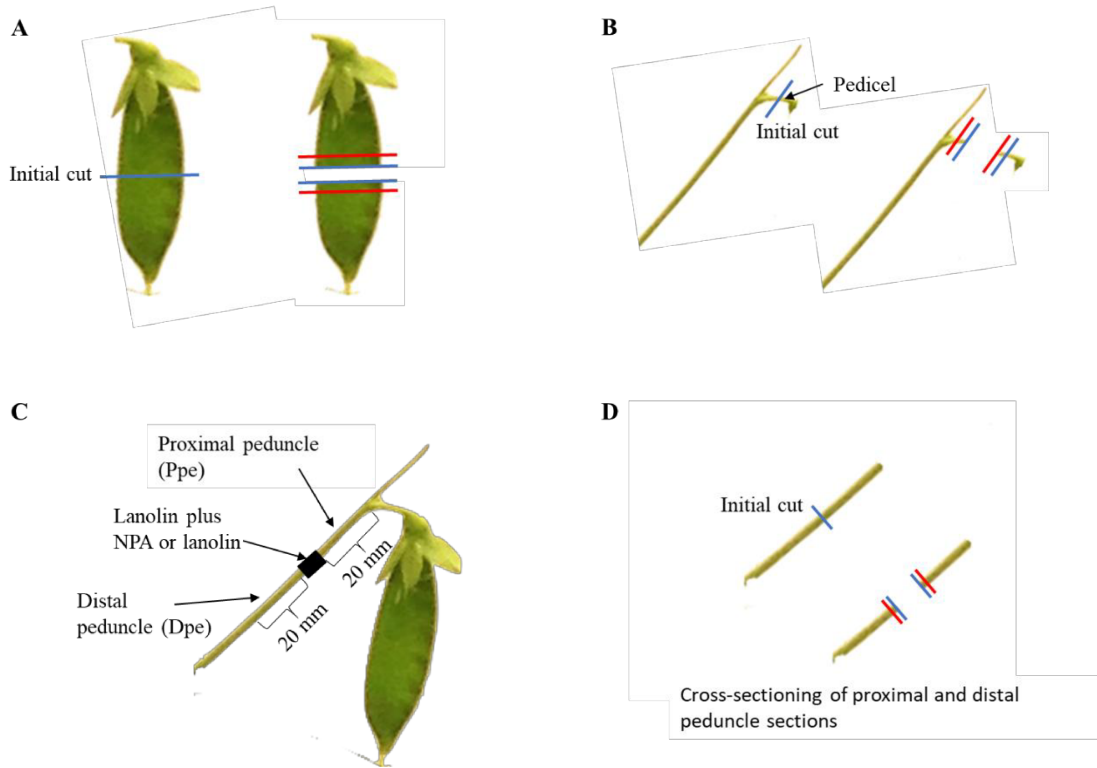


Figure 2.3. A diagram of the fresh-tissue cross-sectioning for GUS staining. Tissue cross-sections were taken from the mid-length region of the ovaries (pericarp with seeds or without seeds) (A) and pedicels (B). The peduncles were partitioned into two regions, proximal to the fruit (Ppe) and distal to the fruit (Dpe), lanolin or lanolin plus NPA was applied to the peduncle between the two regions as marked with a black box (C). Tissues were collected from the mid-region of these two peduncle types (D). The initial cut position is indicated with blue lines and the area where cross-sections were taken noted in red.

2.3.2 GUS histological staining

Tissue cross-sections were placed in 24-well (for pericarp tissues) or 96-well (for pedicels and peduncle tissues) flat-bottom cell culture plates containing GUS staining solution [1

mM 5-bromo-4-chloro-3-indolyl β -D-glucuronide (X-Gluc), 100 mM sodium-phosphate buffer (pH 7), 0.5 mM potassium ferrocyanide, 0.5 mM potassium ferricyanide, 0.1% Triton X100 and 10 mM EDTA (Hull and Devic, 1995)]. Tissues were vacuum-infiltrated for 15 min (to ensure the submergence of the tissues in the buffer), then incubated in dark at 37°C overnight. Tissues were then washed three times with 70% aqueous ethanol (v/v) to remove chlorophylls before micrographs were taken using Olympus SZ61 stereo microscope (Olympus Corporation, Tokyo, Japan) fitted with a digital camera (MDC320; LeadzOptics Ltd, Middlesex, UK) controlled by ScopePhoto 3.0 (Scope Technology Inc, CT, USA) application software. A stage micrometer was used for sizing the micrograph images. A Leica DMRXA microscope (Leica, Germany) with Nomarski configuration fitted with a Qlclick digital camera (QImaging, BC, Canada) controlled by Q-Capture Pro 7 (version 7.0; QImaging, Media Cybernetics. Inc, Maryland, USA) software was used to obtain further cellular details of the fresh tissue cross-sections. Micrographs were also taken with Leica DMRXA microscope (Leica, Germany) under green fluorescent filter mounted with a Qlclick digital camera (QImaging, BC, Canada) controlled by Q-Capture Pro 7 (version 7.0; QImaging, Media Cybernetics. Inc, Maryland, USA) software to further identify the cells using the autofluorescence of lignin in xylem and phloem tissues.

2.4 Fluorometric quantification of GUS enzyme activity.

2.4.1 Tissue dissection for GUS enzyme activity assays

For fluorometric quantification of GUS enzyme activity, 2 DAA pericarps, pedicels, and peduncles were treated as described in section 2.2.1 and 2.2.2. At harvest, the inflorescence was collected onto ice and dissected into the following tissues as shown in Fig. 2.4: pericarp ventral suture (Pvs), the central pericarp wall (Cpw; ~3-4 mm wide section) the pedicel (Pl; entire tissues) and 20 mm long sections of the proximal (Ppe) and distal (Dpe) peduncle. For the intact and SP treatments, the seeds along with the funiculus (Sf) were also collected. After dissection, the tissues were immediately frozen in liquid nitrogen and stored at -80°C until the quantification of GUS enzyme activity.

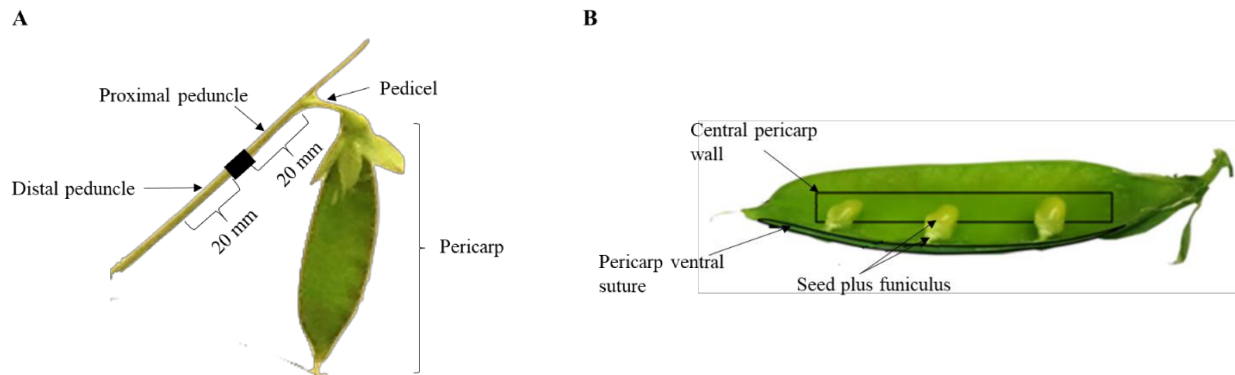


Figure 2.4. A diagram of tissue collected for determining GUS enzyme activity in *DR5::GUS* lines. A 20 mm section of the peduncle above (proximal section) and below (distal section) the lanolin application site, and the entire pedicel were harvested (A). Ovaries were dissected into the central pericarp wall, pericarp ventral suture, and seed plus funiculus tissues (for intact and SP fruits) (B).

2.4.2 Quantification of GUS enzyme activity

GUS enzyme activity was determined using the 4-methylumbelliferyl glucuronide (MUG) assay as described by Jefferson, 1987, with minor modifications. Tissues from six inflorescences were pooled as one biological replicate. Frozen tissues (approximately 150-200 mg fresh weight per biological replicate; 4 biological replicates per treatment) from the pericarp ventral vascular suture (Pvs), the central pericarp wall (Cpw; ~3-4 mm wide section), the pedicel (Pl; entire tissue), seed plus funiculus (Sf), and 20 mm long sections of the proximal (Ppe) and distal peduncle (Dpe) were hand-ground using mortar and pestle. For each ground tissue sample, 200 μ L of GUS extraction buffer [50 mM NaPO₄ (pH 7.0), 10 mM Na₂EDTA, 0.1% sodium lauroyl sarcosinate, 0.1% Triton X-100, 10 mM β -mercaptoethanol] was added and vortex for ~1 min. Then samples were spun down at 14,800 rpm at 4^oC for 10-15 min. The supernatant (protein extract) was aliquoted into new tubes and stored at -80^oC until the next step.

To perform the assay, 20 μ L aliquot of the protein extract was mixed with 200 μ L pre-warmed (37^oC) assay buffer (22 mg MUG in 50 mL GUS extraction buffer) in amber-color microcentrifuge tubes, the mixture was vortexed, immediately, and then incubated at 37^oC in a shaking water bath, for 8, 16 and 24 min time intervals. To stop the reactions at the defined time

points, 60 μL of the reaction mix was mixed with 540 μL stop buffer (0.2 M Na_2CO_3 ; in an amber-color microcentrifuge tubes) at room temperature. The production of fluorescence from 4-methylumbelliferone (4-MU) at the defined time intervals was analyzed using the following fluorometric procedure. Each sample was aliquoted in triplicated into microtiter plate wells (190 μL per well; Costar, black, flat-bottom 96-well plates; Corning Incorporated, NY, USA) and fluorescence was measured using SpectraMax M3 Multi-Mode Microplate Reader (Molecular Devices, CA, USA) at 365 nm, 455 nm and 435nm, excitation, emission, and cut-off bandwidths, respectively. A 7-point dilution series of 4-MU (Biosynth) standard with concentrations ranging from 4000 nM to 62.5 nM was run in each plate to construct the calibration curve. An assay/stop buffer solution (1:9, v/v) was used as a blank. Each sample was analyzed twice, and the average was taken for the calculations.

To normalize GUS enzyme activity to sample total protein content, the total protein concentration of each sample was determined using a Bio-Rad Protein Assay kit (Bio-Rad Laboratories, CA, USA) according to the Bradford (1976) method. Briefly, 2 μL of the original sample protein extract was diluted 50-fold by mixing with 98 μL of milliQ water. A 10 μL aliquot of diluted protein extract was added to 200 μL diluted Bradford dye reagent (dye solution: milliQ water; 1:4, v/v) in the microtiter plate well (Costar 96-well clear, flat-bottom plates; Corning Incorporated, NY, USA). The plate was kept at room temperature for 10 min allowing the reaction to occur before the absorbance was measured using SpectraMax M3 Multi-Mode Microplate Reader (Molecular Devices, CA, USA) at 595 nm. A 4-point dilution series using Bovine Serum Albumin (Bio-Rad) ranging from 0.07 to 0.53 mg/mL was used to construct the calibration curve. MilliQ water was used as a blank. Six technical replicates for each sample were analyzed. Normalized GUS enzyme activity was expressed as nM of MUG per minute per milligram of total protein. Means \pm standard error (SE) of four replicates were calculated. GUS enzyme activity was also monitored in ventral pericarp suture, central pericarp wall, seed plus funiculus (in intact and SP), pedicel, proximal and distal peduncle tissues (2 biological replications per tissue) of non-transgenic pea plants (WT), and no GUS enzyme activity was detected in any of these samples.

2.5 Histochemical analysis of 5 (6)- carboxyfluorescein diacetate movement to identify phloem transport dynamics between the pedicel and the pericarp

Pedicels were abraded and treated with CFDA as described in section 2.2.3 and the pericarps along with the pedicels were collected onto ice as described above at desired time intervals. Fresh tissue cross-sections were taken from the pedicel in regions distal and proximal to the attachment of the pedicel to the fruit (Fig. 2.2), and the ovary in the region proximal to the ovary-pedicel attachment. Fresh tissue sections were immediately placed onto a glass microscope slide, immersed in glycerol and covered with a cover slide. Micrographs were taken using Zeiss AXIO imager-M1 (Carl Zeiss MicroImaging GmbH, Jena, Germany) mounted with a digital camera (Axiocam 506 mono, Carl Zeiss Microscopy GmbH, Jena, Germany) controlled by ZENpro application software (Carl Zeiss Microscopy GmbH, Jena, Germany).

2.6 Statistical analyses

To determine the effect of NPA treatment to the pericarp, peduncle, or simultaneously to the pericarp and peduncle on GUS enzyme activity in ovary, seed, and attachment tissues, a two-way analysis of variance (ANOVA) with treatment being one factor and tissues as another factor was carried out using the PROC MIXED procedure of SAS 9.4 software (SAS Institute Inc. Cary, NC, USA, 2014; the significance of treatment, tissue, and treatment-by-tissue interaction effects were taken into account). Differences between treatment and control at individual tissues were tested using the Least Square Means (LSMEANS) statement (LSD test) with the DIFF option in the SAS PROC MIXED analysis, with significance declared at $P \leq 0.05$.

To determine the effect of pericarp surgical treatments (splitting and splitting and deseeding), and the effect of NPA treatment to the pericarp, peduncle, or simultaneously to the pericarp and peduncle, on pericarp and seed growth parameters, a one-way ANOVA was carried out using the PROC MIXED procedure of SAS 9.4 to test for the significance of treatment effects. Differences between treatments were tested using the LSMEANS statement (LSD test) with the DIFF option in the PROC MIXED analysis, with significance declared at $P \leq 0.05$. Unequal residual variances among different treatments were allowed by specifying the REPEATED statement with the GROUP= option.

For all other experiments, pair-wise mean comparisons were completed using a two-tailed Student's T-test assuming unequal variance (Microsoft Office Excel, 2016, using the Analysis ToolPak). Statistical significance was declared at $P \leq 0.05$ for comparisons between the means.

3. RESULTS

3.1 Pea inflorescence morphology and pedicel and peduncle anatomy

The pea fruit is attached to the floral stem (the peduncle) of the plant through the pedicel. The peduncle is attached to the main stem of the plant (Fig. 3.1 A). In the pea inflorescence at 4 DAA, both the pedicel and peduncle, consist of an outermost epidermal layer, subtended by a few layers of cortical parenchyma cells (cortex), then vascular bundles arranged in distinct rings, with xylem oriented towards the inside and phloem oriented towards the outside of each bundle (Fig 3.1 B and C). The center of both tissue types (the pith) is made up of parenchyma cells (Fig 3.1 B and C). In both 4 DAA pedicels and peduncles, smaller-sized vascular bundles are oriented in the area which is proximal to the pericarp ventral suture, and larger vascular bundles are oriented in the area which is proximal to the pericarp dorsal suture (Fig. 3.1B and C).

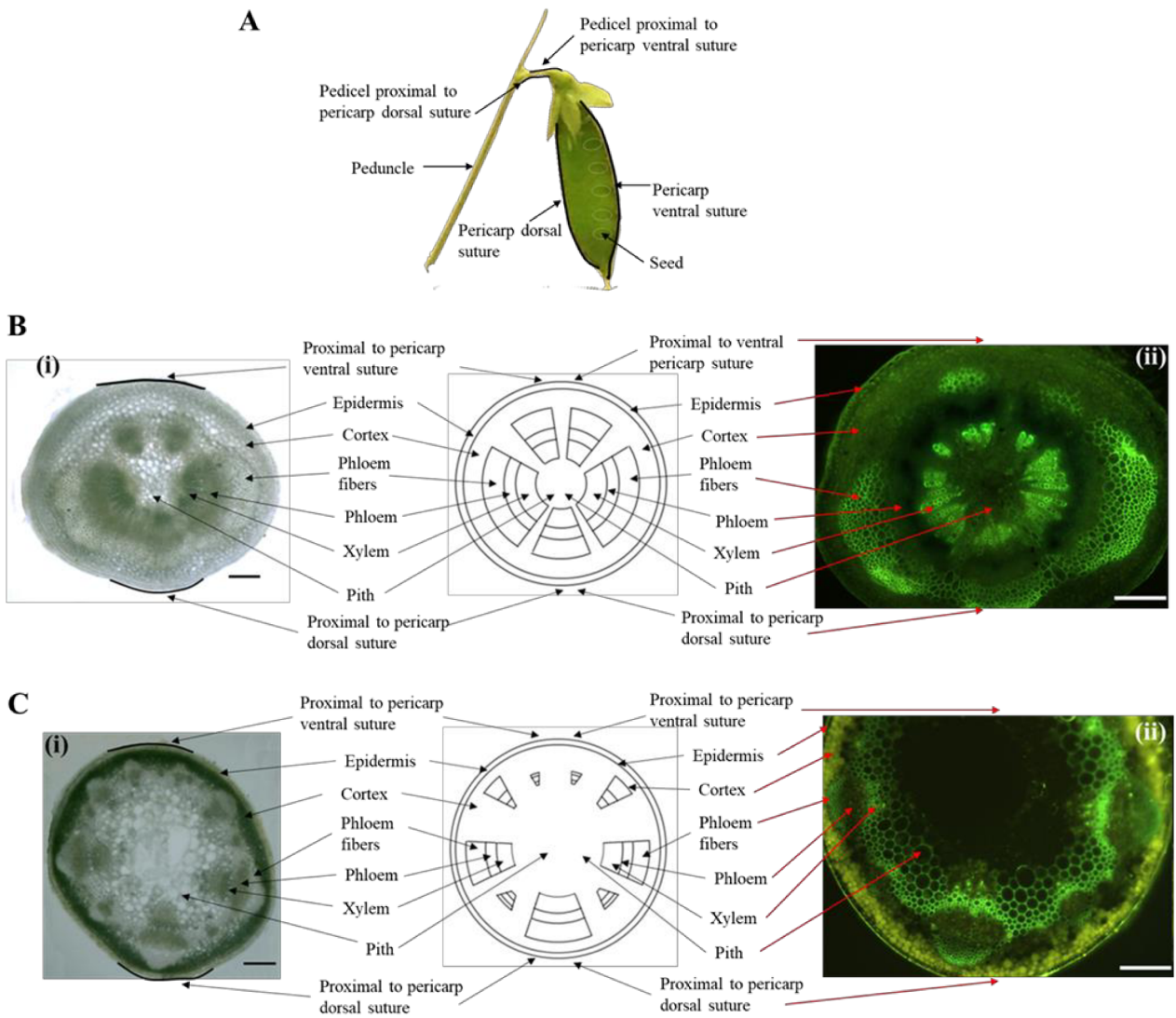


Figure 3.1. Illustrations of the inflorescence, and pedicel and peduncle cross-sectional anatomy of pea (*Pisum sativum* L.). In pea, the fruit is attached to the floral stem (the peduncle) of the plant through the pedicel (A). A representative pedicel (B) and peduncle (C) cross-section from mid-tissue length (attached to a 4 DAA fruit) taken using a light microscope [B (i) and C (i); magnification 4.0X] or a fluorescence microscope under a green fluorescence filter [B (ii) and C (ii); magnification 10X]. B (i) and C (i) scale bar = 200 μm ; B (ii) and C (ii) scale bar = 2000 μm .

3.2 Morphology of the vasculature in the pea ovary

The vascular bundles from the pedicel is converged forming a cylinder as they enter the pericarp. Within the first few millimeters of entering the pericarp, the vascular bundles start to diverge forming distinct ventral and dorsal sutures (Fig. 3.2 A). The pericarp ventral suture vasculature is connected to the developing seeds via the funiculus, and also it is directly connected to the pericarp wall vasculature (Fig. 3.2 B). The dorsal suture is directly connected to the pericarp wall vasculature (Fig 3.2 B). At the tip of the ovary (stigma/style end), the ventral end of the pericarp wraps across the tip, and ventral suture vasculature connects to the style tissue vasculature; the dorsal suture vasculature ends at the tip of the pericarp (Fig.3.2 C).

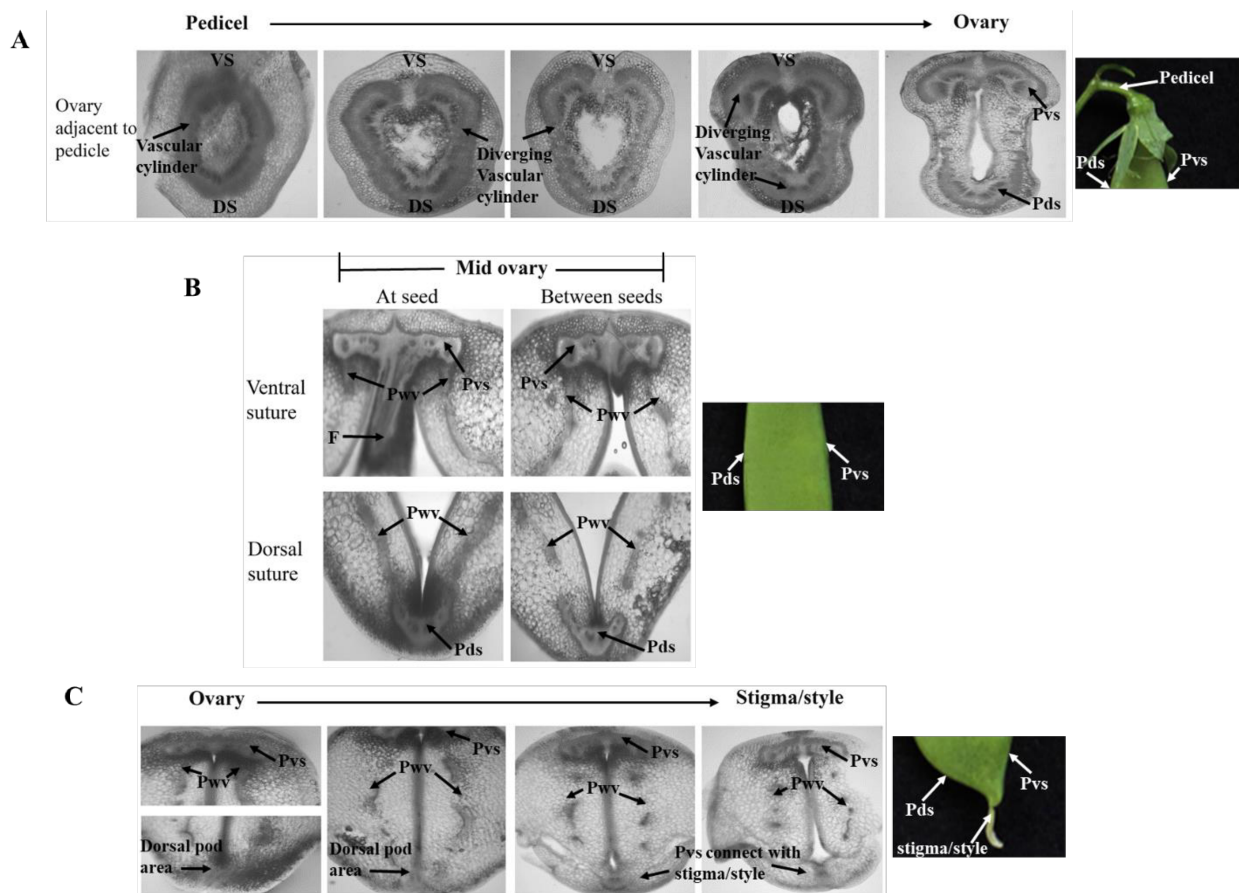


Figure 3.2. Representative micrographs showing the vascular arrangement in the pericarps of ~ approximately 20 DAA ovaries of *Pisum sativum* (Sugar snap pea). Vascular tissue arrangement in the pericarp within 3 mm of pedicel attachment (A), at mid ovary (B), and within 3 mm of the

stigma/style remnant tissue (C). DS, dorsal side; F, funiculus; Pds, pericarp dorsal suture; Pvs, Pericarp ventral suture; Pwv, pericarp wall vasculature; VS, ventral side. Scale bar =100 μ m.

3.3 Vascular transport pathway from the pedicel to the fruit tissues as visualized using 5 (6)- carboxyfluorescein diacetate (CFDA) staining

The phloem mobile dye, 5 (6)- carboxyfluorescein diacetate (CFDA) was applied to the pedicels in the area proximal to the pericarp ventral or dorsal suture to monitor the flow of assimilate in vascular tissues from the pedicel into the fruit. Two hours after CFDA was applied to the abraded surface of the pedicel proximal to the pericarp ventral suture, intense CFDA green fluorescence was observed in the adjacent vascular bundles of the pedicel section proximal to the fruit with less intense CFDA green fluorescence observed in the vascular bundles of the pedicel section distal to the fruit (see the circled area in the proximal and distal pedicels; Fig 3.3 A). In the pericarp, CFDA green fluorescence was also observed in the vasculature of the ventral suture (near the attachment of the pedicel to the pericarp) 2 hours after application to the pedicel proximal to the pericarp ventral suture (Fig 3.3 A). Three hours after application to the pedicel proximal to the pericarp ventral suture, a similar but more intense CFDA green fluorescence was observed in the vasculature of the pedicels and pericarp ventral suture vasculature, and additionally, CFDA green fluorescence was also observed in the pericarp wall and dorsal suture vasculature (Fig 3.3 C). These data suggest CFDA transport from the pedicel vascular bundles adjacent to the pericarp ventral suture to the pericarp ventral suture, into the developing seeds that are connected to this vasculature via the funiculus. CFDA also moves from the pericarp ventral vascular suture into the vasculature of the pericarp wall and then into the dorsal suture vasculature (Fig.3.3 F, red arrows). When CFDA was applied to the abraded surface of the pedicel proximal to the pericarp dorsal suture, a less intense CFDA green fluorescence was observed in the adjacent pedicel vasculature 2 h after application (Fig. 3.3 B, marked by a red circle), but no CFDA green fluorescence was observed in the pericarp vasculature (Fig. 3.3 B). A preliminary experiment suggests that CFDA green fluorescence can also be detected in the pericarp dorsal suture vasculature 4 hr after application to the pedicel proximal to the pericarp dorsal suture (Appendix Fig. A1), but further experimentation is required to verify this result.

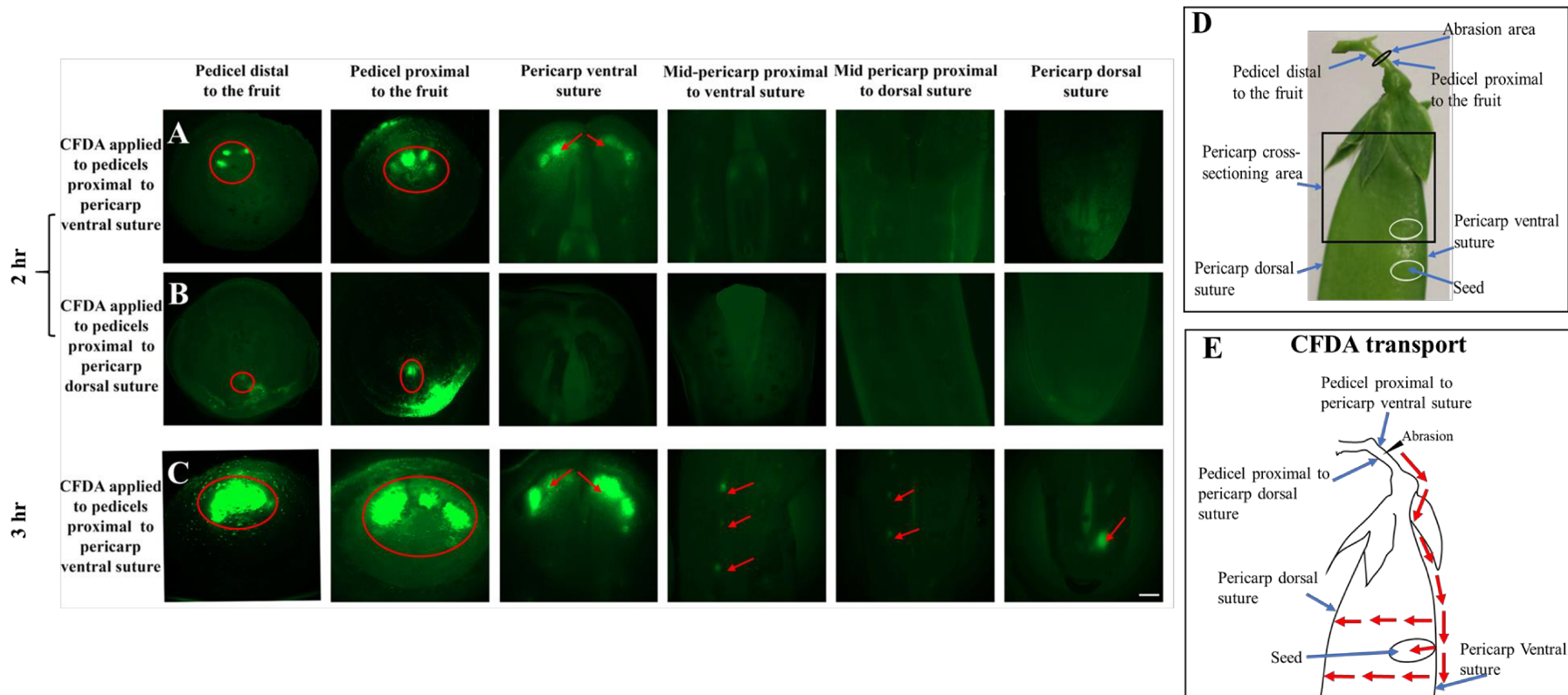


Figure 3.3. Representative micrographs of 5 (6)-carboxyfluorescein diacetate (CFDA) fluorescence (green color) patterns in the pedicels and pericarps of 4-6 DAA pea inflorescences. CFDA green fluorescence observed in the pericarp and pedicel tissues 2 hr after the application of CFDA to the pedicles proximal to the pericarp ventral suture (A) and pericarp dorsal suture (B). CFDA green fluorescence observed in the pericarp and pedicel tissues 3 hr after the application of CFDA to the pedicles proximal to the pericarp ventral suture (C) and 4 hr after the application of CFDA to the pedicles proximal to the pericarp dorsal suture (D). A diagram illustrating the abrasional area in the pedicel and pericarp cross-sectioning area (E). Schematic diagram showing the possible vascular connections between pedicel and the pericarp (F). The vascular bundles in the pedicels proximal to the pericarp ventral suture are attached with the vasculature of pericarp ventral suture (red arrows). Red circles and arrows indicate the green fluorescence observed in the pedicels and pericarp, respectively. Seeds are circled in white. Scale bar = 200 μ m.

3.4 DR5::GUS staining patterns in intact pea fruit and associated attachment tissues

Localization of auxin activity within pea fruit and associated attachment tissues was assessed using pea plants that express a GUS marker gene driven by an auxin-responsive DR5 promoter. In the pericarps of intact pollinated young pea ovaries of DR5::GUS plants at 4 DAA, GUS staining (blue color) was mainly observed in the vascular tissues of the pericarp wall (Pwv), and the ventral (Pvs) and dorsal sutures (Pds; Fig. 3.4 A, A' and B). Intense GUS staining was also observed in the funiculus, and the seed coat tissue adjacent to the seed-funiculus attachment (Fig. 3.4 B). In pedicels attached to 4 DAA pollinated fruits, GUS staining was most intense in the cambium/primary phloem region (C/PP; Fig. 3.4 C and D) of the vascular bundles, with some GUS staining also visible in the cortical cells, mainly proximal to the pericarp dorsal suture attachment (red arrowhead; Fig. 3.4 C and D). This pedicel cortical cell staining pattern was consistent across experiments, although the GUS staining intensities varied between individual pedicels sampled (Appendix A Fig. A2). In peduncle tissue, GUS staining was localized mainly in the cambium/primary phloem region of the vascular bundles (C/PP; Fig. 3.4 E-G). The blue GUS staining of tissues was only observed in tissues of DR5::GUS plants when compared to non-transformed plants of the same cultivar (see micrographs of control non-transformed pea plants, Appendix Fig. A3).

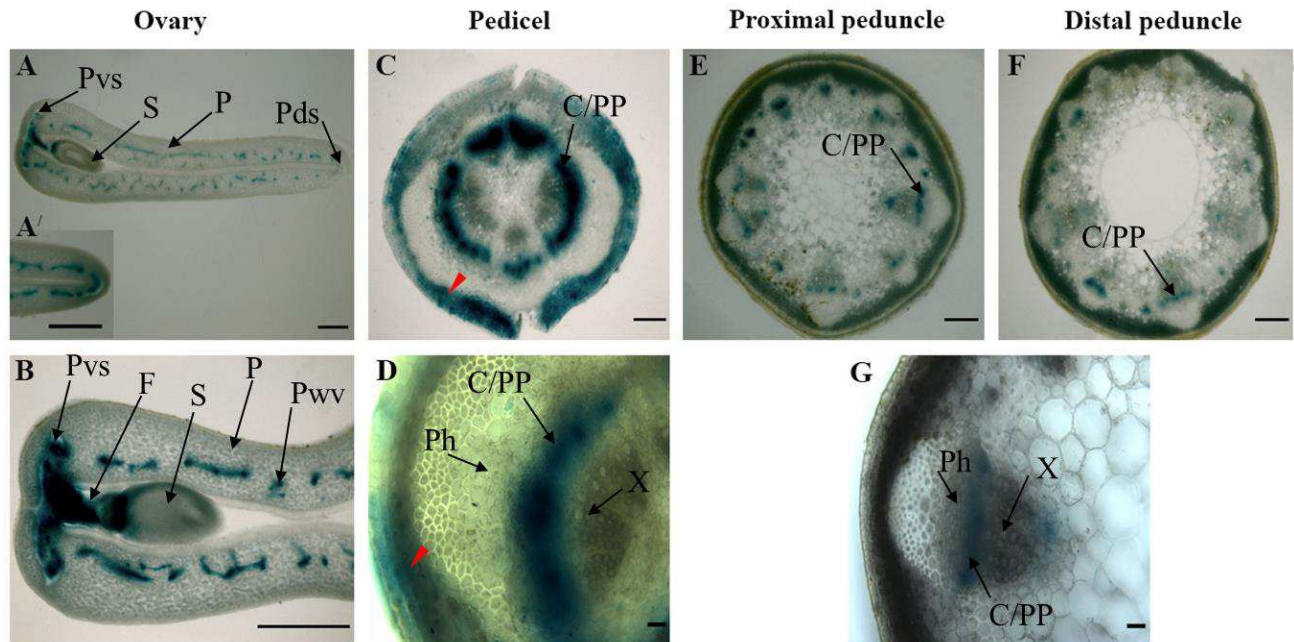


Figure 3.4. Representative micrographs of the GUS staining patterns observed in cross-sections of intact ovaries (pericarp + seeds) of 4 DAA fruits and the attached pedicel, proximal and distal peduncle tissues from DR5::GUS expressing pea plants. GUS staining was mainly observed in the vascular tissues of ovaries (**A**, **A'** and **B**) and the cambium/primary phloem region of attached pedicels (**C** and **D**) and peduncle tissues (**E-G**). In pedicels, GUS staining was also observed in some cortex cells mainly proximal to the pericarp dorsal suture attachment (red arrowhead; **C** and **D**). C/PP, cambium/primary phloem; F, funiculus; P, pericarp; Pds, pericarp dorsal suture; Pvs, pericarp ventral suture; Pwv, pericarp wall vasculature; Ph, phloem; S, seed; X, xylem. A and B scale bar = 1000 μ m; C-G scale bar = 200 μ m.

3.5 DR5::GUS staining patterns in pedicels attach to pollinated or nonpollinated ovaries

In -2 DAA pedicels (prior to ovary pollination), intense GUS staining was observed in the cortical tissue proximal to ventral pericarp suture attachment (Fig. 3.5). By 2 DAA, the ratio of cortical to vascular tissue in the pedicel decreased, and cortical tissue staining for GUS activity was localized proximal to dorsal pericarp suture attachment in pedicels attached to both pollinated and non-pollinated ovaries (Fig. 3.5). GUS staining intensity was higher in the

pedicels attached to pollinated ovaries at 2 and 3 DAA compared to that from nonpollinated ovaries (Fig. 3.5).

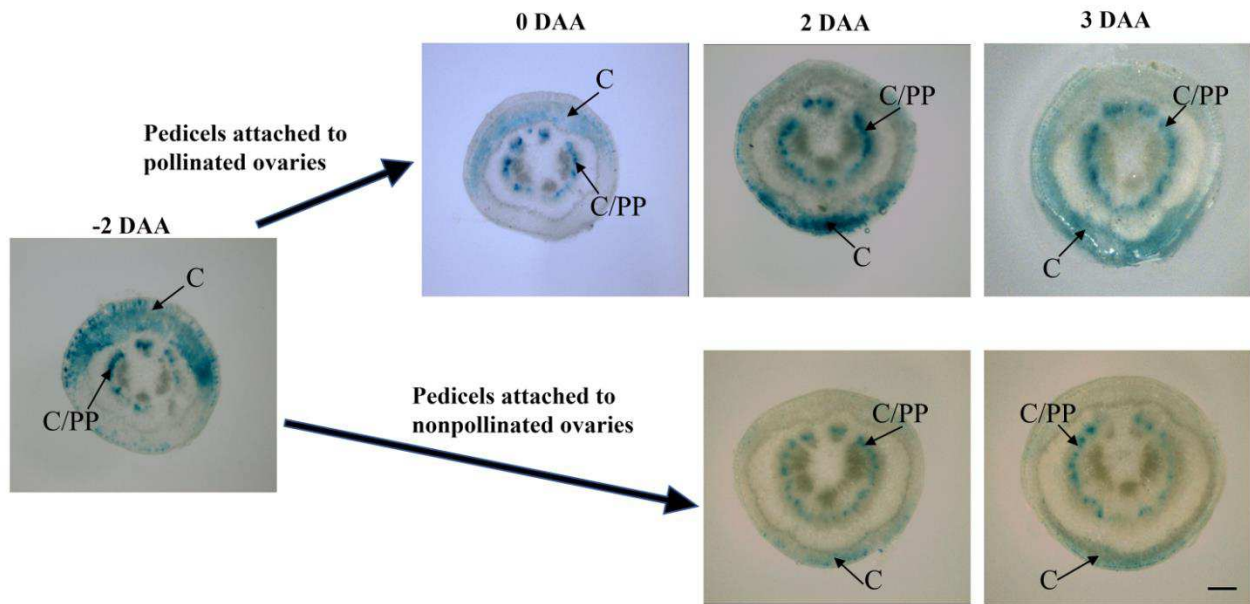


Figure 3.5. Representative micrographs of the cross-section of pedicels attached to pollinated and nonpollinated ovaries at -2, 0, 2, and 3 DAA from DR5::GUS expressing pea plants. Ovaries were either emasculated at -2 DAA (nonpollinated) or allow to pollinate, and pedicel fresh-tissue cross-sections were taken mid-tissue length and processed for GUS staining. C, cortical cells staining for GUS activity; C/PP, cambial/primary phloem tissue. Scale bar = 200 μ m.

3.6 GUS staining and enzyme activity in pea fruit and associate attachment tissues in response to pericarp splitting and seed removal

To test if the seeds are a source of auxin for the developing pea fruit, auxin-responsive DR5 promotor driven GUS staining localization was assessed in the pericarp and associated attachment tissues in the presence and absence of developing seeds using the pea split pericarp assay system (Ozga et al., 1992) in DR5::GUS expressing pea plants. In this assay, 2 DAA pollinated ovaries were split down the dorsal pericarp suture (Fig. 3.6 A) to access the seeds. Seeds were either not disturbed (remained attached to the ventral suture via the funiculus; Fig. 3.6 A; SP treatment), or they were removed (SPNS treatment) from the pericarp. Although

splitting of the pericarp along the dorsal suture did not change the GUS staining pattern in the pericarp or attached pedicel and peduncle cross-sections (Appendix Fig.A4) GUS enzyme activity was higher in the pedicel and peduncle tissues attached to SP fruits compared to that attached to intact fruits (Fig. 3.6 B and C).

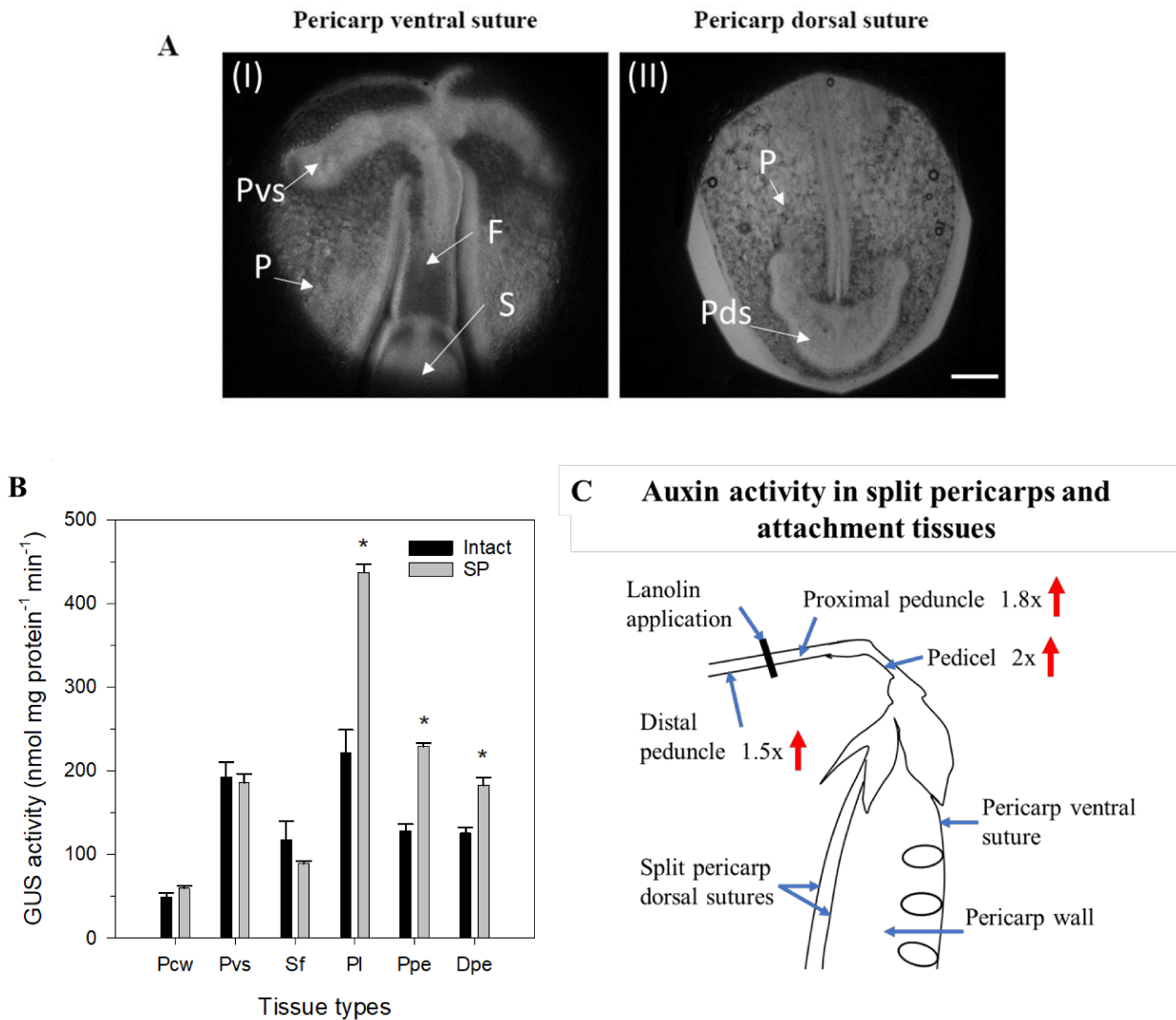


Figure 3.6. The effect of pericarp splitting on the GUS enzyme activity in fruit and attachment tissues of DR5::GUS expressing pea plants. Micrographs showing the tissue arrangement in the intact ovary focusing on the seed attachment to the pericarp ventral suture via funiculus [A (I)] and the pericarp dorsal suture [A (II)]. F, funiculus; P, pericarp; Pds, pericarp dorsal suture; Pvs, pericarp ventral suture; S, seed. Scale bar = 200 μ m. Fruits (2 DAA) were left intact or were split

down the dorsal suture (SP) and GUS enzyme activity assessed at 4 DAA in the central pericarp wall (Cpw), pericarp ventral suture (Pvs), seed plus funiculus (Sf), pedicel (Pl), and peduncle [proximal (Ppe) and distal (Dpe)] tissues from or attached to intact or SP fruits (**B**). Data are means \pm SE (n=4 biological replicates, each biological replicate is composed of tissues from six fruits). Asterisks denote significantly different treatment means within tissues at $P < 0.05$. Illustration showing the effect of splitting on the GUS enzyme activity in pericarp and attachment tissues (**C**).

Seed removal from the ovary (SPNS treatment) at 2 DAA did not affect the GUS staining patterns observed in the pericarp, pedicel or, peduncle tissues at 4 DAA; however, GUS staining intensities were lower in all tissue types when compared to pericarps with seeds (SP; Fig. 3.7A and B). Consistent with the observed GUS staining intensities, seed removal decreased GUS enzyme activity 2-fold in the ovary (pericarp ventral suture and central wall), pedicel, and proximal peduncle tissues. In distal peduncle tissues, GUS enzyme activity was reduced approximately 4-fold in SPNS pericarps compared to seed-bearing pericarps (SP; Fig. 3.7C and D).

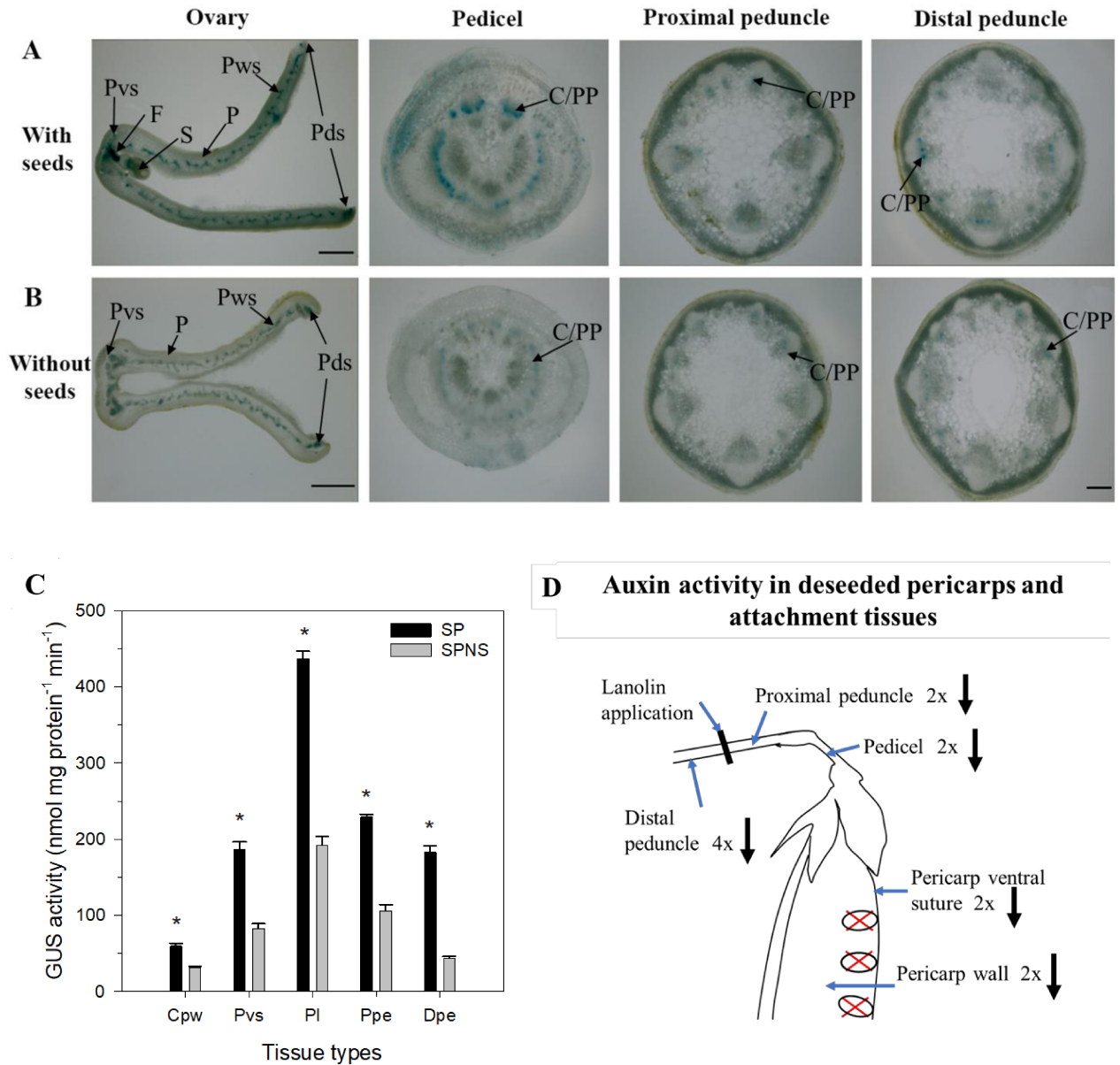


Figure 3.7. The effect of seed removal on DR5-GUS staining patterns and GUS enzyme activity in 4 DAA fruit and attachment tissues of DR5::GUS expressing pea plants. Representative micrographs of the GUS staining patterns of fresh tissue cross-sections taken from the mid-region of the ovary, pedicel and peduncle (sections proximal and distal to the pedicel attachment) when seeds were present (**A**; SP), or 2 days after seeds were removed (**B**; SPNS) from the pericarp. C/PP, cambium/primary phloem; F, funiculus; P, pericarp; Pds, pericarp dorsal suture; Pvs, pericarp ventral suture; Pwv, pericarp wall vasculature; S, seed. Ovary scale bar = 1000 μ m; pedicel and peduncle scale bar = 200 μ m. GUS enzyme activity assessed in the central pericarp

wall (Cpw), pericarp ventral suture (Pvs), and the associated attachment tissues (pedicels; Pl, proximal; Ppe, and distal; Dpe peduncles) in presence of seeds (SP) or absence of seeds (SPNS) in the ovaries (C). Data are means \pm SE (n=4 biological replicates, each biological replicate contains tissues from six fruits). Asterisks denote significantly different treatment means within tissues at $P < 0.05$. Illustration showing the effect of deseeding on the GUS enzyme activity in pericarp and attachment tissues (D).

3.7 Effect of the polar auxin transport inhibitor NPA on GUS staining and enzyme activity in pea fruit and associate attachment tissues

3.7.1 Effect of NPA application to the peduncle

The application of polar auxin transport inhibitor NPA to the peduncle (2 cm away from the pedicel-peduncle junction) attached to intact 2 DAA fruits did not alter the general GUS staining patterns observed when assessed 2 days after NPA application (Fig. 3.8 A and B). However, GUS enzyme activity was higher in the vascular tissues of the ovary (pericarp), pedicel, proximal and distal peduncle tissues (2 days after NPA application; Fig. 3.8 C). Specifically, GUS enzyme activity increased in the proximal peduncle tissue by 4-fold (immediately above the NPA application site), followed by the pedicel and ventral suture (3-fold increase), and then the central pericarp wall (2-fold increase; Fig. 3.8 C and D).

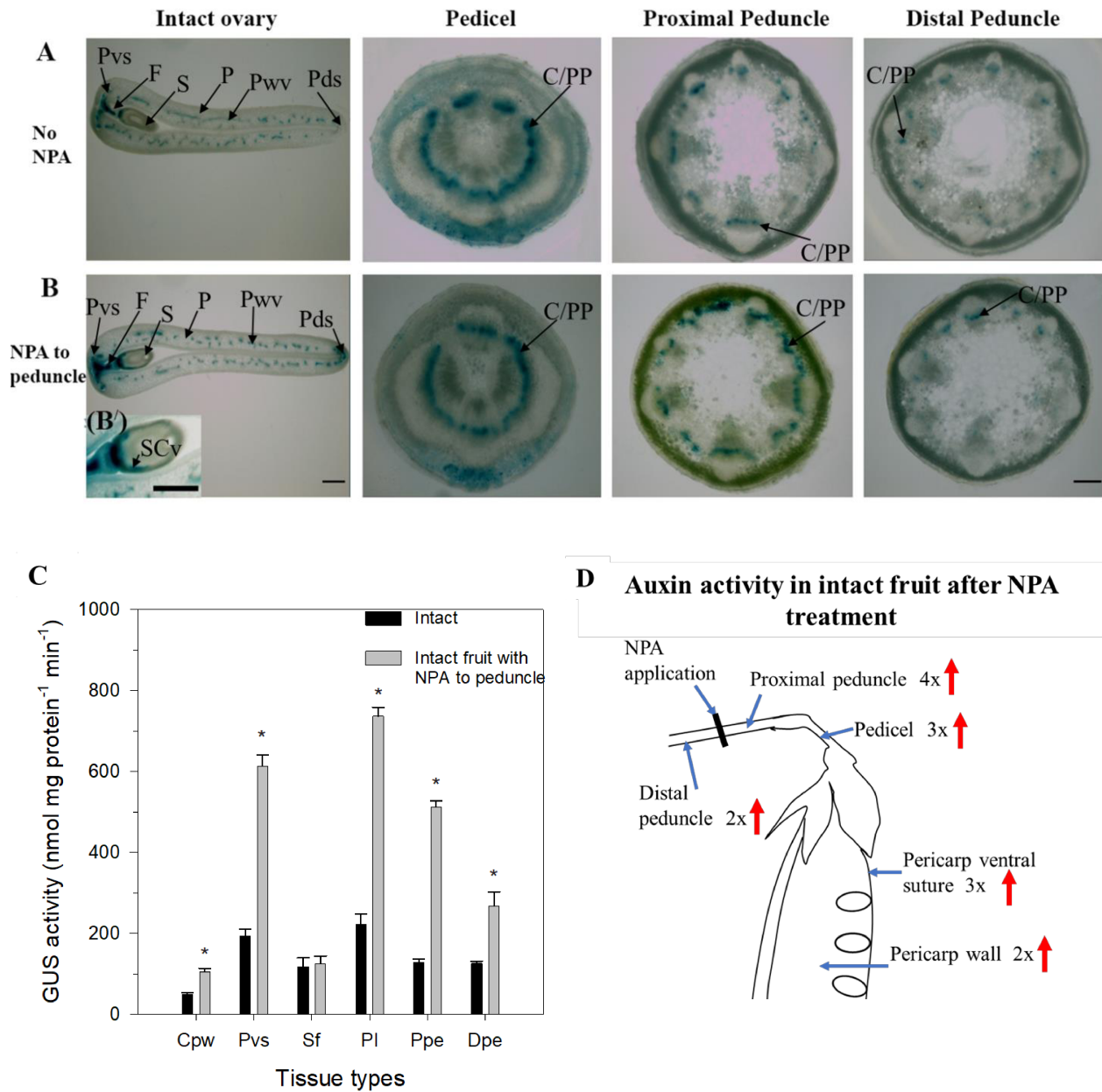


Figure 3.8. The effect of NPA (polar auxin transport inhibitor) applied to the peduncle on DR5-GUS staining patterns and GUS enzyme activity in 4 DAA intact fruit and attachment tissues of DR5::GUS expressing pea plants. Representative micrographs of fresh tissue cross-sections taken from the mid-region of the ovary, pedicel and peduncle (sections proximal and distal to the lanolin or NPA in lanolin application site) 2 days after application of lanolin (control; **A**) or NPA in lanolin to the peduncle (**B**). GUS staining observed in the vascular tissues of seed coat (**B'**) C/PP, cambium/primary phloem; F, funiculus; P, pericarp; Pds, pericarp dorsal suture; Pvs,

pericarp ventral suture; Pwv, pericarp wall vasculature; S, seed. Ovary scale bar = 1000 μm ; Pedicel and peduncle scale bar = 200 μm . GUS enzyme activity assessed in the ovary (central pericarp wall; Cpw, seed plus funiculus; Sf, ventral pericarp suture; Pvs) and the associated attachment tissues (pedicel; Pl, proximal; Ppe, and distal; Dpe peduncles) 2 days after application of lanolin (control) or NPA in lanolin to the peduncle (**C**). Data are means \pm SE (n=4 biological replicates, each biological replicate contains tissues from six fruits). Asterisks denote significantly different treatment means within tissues at $P < 0.05$. Illustration showing the effect of NPA application to the peduncle of intact fruit on GUS enzyme activity in pericarp and attachment tissues (**D**).

The GUS staining pattern in the ovary, proximal and distal peduncle sections of the NPA treated (to the peduncle) split pericarps (SP; Fig. 3.9 B) was similar to the staining pattern observed in SP (control; Fig 3.9 A). However, it was observed that NPA application to the peduncle attached to SP fruit resulted in GUS staining in primary xylem as well as the cambium/primary phloem regions of the vascular bundles of the pedicels, in 43% (6 out of 14 pedicel replicates across four independent experiments) of the pedicels studied (red arrowhead; Fig. 3.9 D and Appendix A Fig. A5). GUS staining intensities of the ovary and the peduncle tissues were also higher when the peduncle was treated with the NPA (Fig. 3.9 A and B). Consistent with the GUS staining intensities of these tissues, application of NPA to the peduncles attached to the SP fruits also increased the GUS enzyme activity in the proximal peduncle by 1.5-fold (immediately above the NPA application site), pericarp ventral suture by 3-fold, and central pericarp wall by 2-fold (Fig. 3.10 A and C). In contrast to intact fruit (Fig 3.8 C and D), NPA application to the peduncle of the SP fruit did not affect the GUS enzyme activity in the pedicel tissue, as levels were already high in the pedicel as a result of pericarp splitting (Fig 3.10 A and C).

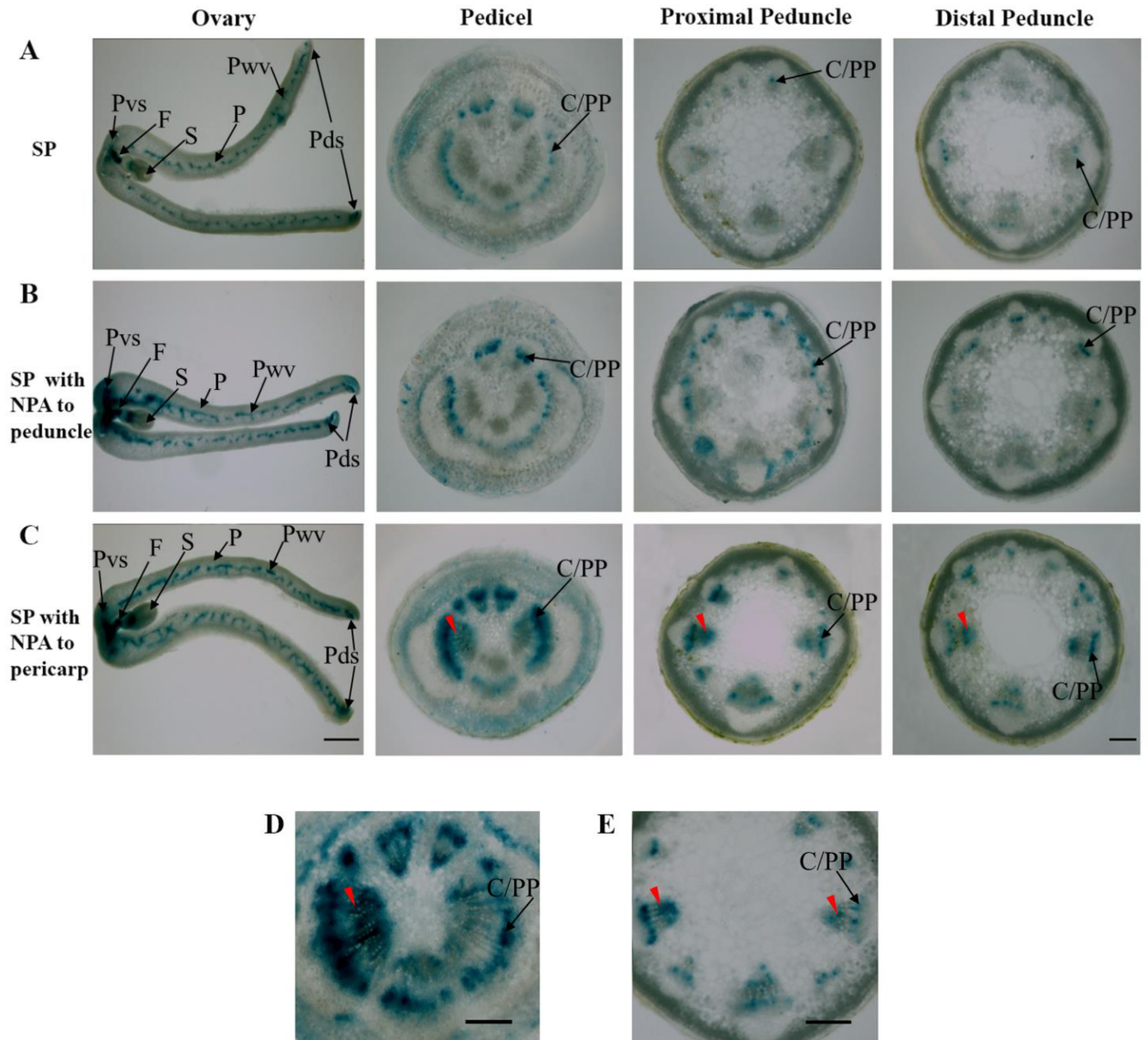


Figure 3.9. GUS staining patterns from tissues with no NPA application (control; **A**), NPA treatment to peduncle only (**B**) or NPA treatment to pericarp only (**C**). GUS staining in the xylem of pedicels after NPA treatment to peduncle (red arrowhead; **D**) and in proximal peduncle after NPA treatment to inner pericarp wall (red arrowheads; **E**). C/PP, cambium/primary phloem; F, funiculus; P, pericarp; Pds, pericarp dorsal suture; Pvs, pericarp ventral suture; Pwv, pericarp wall vasculature; S, seed. Ovary scale bar = 1000 μ m; Pedicel and peduncle scale bar = 200 μ m.

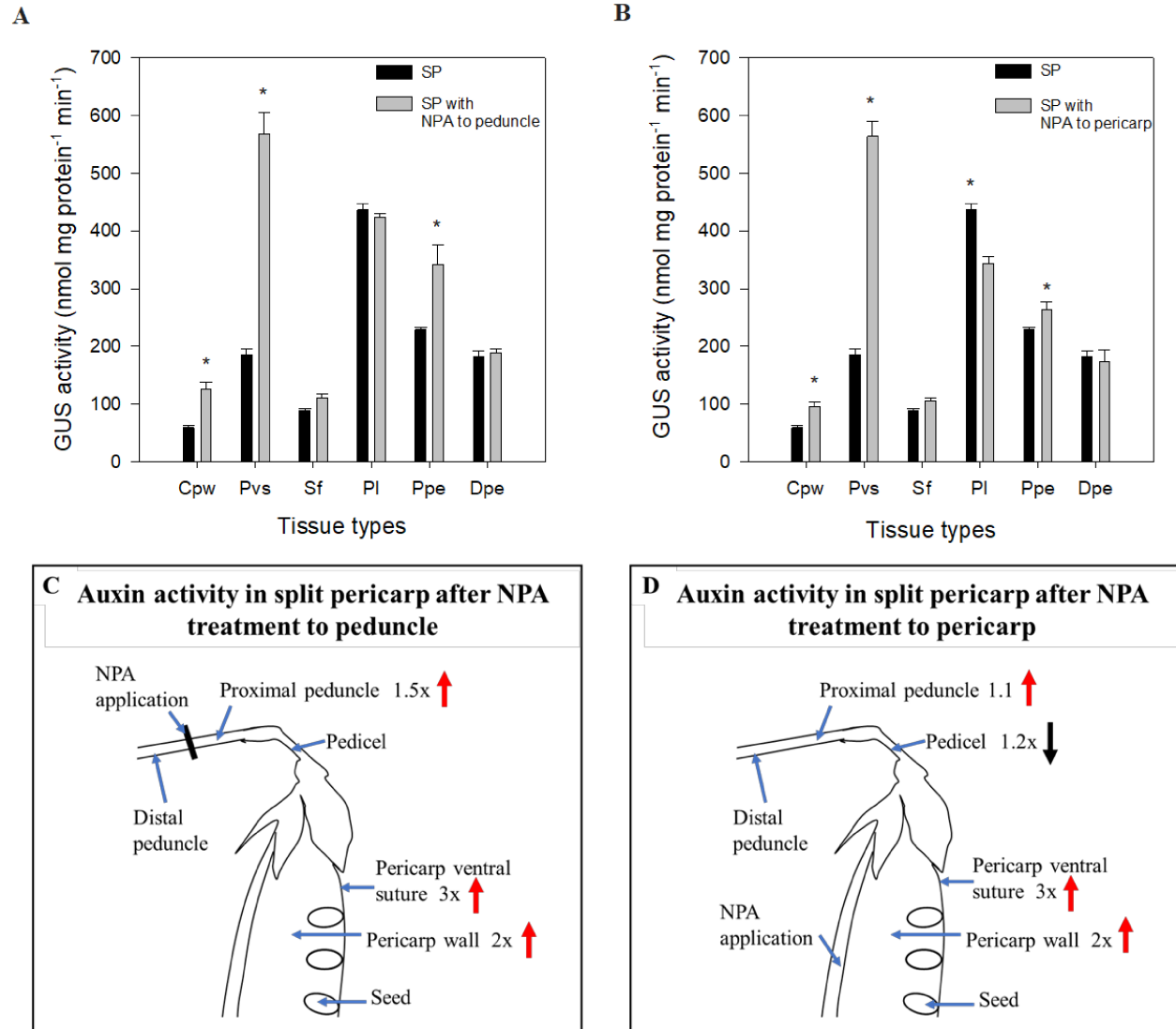


Figure 3.10. The effect of NPA application to the peduncle or inner pericarp wall of 4 DAA split pericarps on GUS enzyme activity in the ovary and attachment tissues of DR5:: GUS expressing pea plants. GUS enzyme activity in the central pericarp wall (Cpw), pericarp ventral suture (Pvs), seed plus funiculus (Sf), pedicels (PI), and peduncle [proximal (Ppe) and distal (Dpe)] tissues from or attached to NPA-treated peduncles (A), NPA-treated pericarps (B) or non-NPA-treated controls (A and B). Data are means \pm SE (n=4 biological replicates, each biological replicate contains tissues from six fruits). Asterisks denote significantly different treatment means within tissues at $P < 0.05$. Illustrations showing the effect of NPA application to the peduncle (C) or inner pericarp wall (D) on GUS enzyme activity in the ovary and attachment tissues.

3.7.2 Effect of NPA application to the pericarp

The application of NPA to the inner pericarp wall of 2 DAA SP fruits generally did not alter the GUS staining patterns observed in the ovary when assessed 2 days after NPA application (4 DAA); however, the GUS staining intensities were higher compared to non-treated controls (Fig. 3.9 A and C). Also, in addition to GUS staining in the cambium/primary phloem region of the vascular bundles in tissues attached to NPA-treated pericarps, GUS staining was observed in the xylem of pedicels (60% of tissues examined; 9 out of 15 pedicel replicates across four independent experiments, red arrowhead; Fig 3.9 C and Appendix A Fig. A6), and distal and proximal peduncles (53%; 7 out of 13 proximal peduncle replicates and 50%; 6 out of 12 distal peduncle replicates examined across four independent experiments, red arrowheads Fig. 3.9 C and E, and Appendix Fig. B19 and B20).

Consistent with the higher GUS staining intensities observed in the ovary tissues of NPA-treated fruits, GUS enzyme activity was higher in the pericarp ventral suture by 3-fold and the central pericarp wall by 1.6-fold compared to non-treated fruits (Fig. 3.10 B and D). However, GUS enzyme activity was significantly reduced (1.3-fold) in the pedicels attached to NPA-treated pericarps (Fig. 3.10 B and D). GUS enzyme activity in the proximal peduncle tissue was marginally increased (1.1-fold) after NPA application to the inner pericarp wall.

3.7.3 Effect of NPA application simultaneously to the peduncle and pericarp

Simultaneous NPA application to the peduncle and pericarp wall of 2 DAA SP fruits, in general, did not alter the GUS staining pattern observed in the ovaries 2 days after NPA treatment (Fig 3.11 A), but led to a higher frequency of pedicels with GUS staining in the xylem (86%; 12 out of 14 pedicel replicates across four independent experiments, red arrowheads; Fig 3.11 A and Appendix A Fig. A7) than that observed when NPA was applied to the peduncle (43%) or pericarp (60%) alone. In proximal peduncles, similar to the peduncles attached to NPA-treated SP fruits, GUS staining was also observed in the xylem and the cambium/primary phloem region of the vascular bundles (50% of tissues examined; 6 out of 12 peduncles across four independent experiments, Appendix B Fig.B23 and arrowhead; Fig. 3.11 A). Simultaneous application of NPA to the peduncle and pericarp wall of 2 DAA SP fruits further increased the GUS enzyme activities in the central pericarp wall, pericarp ventral suture and pedicel tissues 2

days after NPA application compared to the SP fruits treated with NPA to the peduncle only (Fig. 3.11 B). In contrast, simultaneous NPA application reduced the GUS enzyme activity of the proximal peduncle tissues with respect to NPA-peduncle only treatment (Fig. 3.11 B). When compared to NPA-treated pericarp tissues, simultaneous application of NPA to the peduncle and the pericarp tissues increased the GUS enzyme activities in the pericarp ventral suture and pedicels tissues (Fig. 3.11 C).

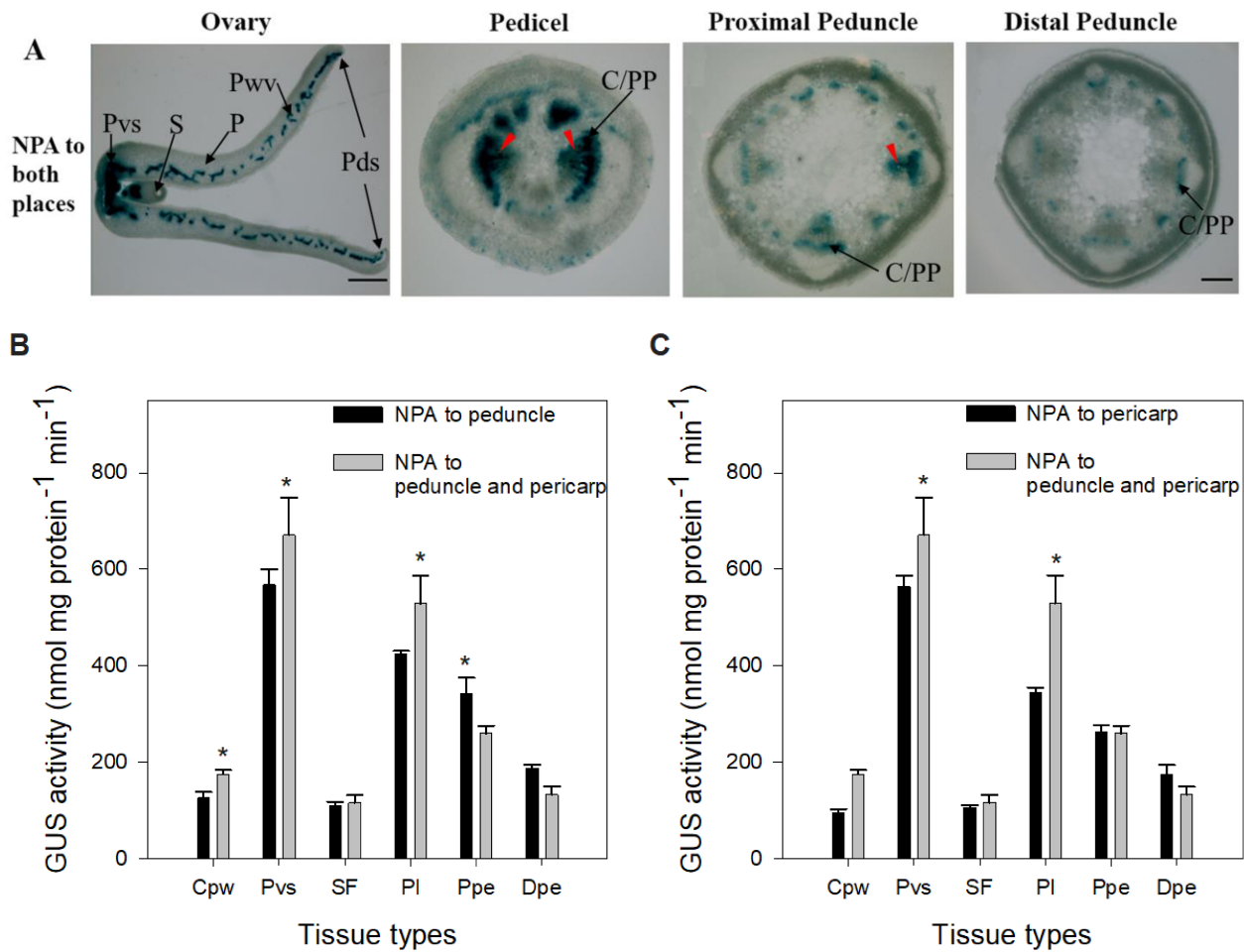


Figure 3.11. Representative micrographs showing the effect of NPA applied simultaneously to the peduncle and inner pericarp wall of 4 DAA fruits split along the dorsal pericarp suture (SP) on GUS staining patterns and GUS enzyme activity in the ovary, pedicel, proximal and distal peduncle tissues from DR5::GUS expressing pea plants. Fresh tissue cross-sections were taken from the mid-region of each tissue types and assessed for GUS staining (A). Arrowheads

indicate the GUS staining in the xylem tissues of pedicels and proximal peduncles. C/PP, cambium/primary phloem; F, funiculus; P, pericarp: Pds, pericarp dorsal suture; Pvs, pericarp ventral suture; Pwv, pericarp wall vasculature; S, seed. Ovary scale bar = 1000 μm ; Pedicel and peduncle scale bar = 200 μm . GUS enzyme activity in the central pericarp wall (Cpw), pericarp ventral suture (Pvs), pedicel (Pl), proximal peduncle (Ppe), and distal peduncle (Dpe) tissues from or attached to NPA-treated peduncle and pericarps compared to NPA-treated peduncles (**B**) and NPA-treated pericarps (**C**). Data are means \pm SE (n=4 biological replicates, each biological replicate contains tissues from six fruits).

3.7.4 Effect of NPA application on GUS enzyme activities in deseeded pericarps

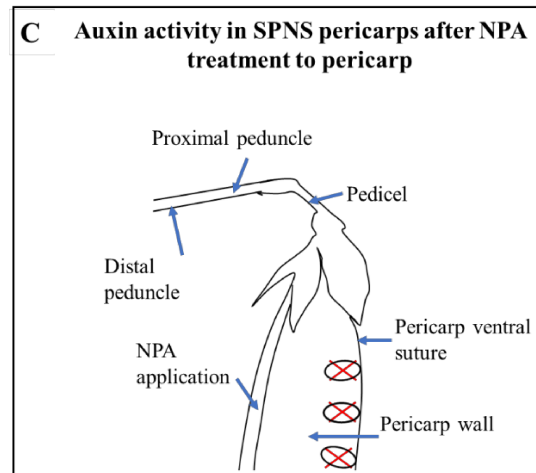
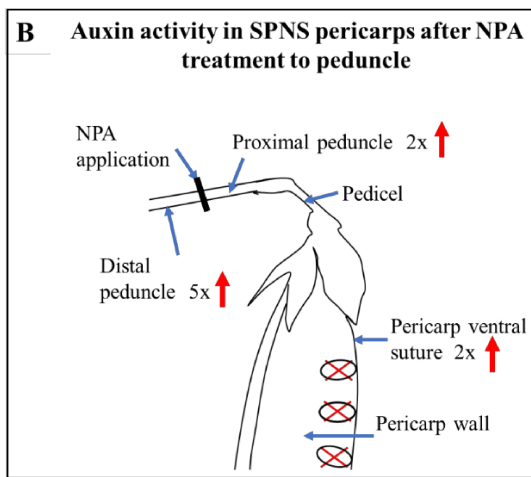
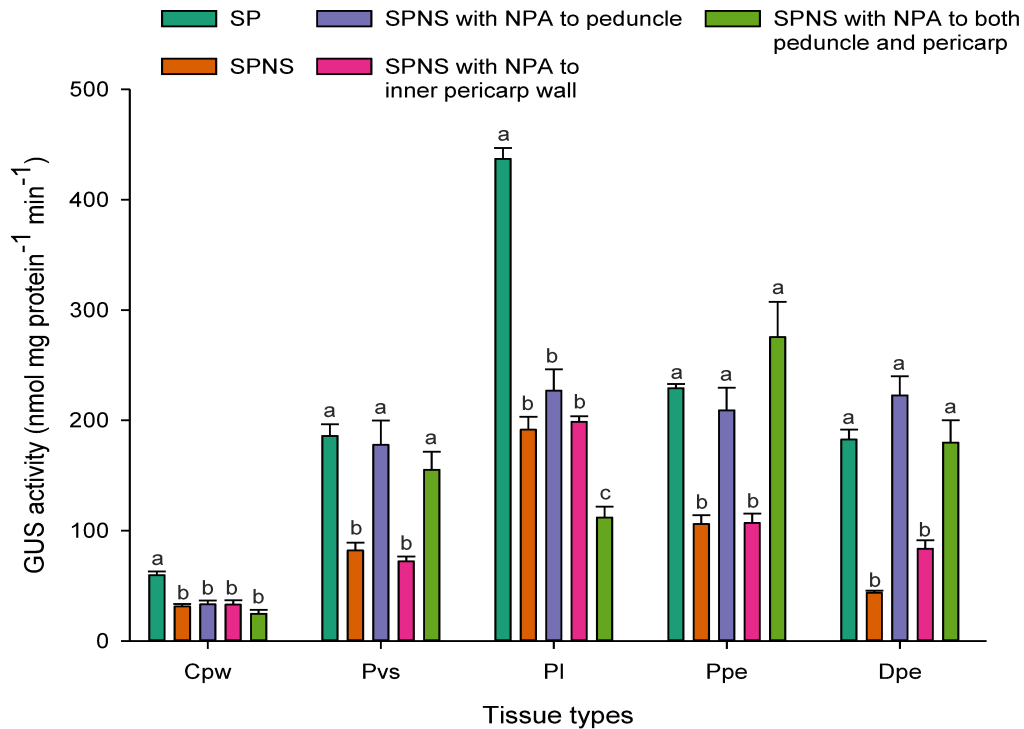


Figure 3.12. The effect of NPA application to the pericarp, peduncle, or simultaneously to the pericarp and peduncle on GUS enzyme activity in 4 DAA split and deseeded fruit (SPNS) and attachment tissues of DR5::GUS expressing pea plants. GUS enzyme activity in the central pericarp wall (Cpw), pericarp ventral suture (Pvs), pedicel (PI), proximal peduncle (Ppe), and distal peduncle (Dpe) tissues from Pvs attached to SP or SPNS pericarp, or SPNS pericarps treated with NPA, SPNS pericarps attached to NPA-treated peduncles, or SPNS pericarps treated with NPA attached to NPA-treated peduncles (A). Data are means \pm SE (n=4 biological replicates,

each biological replicate contains tissues from six fruits). Means with different letters (a, b, c) are significantly different within tissue at $P \leq 0.05$ using a one-way ANOVA with means separation using the Holm-Sidak method. Illustrations showing the effect of NPA application to the peduncle (**B**) or inner pericarp wall (**C**) on GUS enzyme activity in the ovary and attachment tissues of split and deseeded fruits.

Seed removal from the ovaries reduced GUS enzyme activity in the pericarp, pedicel and peduncle tissues (compare SP with SPNS; Fig. 3.12), as mentioned previously (Fig. 3.7 C and D). NPA application to the inner-pericarp wall of deseeded pericarps (SPNS) had no effect on GUS enzyme activity in any of the tissues assessed (Fig. 3.12 A and C). When SPNS pericarps were treated with NPA at the peduncle (application to peduncle only or simultaneously to the peduncle and pericarp), GUS enzyme activity was equivalent to that observed in tissues from pericarps with seeds in the pericarp ventral suture, and proximal and distal peduncle tissues, but not the pedicel tissue (Fig 3.12 A and B).

3.8 Effect of seeds and NPA application on pericarp growth

3.8.1 Effect of seed on pericarp growth

Splitting the pericarp of 2 DAA fruit down the dorsal suture results in a small reduction in pericarp growth (13-14% in length and fresh weight) and seed number (1-2 seeds per fruit) by 4 DAA (Table 3.1). Seed removal markedly decreased pericarp growth by 4 DAA 79% decrease in length and 68% in fresh weight compared to the intact; 76% decrease in length and 63% in fresh weight compared to SP (Table 3.1).

Table 3.1. Effect of pericarp splitting and splitting and deseeding at 2 DAA on pericarp growth and number of seed present at 4 DAA.^a

	Pericarp		Seed number
	Increase in length (mm) ^b	Fresh weight (g)	
Intact	27.46 ± 0.82 ^c a	0.612 ± 0.03 a	7.91 ± 0.29 ^d a
Split pericarps (SP)	23.96 ± 0.91 b	0.528 ± 0.02 b	6.09 ± 0.21 b
Split and deseeded (SPNS)	5.80 ± 0.51 c	0.193 ± 0.01 c	-
			-

^a Pericarp and seed data are from separate experiments.

^b Pericarp length at 4 DAA- length at 2 DAA.

^c Pericarp data are means ± SE, n=23.

^d Seed data are means ± SE, n=11.

A one-way ANOVA was used to test the significance of treatment effects. Means with different letters (a-c) are significantly different within parameter by LSD at P≤0.05.

3.8.2 Effect of NPA application on pericarp growth

When assessed 2 days after NPA application, NPA applied to the peduncle did not affect pericarp growth in length or seed number in attached intact or SP fruits (Table 3.2). NPA applied to the inner pericarp wall of the SP fruit decreased pericarp growth compared to the SP control (Table 3.2). Simultaneous application of NPA to the peduncle and the inner pericarp wall of the SP fruits inhibited pericarp growth to a greater extent than NPA application to the pericarp alone (Table 3.2). NPA treatments generally increased the SPNS pericarp growth 2 days after application (Table 3.2).

Table 3.2. The effect of NPA application to the pericarp, peduncle, or pericarp and peduncle on ovary growth and seed number 2 days after application.^w

	Pericarp		Seed number
	Increase in length (mm) ^x	Fresh weight (g)	
Intact	27.46 ± 0.82 ^y a	0.612 ± 0.03 a	7.91 ± 0.29 ^z a
Intact-NPA to the peduncle	29.63 ± 0.91 a	0.667 ± 0.03 a	7.55 ± 0.37 ac
Split pericarps (SP)	23.96 ± 0.91 b	0.528 ± 0.02 b	6.09 ± 0.21 b
SP-NPA to the peduncle	22.09 ± 0.95 b	0.451 ± 0.03 c	6.58 ± 0.19 b
SP-NPA to the inner pericarp wall	18.58 ± 1.05 c	0.406 ± 0.03 c	6.55 ± 0.41 bc
SP-NPA to both peduncle and inner pericarp wall	15.26 ± 0.81 d	0.302 ± 0.02 d	6.50 ± 0.27 b
Split and deseeded (SPNS)	5.80 ± 0.51 e	0.193 ± 0.01 e	-
SPNS-NPA to the peduncle	7.83 ± 0.65 f	0.216 ± 0.01 ef	-
SPNS-NPA to the inner pericarp wall	7.21 ± 0.45 f	0.245 ± 0.02 f	-
SPNS-NPA to both peduncle and inner pericarp wall	7.68 ± 0.69 f	0.243 ± 0.02 f	-

^w Pericarp and seed data are from separate experiments.

^x Pericarp length at 4 DAA- length at 2 DAA.

^y Pericarp data are means ± SE, n=23.

^z Seed data are means ± SE, n=11.

A one-way ANOVA was used to test the significance of treatment effects. Means with different letters (a-c) are significantly different within parameter By LSD at $P \leq 0.05$.

Although NPA application to the inner pericarp wall of SP fruits reduced pericarp growth 2 days after application (Table 3.2), no difference in pericarp growth was observed when

measured 7 days after NPA treatment (9 DAA) compared to the control (Table 3.3). NPA application also did not affect the growth or days of pericarp abscission of split and deseeded (SPNS) fruits 7 days after application (Table 3.3).

Table 3.3. Effect of NPA applied to the inner pericarp wall of 2 DAA split or split and deseeded pericarps on pericarp growth, seed number and size, and abscission 7 days after application.

	Pericarp		Seed		Day of abscission *
	Increase in length (mm) †	Fresh weight (g)	Number	Fresh weight (g)	
SP	44.83 ± 2.39 a	1.982 ± 0.17 a	5.67 ± 0.33 a	0.230 ± 0.05 a	-
SP-NPA	48.00 ± 1.72 a	1.923 ± 0.19 a	6.43 ± 0.35 a	0.298 ± 0.04 a	-
SPNS	1.89 ± 0.56 b	0.078 ± 0.01 b	-	-	6.33 ± 0.24 a
SPNS-NPA	2.33 ± 0.33 b	0.063 ± 0.01 b	-	-	5.50 ± 0.34 a

* Calculated starting from the day of NPA or Tween treatment (12 hr after SP or SPNS treatment)

† Pericarp length at 9 DAA minus pericarp length at 2 DAA

All data are mean ± SE, n= 6 to 9

A one-way ANOVA was used to test the significance of treatment effects. Means with different letters (a-c) are significantly different within parameter by LSD at P≤0.05

3.9 Effect of NPA on pea fruit set and pericarp growth

To understand the effect of polar auxin transport on pea fruit set, NPA was applied to the peduncle or pedicel of the pollinated or non-pollinated ovaries at -2 DAA (prior to self-pollination). Although NPA application did not affect pericarp growth in the pollinated fruits (Fig 3.13 A and B), NPA application to either the peduncle or pedicel of non-pollinated fruits resulted in a minor increase in pericarp growth, and it maintained pericarp tissue integrity 7 days after NPA treatment (5 DAA; Fig 3.13A and C). However, NPA application did not produce parthenocarpic fruits, as 100% (16 out of 16 fruits) of the non-pollinated fruits abscised within two weeks of NPA application.

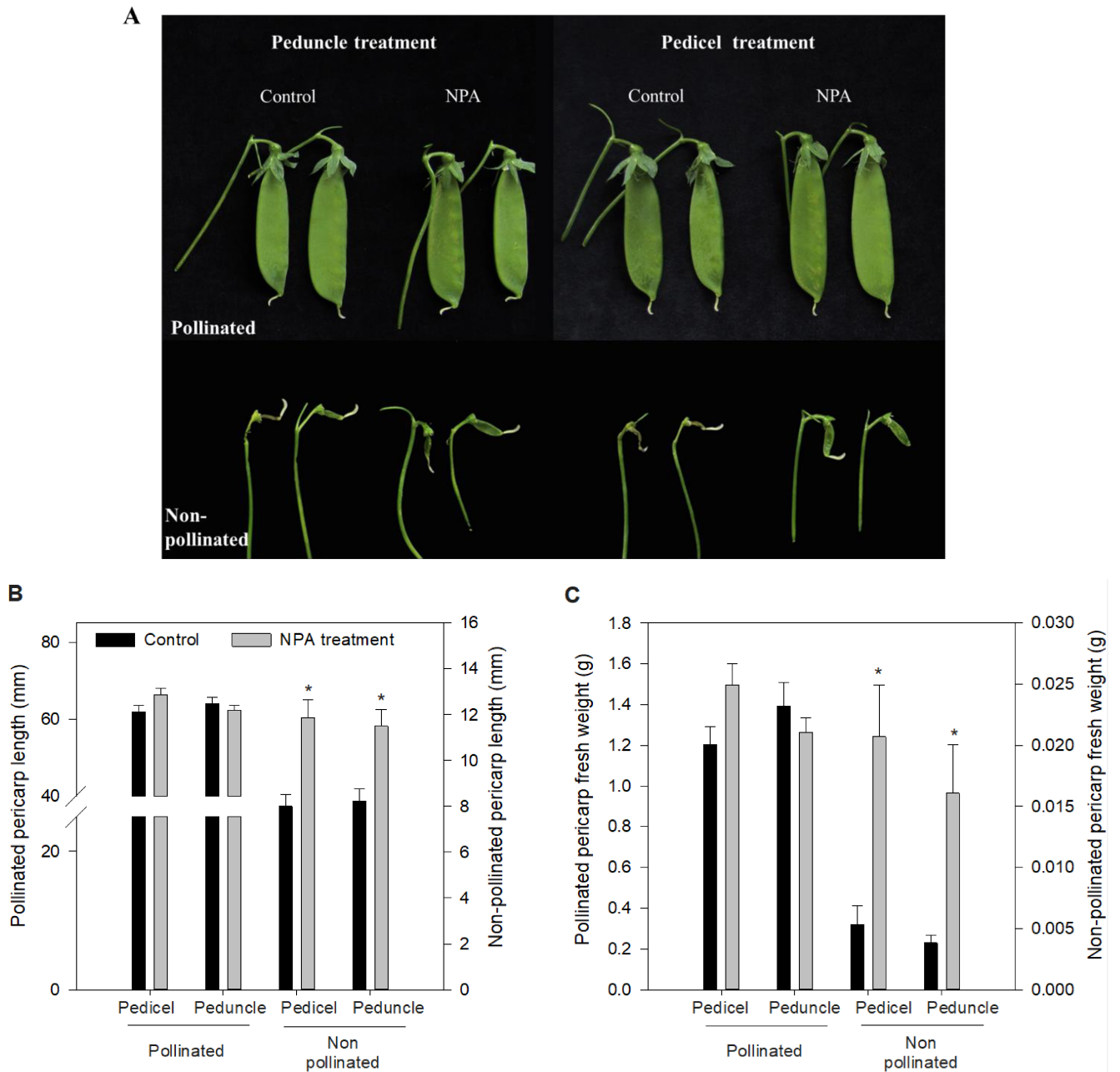


Figure 3.13. Effect of NPA application to pedicels or peduncle of emasculated (non-pollinated) or pollinated fruits on the growth of fruits. Flowers were emasculated prior to pollination (at -2 DAA) or allowed to pollinate. At the same date of the surgical manipulation, pedicels and peduncles of both non-pollinated and pollinated fruits were treated with NPA in lanolin paste. Lanolin paste alone was used as a control. Fruits were harvested 7day after treatment. Representative pollinated fruits and non-pollinated fruits 9 DAA after treatment (A). Effect of different NPA treatments on pericarp length (B) and fresh weight (C) of pollinated and non-

pollinated fruits. Data are means \pm SE, n= 8 to 10. Asterisks denote significantly different mean of control than the NPA treatment within tissues at $P < 0.05$.

4. DISCUSSION

In pea, the presence of developing seeds is required for fruit development (Ozga et al., 1992). In the absence of seeds, auxin (4-Cl-IAA, that occurs naturally in pea seeds) can mimic seeds in stimulating pericarp growth and development by regulating GA levels (Ozga et al., 1992; Ozga et al., 2009) and ethylene signalling and/or ethylene action (Johnstone et al., 2005; Jayasinghe, 2017) in pea pericarps. Furthermore, an auxin gradient from seeds to the pericarp tissues has been observed during pea fruit development suggesting seeds as a source of auxins for the pericarp tissues (Magnus et al., 1997). However, information is scarce about tissue-specific auxin localization patterns and activity in pea fruits. In this thesis, a histochemical approach using pea plants that express the auxin-responsive DR5 promoter linked to the GUS marker gene was employed to localize auxin activity within the pea fruit and attachment tissues to provide evidence for auxin gradients within these tissues and determine if polar auxin transport is involved in the establishment of any observed auxin gradients.

4.1 Ovary and pedicel vasculature in *Pisum sativum*

Developing pea fruit is attached to the parent plant via pedicel and peduncle tissues, and they provide the vascular connection between fruit and parent plant (Fig 3.1 A). At 4 DAA, 4 to 7 vascular bundles were observed in the pedicels, with 8-12 vascular bundles observed in the peduncles (Fig. 3.1 B and C). In the pericarps, vascular bundles adjacent to the pedicel are arranged as a central cylinder, and they gradually diverge into the ventral suture and the dorsal suture vasculature (Fig. 3.2 A). The typical vascular arrangement of legume fruits was observed, where the ventral suture consists of two adjacent longitudinal veins, representing the marginal veins of the carpel, and the dorsal suture consists of a single vein representing the mid-rib vein of the carpel (Fig. 3.2 B; Sutcliffe and Pate, 1977). The two veins of the ventral suture alternatively provide vascular traces to the seeds (Fig. 3.2 B). The ventral suture also connects with the pericarp wall vasculature, which consists of a network of minor veins running throughout the pericarp wall (Fig. 3.2 B). The dorsal suture also connects to the pericarp wall network of minor veins (Fig. 3.2 B). The vasculature of the ventral and dorsal sutures does not connect to each other at the stigma/style end of the pericarp (Fig. 3.2 C).

The pattern of transport of the phloem-mobile (Truernit, 2014; Cui et al., 2015) CFDA green fluorescent dye from the pedicel to the ovary (Fig. 3.3) supports that vascular bundles in the pedicels proximal to the pericarp ventral suture are a major transport pathway for supplying phloem assimilates to the developing seeds that are attached to the ventral pericarp vasculature, as well as the pericarp wall.

4.2 Auxin and auxin activity in pea seeds

Evidence suggests that auxins are important for early seed development. Figueiredo et al (2016) showed that expression of auxin biosynthetic genes, *TAA1* and *YUC6*, under control of the central cell (forms the endosperm after fertilization) and early endosperm-specific promoters, can induce seed coat development in the absence of fertilization. Therefore, these authors proposed that fertilization-dependent activation of auxin biosynthesis occur in the endosperm tissues and these auxins are subsequently transported to the seed coat tissues to stimulate seed coat growth. However, in the present study, the developing embryo and endosperm were lost during sectioning and GUS staining process, therefore, GUS staining was only observed at the base of the seed coat adjacent to the funiculus attachment point (Fig. 3.4 A and B). Moreover, if the section transected the seed coat vascular strands, GUS staining was also observed in these vascular traces (Fig. 3.8 B'). In tomato, DR5 driven expression of the red fluorescent tag (DR5rev::mRFP_{er}) detected auxin activity throughout the fertilized tomato ovules (seeds) starting at 2 DPA (days post anthesis; Pattison and Catalá, 2012). A detailed study that focused on auxin biosynthesis, transport and responsiveness (using the R2D2 ratiometric fluorescent reporter system) in the developing *Arabidopsis* embryo also showed higher auxin activity in all seed tissues after ovary fertilization (a stage after the first endosperm cell division and before embryo cell division; Larsson et al., 2017). These data are consistent with the transcriptomic studies in 4 DPA tomato fruit that showed a peak of expression of the auxin biosynthetic genes *TRYPTOPHAN AMINOTRANSFERASE RELATED 2 (TAR2)* and *FZY6* (a YUCCA-related gene) in the embryos of the developing fruit at this stage (Pattison et al., 2015). Along with above data, evidence that auxin (IAA and 4-Cl-IAA) concentration is higher in pea seeds than the pericarp [in 3-8 DAA (days after anthesis) fruits; Magnus et al., 1997] support the hypothesis that developing seeds are a main source of auxins within the developing pea fruits.

4.3 Auxin transport patterns in fruit and attachment tissues when seeds are present

The 4 DAA fruit is an ideal developmental period to study the involvement of seed-derived auxins in pericarp and attachment tissue development as rapid development of pea fruit occurs between 2 to 6 DAA (van Huizen et al., 1997; Ozga and Reinecke, 1999).

4.3.1 Funiculus

Intense GUS staining was observed in the funiculus, the tissue that attaches the seed to the pericarp (Fig. 3.4 B). The observation of localized auxin activity in the pea funiculus is consistent with observations using auxin sensitive promotor-reporter systems in tomato (at 6 DPA and onwards; Pattison and Catalá, 2012) and *Arabidopsis* (around anthesis; Larsson et al., 2017). In *Arabidopsis*, following ovule fertilization, *AtPIN3* genes were found to be expressed and basally localized in a single cell file in the funiculus that lacks the characteristics of either xylem or phloem, and most likely retains a cambial fate (Larsson et al., 2017). These data suggest that polar transport of seed-derived auxins towards the pericarp tissues via the funiculus takes place at the early stages of fruit development in *Arabidopsis* (Larsson et al., 2017). Supporting this, Pattison et al. (2015) also observed high expression of the auxin influx carrier *SILAX2* and the auxin efflux carrier (*SIPIN1,3,4,7,9*) genes in the funiculus tissue of tomato fruit at the beginning of the exponential fruit growth stage (4 DPA). Moreover, increased expression of the auxin biosynthetic genes, *TAR2* and *YUCCA* genes (*toFZY2* and *6*) in the funiculi was also observed in 4 DPA tomato fruits (Pattison et al., 2015). These synthesized auxins as well as the auxins transported from the seed may be important to maintain high auxin levels in the funiculus and thus to prevent pre-mature seed abscission as the fruit develops, which is common to the orthodox seeds (desiccation tolerant seeds such as cereals and legume seeds; Berry and Bewley, 1991; Pattison and Catalá, 2012).

4.3.2 Pericarp

In pea cv. I₃ Alaska-type, fruit growth in length mainly occurs between 1 and 7 DAA (Ozga et al., 2002, 2003) and evidence suggests that seed-derived auxin is important to regulate the cell division and elongation in the pea pericarps (Ozga et al., 2002). GUS staining and GUS enzyme activities were higher in the pericarp ventral sutures than that in the central pericarp wall

tissues (Fig. 3.4 A and B and Fig 3.6 B intact). Consistently, free IAA and IAA-aspartate (IAA-Asp; the main conjugated form of auxin in pea) levels were higher in the pericarp ventral suture than the central pericarp wall of 5 DAA pollinated pea fruits (Jayasinghege, 2017). In 8 DAA pollinated pea fruits, much higher free IAA and IAA-Asp levels (ng gfw^{-1}) were present in the seeds than the pericarp ventral sutures (87-fold and 95-fold higher, respectively), or the central pericarp wall (215-fold and 2247-fold higher, respectively; Jayasinghege, 2017). As the pericarp ventral sutures are directly attached to the seed via the funiculus, (Fig. 3.6 A (I)), these data suggest that a source of auxin for the pericarp ventral sutures is the seeds, and this auxin can then be redistributed throughout the pericarp tissues. Moreover, as long as seeds are present, splitting the ovaries along the pericarp dorsal suture (SP) did not affect the GUS staining pattern (Appendix Fig. A4) or the GUS enzyme activity (Fig. 3.6 B) observed in the pericarp tissues, pericarp ventral suture, or the central pericarp wall. These data support the involvement of seeds as a source of auxin for the pericarp tissues.

4.3.3 Pedicel and peduncle

Attachment tissues, pedicels and peduncles, provide the vascular and structural connection between the pea ovary and parent plant. In both pedicels and peduncles attached to intact fruit, GUS staining was mainly localized to the cambium/primary phloem region of the vascular bundles (Fig. 3.4 C -G), suggestive of polar transport of auxins from the seeds through the cambial/primary phloem tissues to these attachment tissues. Consistently, GUS enzyme activity was evident in the pedicels and peduncle tissues attached to intact fruit (Fig. 3.6 B; intact). In tomato, higher auxin response (as measured by DR5::GUS expression) was also observed in the peduncles compared to other fruits tissues in the early stages of fruit development (Nishio et al., 2010; Pattison and Catalá, 2012). Therefore, it can be postulate that a minimal level of auxin in the fruit attachment tissues may crucial to prevent premature abscission of the fruits (Oberholster et al., 1991; Brown, 1997; Else et al., 2004; Meir et al., 2010; Ito and Nakano, 2015; Ma et al., 2015; Meir et al., 2015).

Additionally, in pedicels, GUS staining was also observed in the cortical region (Fig. 3.4 C and D, Fig. 3.5 and Appendix A Fig. A2). From -2 DAA (prior to self-pollination) to 0 DAA (after self-pollination), GUS staining in the cortical tissues of the pedicel was intense in the region proximal to pericarp ventral suture attachment. By 2 to 3 DAA, cortical tissue staining for

GUS activity was located at the opposite side of the pedicel (proximal to pericarp dorsal suture attachment; Fig. 3.5). As this cortical staining pattern was similar in the pedicels attached to both pollinated and non-pollinated ovaries, the change in GUS staining localization in the cortical cells was not related to the presence of developing seeds in the attached ovaries. However, the intensity of the GUS staining in the cortical tissues was higher in pedicels attached to pollinated ovaries compared to those attached to non-pollinated ovaries (Fig.3.5). It is possible that auxin biosynthesized in the unfertilized (non-pollinated) ovules or ovary tissue are transported to the pedicels via cortical tissues (as well as pedicel vascular tissues) resulting in the observed cortical GUS staining in the pedicels attached to non-pollinated ovaries. In the absence of fertilization, ovules gradually degenerate, and this may coincide with the less cortical staining observed in the pedicels attached to non-pollinated ovaries. It is also possible that acropetal transport of auxins from parent plant towards the fruits occurs via the cortical cells of the pedicel. However, the proportion of auxin movement in this direction is less compared to basipetal (from fruit towards attachment tissues) auxin transport (Homan, 1964; Sastry and Muir, 1965; Else et al., 2004). Supporting this, in tomato radiolabel IAA applied to the apex was not found in either the pedicel or fruit tissues (Serrani et al, 2010). Therefore in summary, these results postulate that the auxin present in the cortical region of the pedicel may have a role in delaying the formation of an abscission zone between the pedicel and the peduncle until the developing seeds are exporting auxins to these tissues. However, further experiments are needed to understand the source and function of the cortical auxins present in the pedicels.

It was also noted that splitting the ovaries along the dorsal suture (SP) increased the GUS enzyme activity in the fruit attachment tissues compared to that observed in the intact fruit (Fig. 3.6 B). In citrus, disturbing the specific mass transfer by removing phloem tissues (by partial girdling) showed a compensatory increase of specific mass transfer in the remaining phloem tissues (Garcia-Luis et al., 2002). Similarly, the splitting of the pericarp dorsal vascular suture appears to have disrupted auxin transport dynamics within the pericarp tissue resulting in a greater amount of auxin transported from the seeds to the pedicels and peduncles (leading to greater GUS enzyme activity in these tissues; Fig. 3.6 B). This apparent change in auxin flow dynamics may be required to prevent auxin accumulation in the ovaries following the splitting of the pericarp dorsal suture.

4.4 Auxin activity patterns in fruit and attachment tissues in the absence of seeds

Seed removal (SPNS) did not affect the GUS localization pattern in any of the tissues studied (Fig. 3.7 A and B). However, seed removal reduced both GUS staining intensity and GUS enzyme activities by 2-fold in all studied tissue types, with one exception, the distal peduncle tissues decreased by 4-fold (Fig. 3.7 B and D). In tomato, Pattison et al (2015) did not detect auxin biosynthetic gene expression in the placental tissues of 4 DPA fruit. However, these authors did observe that higher expression of auxin transport-related genes in the placenta (*LAX2* and *SIPINI*, 3, 4, 7 and 9) coincided with higher auxin biosynthetic gene expression in seeds (*TAR2*, *toFZY1* and 2) and transport (*LAX2* and *SIPINI*, 3, 4, 7 and 9) gene expression in the funiculus tissues, reflecting the possibility of auxin transport from seeds and or its surrounding tissues towards the outer layers of the fruit.

Moreover, previous studies in *Prunus avium* have shown that basipetal auxin movement coincides with the period of rapid pedicel expansion (cross-sectional area; Else et al., 2004). Increases in the cross-sectional area of the pedicels is mainly due to the cell division and differentiation in the cambial zone (in *Malus domestica*; Dražeta et al., 2004; reviewed by Aloni, 2010) and therefore auxins are important to stimulate vascular development in the pedicels, before and after anthesis, to ensure the developing fruit/seeds are supplied with a sufficient nutrients from the parent plant (Else et al., 2004). In our study, the pedicel cross-sectional area increased from 2 days before anthesis to 3 DAA (Fig. 3.5). Furthermore, as the pedicel cross-sectional area increased, the ratio of cortical tissue to vascular tissue decreased (Fig. 3.5), supporting that the increase in the pedicel cross-sectional area at this stage is mainly due to the developing vascular bundles. However, we did not observe any difference in the vascular development or the ratio of cortical to vascular bundle between the pedicels attached to pollinated fruits and those attached to non-pollinated fruits, indicating a pre-determined developmental program controlling pedicel vascular development. These data in pea are consistent with those in *Prunus avium* fruit pedicels (Else et al., 2004), supporting that abscission of non-pollinated ovaries is not due to the absence of proper vascular development and thus the limited capacity of the vascular system to export essential materials to the developing fruits (Else et al., 2004). A continuous polar flow of auxin through abscission zone has been suggested to be vital to prevent the premature abscission of the attached organ (leaves, flowers or fruits), and in some species this is suggested to involve an auxin-induced decrease in ethylene sensitivity

(Oberholster et al., 1991; Brown, 1997; Else et al., 2004; Meir et al., 2010; Ito and Nakano, 2015; Ma et al., 2015; Meir et al., 2015). In pea, an abscission zone can be formed at the junction of the pedicel and peduncle tissues result in fruit abscission (Glazinska et al., 2017). The reduction of auxin activity in pedicels attached to deseeded ovaries (Fig. 3.7) supports that the abscission of ovaries without developing seeds (Fig.3.5; pedicels attached to non-pollinated ovaries) observed in our studies are at least partially due to an inadequate supply of auxin to the pedicel which leads to the formation of an abscission zone at the pedicel-peduncle junction.

4.5 Auxin activity patterns in fruit and attachment tissues after NPA treatments

Polar transport of auxin is mediated by PIN proteins asymmetrically localized in the plasma membrane (Morris et al., 2010). Polar auxin transport inhibitors such as NPA can inhibit carrier-mediated polar auxin transfer (Lomax et al., 1995; Morris et al., 2010) without itself being transported in a polar manner (Thomson et al., 1973). Therefore, NPA was used to determine the influence of polar auxin transport on the relative distribution of auxin activity in pea fruits from 2 to 4 DAA.

4.5.1 NPA application to the peduncle

In general, NPA application to the peduncles attached to intact or split pericarps with seeds (SP) did not affect the GUS localization patterns in the ovaries or the attached pedicel and peduncle tissues; however, it led to increased GUS staining intensity in the tissues above the NPA application point (Intact, Fig.3.8 A and B; SP, Fig.3.9 A and B). The greatest increase in auxin activity above the NPA application site was observed in the intact ovaries. When NPA was applied to the peduncle of the intact ovaries, GUS enzyme activity increased in the proximal peduncle (tissue just above the NPA application point) by 4-fold, and 3-fold in the pedicel tissues followed by the 3-fold and 2-fold increase in pericarp ventral suture and central pericarp wall, respectively (Fig.3.8 C and D). Similar to the intact fruit, increased GUS enzyme activity was also observed in the ovary tissues of SP fruits when NPA was applied to the peduncle (Fig. 3.10 A and C). As auxin activity was already elevated in the pedicel tissue attached to SP fruits due to the splitting of the pericarp dorsal suture, NPA application to the peduncle did not further increase auxin activity in that tissue (Fig. 3.10 A and C). Overall, these observations suggest that

NPA application to the peduncle results in auxin accumulation in tissues above the application point. Therefore, we postulate that the flow of auxin is basipetal from the seed in the fruit to the attachment tissues, and at least part of this movement is facilitated by the polar auxin transport system. Consistent with these data, NPA application to the pedicels of tomato fruits also increased the amount of applied radiolabeled IAA remaining in the ovaries while reducing the amount observed in the pedicel tissues below the NPA application (Serrani et al., 2010). Moreover, application of another auxin transport inhibitor TIBA to the peduncles of tomato led to an increase in the auxin content in the fruits (Hamamoto et al., 1998). These data in tomato along with the higher expression of *SIPIN1* and *SIPIN2* in the ovary and seed tissues, respectively (Nishio et al., 2010) supports that auxin from the young developing seeds are transported to the pedicels via a polar transport-dependent pathway.

4.5.2 NPA application to the pericarp

NPA application to the pericarp also increased both GUS staining intensity and GUS enzyme activity in the ovary tissues including pericarp ventral suture by 3-fold and the central pericarp wall by 2-fold (Fig 3.9 A and C, and Fig. 3.10 B and D). However, the GUS localization pattern in the ovary tissues was unaffected (Fig. 3.9 A and C). Along with above observations, Dorcey et al (2009) observed that parthenocarpic fruit set in *Arabidopsis* when NPA applied to the *cer6-2* male sterile flowers at the anthesis and therefore, they concluded that NPA could block the auxin flow in *Arabidopsis* ovaries which intern trigger the auxin accumulation in ovary tissues leading to fertilization-independent fruit set. Additionally in pea, we observed a 1.2-fold reduction of auxin activity in the pedicel tissues after NPA treatment to the ovaries (Fig. 3.10 B and D), supporting the hypothesis that the ovary is responsible for maintaining the auxin levels in pea pedicels, and the auxin flux across the pericarp/ovary tissues towards the attachment tissues is at least partially mediated by the polar auxin transport system. Strengthening the above observations, higher expression of *PIN* genes, which are susceptible for NPA inhibition, was observed in the seed (*AtPIN1,3,7*, *SIPIN1* and 2), funiculus and placental tissues (*SIPIN1,3,4,7* and 9), and pericarp (*PIN-LIKE* genes; *SIPILS2* and 5) of *Arabidopsis* and tomato during the early stages of the fruit development (Friml et al., 2003; Nishio et al., 2010; Pattison et al., 2015; Larsson et al., 2017).

Although the pericarp NPA treatment did not affect the GUS localization patterns in the ovaries, it led to GUS staining in the primary xylem tissue of the pedicels and peduncles along with staining in the cambial/primary phloem region (Fig. 3.9 C and E). This GUS staining pattern was also observed in the pedicel tissues when NPA was applied to the peduncles attached to split pericarps with seeds (SP; Fig. 3.9 D). This alternate GUS staining pattern may be a result of auxin redistribution to the xylem tissues to remove excess auxins from the ovaries in order to prevent accumulation of supraoptimal auxin levels after the NPA application.

4.5.3 NPA application simultaneously to the peduncle and pericarp

Simultaneous NPA application to peduncle and inner pericarp wall of the SP fruits generally increased both GUS staining intensity and GUS enzyme activity in the ovary tissues compared the single application to either peduncle or pericarp wall (compare Fig. 3.11 A with Fig. 3.9 B and C, and Fig. 3.11 B and C). Simultaneous NPA application to peduncle and pericarp wall further increased the frequency of pedicels with GUS staining in the xylem (86%; Fig. 3.11 A and Appendix A Fig. A7) compared to single site applications. Consistent with GUS staining in the xylem, GUS enzyme activity in the pedicels was higher after dual site compared to single site NPA application (Fig. 3.11 B and C). The GUS staining activity in the proximal peduncle was reduced after simultaneous NPA application to the peduncle and pericarp compared to NPA application to the peduncle only (Fig. 3.11 B). This is may due to the perturbation of seed auxin flow toward the peduncle by applied NPA to the ovaries in dual NPA application. Altogether, the GUS enzyme activity in the pedicels and peduncle after simultaneous NPA application to the peduncle and pericarps further supports that seeds are a source of auxins for developing pea fruits and when normal auxin transport is disrupted by NPA, it appears that auxins are loaded into xylem tissues to prevent supraoptimal auxin accumulation in these tissues.

4.5.4 NPA application to the deseeded fruits

GUS enzyme activities were greatly reduced by seed removal in the ovary and fruit attachment tissues (SP compared to SPNS; Fig. 3.7 C and Fig. 3.12 A). NPA application to the peduncle (peduncle alone or peduncle plus pericarp) increased the GUS enzyme activity in the peduncle and pericarp ventral suture tissues of deseeded fruits to levels similar in SP fruits (Fig.

3.12). These data indicate that the NPA-related auxin redistribution (when NPA is applied to the peduncle) led to higher auxin levels which increased auxin activity in the peduncle and pericarp ventral suture tissues. NPA treatment to the inner pericarp wall of the deseeded pericarps did not change GUS enzyme activity within the ovary, or in the fruit attachment tissues (Fig. 3.12), confirming the importance of the developing seeds in providing auxin to these tissues.

4.6 Effect of pericarp splitting, deseeding, and NPA applications on pericarp growth

4.6.1 Pericarp splitting, and splitting and deseeding

Pericarp growth in the split pericarps (SP) was approximately 13-14% less than that in intact ovaries (Table 3.1). These data are consistent with previous data in our lab (Ozga et al., 1992). This small reduction of pericarp growth may be due to the disturbance of the normal auxin flow associated with the dorsal suture and the wound-related ethylene evolution as a result of splitting. However, removal of seeds reduced pericarp growth more than 50% within two days after seed removal (Table 3.1), and the pericarp subsequently abscises within 7 days (Johnstone et al., 2005). Removal of the seeds reduced bioactive gibberellin levels (Ozga et al., 2009) and induced ethylene signaling and/or action (Johnstone et al., 2005; Jayasinghe, 2017) in the pericarp, and these processes may lead to the gradual abscission of deseeded ovaries.

4.6.2 NPA applications

NPA application to the pericarp or to both the peduncle and the pericarp reduced SP pericarp length and fresh weight when assessed 2 days after NPA application (Table 3.2). The reduction of pericarp growth in SP fruits may occurred due to the accumulation of auxin to a supraoptimal level as a result of the altered auxin transport by NPA together with splitting of the pericarps. Quantification of auxins in the ovary tissues after NPA application is required to confirm this possibility. In deseeded pericarps, NPA application increased deseeded pericarp growth when assessed 2 days after application (Table 3.2). These data further indicate that NPA could transiently increase the auxin levels within the pericarp resulting in greater pericarp growth. However, in absence of seeds this transient increase was not sufficient to maintain pericarp growth, as in longer-term growth assays, deseeded pericarps (SPNS) did not continue to grow and they abscised (Table 3.3). NPA treatment also did not affect pericarp growth or seed

number per fruit in pericarps with seeds (SP) when assessed 7 days of NPA treatment (Table 3.3). These data support that sustained pea ovary growth requires seed-derived auxins. It would be interesting to determine if several applications of NPA would affect pericarp growth in seeded and deseeded pea fruits, as the effect of NPA on PIN auxin efflux carriers may be influenced by PIN protein recycling or synthesis and/or by the activation of auxin homeostasis mechanisms (e.g., conjugation and/or catabolism of auxins).

4.7 Effect of NPA applications on pollinated and non-pollinated ovary growth

NPA application to either the peduncle or pedicel of pollinated (intact) pea ovaries also did not affect fruit growth 7 days after treatment (Fig. 3.13 A and B). However, NPA application to these tissues attached to non-pollinated fruits slightly increased the pericarp growth and maintained the fruit integrity for at least 7 days after treatments, but did not induce parthenocarpy, as all non-pollinated fruits abscised within two weeks after treatments (Fig 3.13 A and C). The transient induction of the pericarp growth in the non-pollinated pea ovaries attached to NPA-treated peduncles or pedicels may be due to a small amount of auxin accumulation in the fruit as the result of NPA application. In contrast, NPA application to the pedicels of pollinated tomato ovaries completely blocked fruit set while application to pedicels attached to non-pollinated ovaries induced parthenocarpic tomato fruit set, and the fruits were similar in size to that of pollinated fruits (Serrani et al., 2010). In *Arabidopsis*, disruption of auxin flow in the male sterile *cer6-2* flowers by NPA led to set the parthenocarpic fruits with a final length similar to GA₃ or NAA induced fruits (but less than pollinated fruit length; Dorcey et al., 2009). The ability of NPA application to induce sustained ovary growth in the non-pollinated fruit of tomato and *Arabidopsis*, but not in pea, may suggest that auxin synthesis in non-pollinated pea fruit is minimal and not enough auxin accumulates in the non-pollinated fruits after NPA application to induce sustained ovary growth.

5. CONCLUSION

Presence of viable seeds is vital for fruit development. Removal of seeds early in the fruit development cease pericarp (fruit) growth and eventually leads to pericarp abscission (Ozga and Reinecke, 1999; Ozga et al., 2002; Johnstone et al., 2005). Mounting evidence supports the hypothesis that seed-derived signals, particularly auxin (4-Cl-IAA in pea), promotes pericarp growth (Magnus et al., 1997; Ozga et al., 2009; McAtee et al., 2013; Kumar et al., 2014). The data presented in this study provide evidence to further strengthen the seed-auxin hypothesis in relation to pea fruit development. Additionally, the involvement of polar auxin transport in regulating the tissue-specific auxin accumulation in fruit tissues has been evaluated.

5.1 Seeds serve as a source of auxins for the fruit and attachment tissues

Fertilization dependent synthesized-auxins in the central cell, diffuse to the seed coat tissues to induce seed coat development (Figueiredo et al., 2016). Fertilization also reduces the auxin conjugation in seeds, increasing the pool of free- auxins. The accumulating free-auxin in the seeds is then transported to the surrounding pericarp tissues to promote fruit growth (Figueiredo et al., 2016; Larsson et al., 2017). Cells associated with the vasculature of the seed, funiculus, pericarp and attachment tissues provide a continuous route for the distribution of seed-derived auxin throughout the fruit, pedicel and the peduncle. In accordance with this, removing the developing seeds from 2 DAA pollinated ovaries reduced the GUS staining and the GUS enzyme activity in the ovary, the pedicel and the peduncle tissues (Fig. 3.7). Seed removal also arrested the pericarp growth (Table 3.1) and caused subsequent pericarp abscission (Johnstone et al., 2005), implying the importance of seed-auxin as a coordinative signal for fruit growth.

Seed-derived auxins are transported to the pericarp ventral suture via the funiculus. It has shown that maintaining a high auxin level in the funiculus is important to prevent the seed abscission (Berry and Bewley, 1991; Pattison and Catalá, 2012). The GUS staining and GUS enzyme activity in the pericarp ventral suture and the central wall dictate an auxin gradient towards the central pericarp wall (Fig. 3.4 A and B and Fig.3.6 B), indicating the direction of the auxin flow from ventral suture to the central wall. Auxin (4-Cl-IAA) transported to the pericarp tissues induces pericarp bioactive gibberellin level by stimulating the expression of gibberellin

biosynthesis genes *PsGA20ox1* and *PsGA3ox1*, and repressing gibberellin catabolism gene *PsGA2ox1* (Ozga et al., 2009). 4-Cl-IAA also reduce the pericarp ethylene action, potentially by suppressing ethylene signaling (Johnstone et al., 2005; Jayasinghege, 2017). High level of auxin, together with high level of bioactive gibberellin and reduced ethylene activity stimulate the pericarp growth.

Pericarp dorsal suture receives seed-auxin via the vasculature of central pericarp wall (Fig. 3.2B) and auxin present in the dorsal sutures important to prevent pre-mature dehiscence of the pericarps (Chauvaux et al., 1997; Sorefan et al., 2009). Ventral sutures also redistribute the auxin to the attachment tissues (Fig.3.3). A continuous Auxin flow (mainly in the cambium/primary phloem region; Fig 3.4 C-G) in the attachment tissues is important to prevent the pea fruit abscission during development at the pedicel-peduncle junction (Glazinska et al., 2017).

5.2 Tissue-specific distribution of seed-derived auxins depends on the polar auxin transport

Disturbing the auxin flow in the fruit tissues by applying polar auxin transport inhibitor *N*-1-naphthylphthalamic acid (NPA) to the peduncle or pericarp resulted in an auxin accumulation in the tissues above application point. Application of NPA to the peduncles generally increased the GUS staining and GUS enzyme activity in proximal peduncle, pedicel and ovary tissues of intact and SP fruits (Fig. 3.8 C, Fig. 3.9 A and B and Fig. 3.10 A and C); whereas, NPA application to the inner pericarp wall increased GUS staining and activities in all the ovary tissues (Fig. 3.9 A and C and Fig. 3.10 B and D). This pattern suggests a basipetal polar flow of auxin in the developing fruits and attachment tissues. Blocking this polar flow of auxin in the pericarp tissues (single application to pericarp or simultaneous application to both pericarp and peduncle) reduced the pericarp growth at two days after the treatment (Table 3.2). Although, in deseeded pericarps, application of NPA to the peduncle, pericarp, or simultaneous application to both tissues restored the pericarp growth (Table 3.2) the effect was diminished in both SP and SPNS fruits in long-term growth assays (Table 3.3). Similarly, NPA application did not induce the parthenocarpic fruit set from emasculated ovaries (Fig. 3.13). Together, these data indicate the importance of seeds as an auxin source. Availability of an optimal level of auxin, but not a sudden transient increase, is required for the coordination of fruit set and subsequent fruit development.

Overall, these data support the seed-derived auxin model for developing pea ovary and attachment tissues. Further, this study shows that auxin distribution in both ovary and attached pedicel and peduncle tissues is at least partially mediated by the polar auxin transport mechanism. Figure 5.1 illustrates the proposed route for seed-derived auxins in ovary and attachment tissues, based on data from the present study.

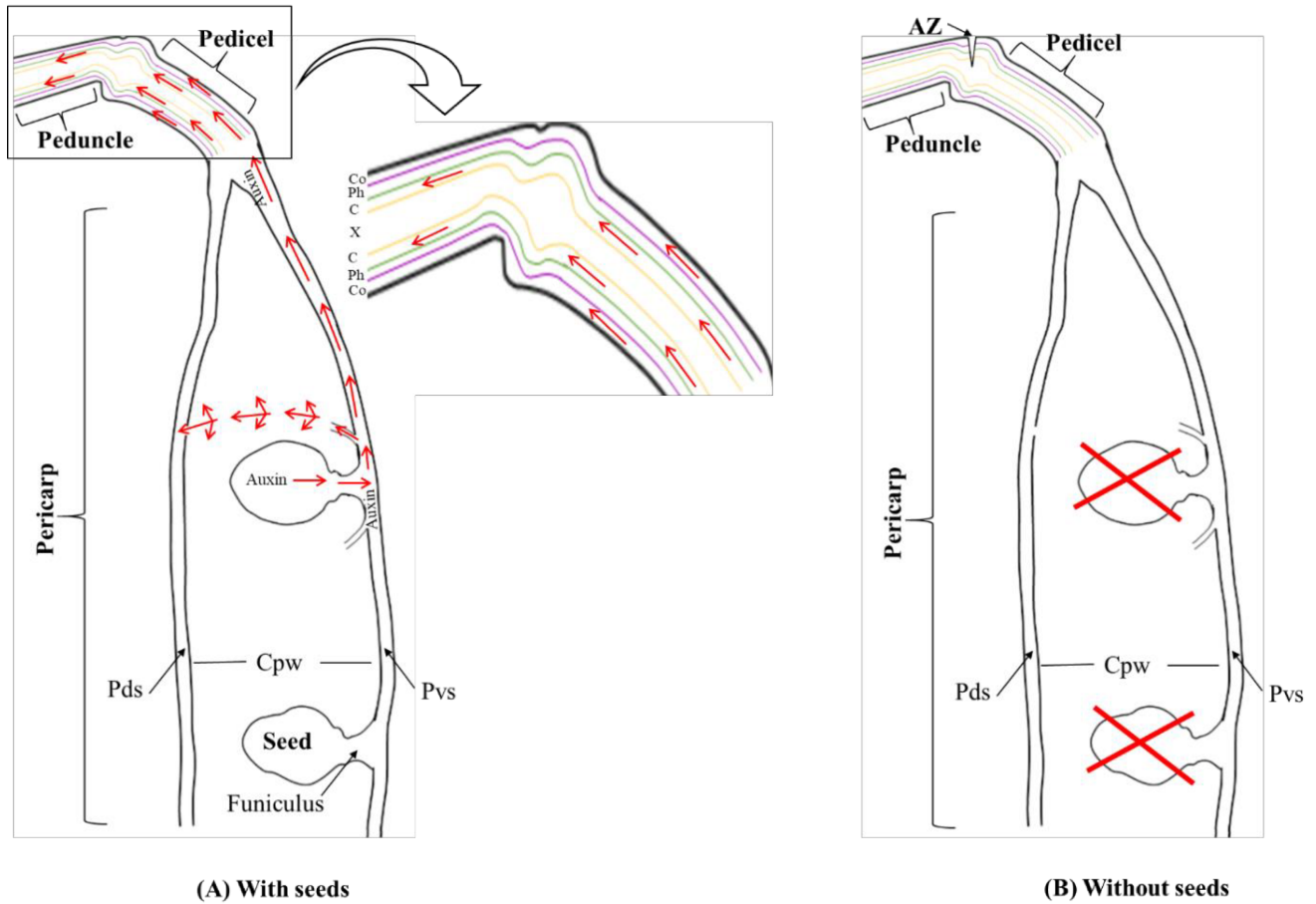


Figure 5.1. Proposed model for the source and possible transport routes of auxins in developing pea fruits. Seeds are the source of auxins in developing pea fruits (A). Removal of seeds (B) reduces the auxin levels in all pericarp and attachment tissues, which promotes subsequent pericarp abscission (Johnstone et al., 2005). seed-derived auxin is transported polarly towards the pericarp ventral suture (Pvs) via the funiculus (Larsson et al., 2017). Polar auxin transport in the ventral suture redistributes this seed-auxin to the central pericarp wall (Cpw), and to the attachment tissues, pedicel, and peduncle. Ventral suture also supplies auxin to the dorsal suture (Pds) through the vascular connections in the central pericarp wall. In the attachment tissues, the

polar flow of auxin occurs through the cambium/ primary phloem cells. However, at 4 DAA, an auxin flow through cortical cells towards the abscission zone (AZ) is also taking place. C; cambium, Co; cortex, Ph; phloem, X; xylem.

5.3 Future perspectives

In the study with the phloem mobile dye, 5 (6)- carboxyfluorescein diacetate (CFDA; section 3.3), we observed that the vascular strands in the pericarp ventral suture are connected with the vascular bundles of pedicels, oriented in the area proximal to pericarp ventral suture. However, at studied time points in our preliminary study, data were not sufficient to conclude such a connection between the vasculature in pericarp dorsal suture and pedicel. Therefore, repeating the experiment with longer time points (6, 8 and 10 hr after CFDA application to the abraded surface of the pedicel proximal to the dorsal suture) and at least 8-10 replicates per time point would be useful to understand the vascular connection between dorsal sutures and pedicel tissues.

Data from the present study (section 3.5 – 3.8) and previous studies (Magnus et al., 1997; Ozga et al., 2009) show the importance of seeds in maintaining auxin levels in developing fruit and attachment tissues. However, we were not able to study the auxin distribution within the seed tissues in this study. In the seeds, GUS activity was detectable only in the outer most seed coat tissues due to the loss of internal tissues during sectioning and GUS staining procedure. Transgenic plants expressing efficient and more sensitive novel fluorescent reporter constructs such as DR5rev::mRFP_{er} or R2D2 can be used to overcome this issue. Fluorescence signals under high resolution confocal microscopes will provide a detailed picture of the auxin distribution in the seeds with a reduced risk of losing embryo and other internal tissues during tissue processing. Moreover, fluorescent reporter fusions of auxin biosynthetic genes such as *PsTAR1* and *PsTAR2* (Tivendale et al., 2012; Ligerot et al., 2017), auxin transporter genes such as *PsPIN1* (Chawla and DeMason, 2004), and the recently cloned auxin conjugating gene *PsGH3* (Ostrowski et al., 2016) will provide more comprehensive picture on the spatiotemporal regulation of auxin readout during pea fruit development. However, given that the generation of transgenic pea plants is a laborious and lengthy process (Atif et al., 2013; Smýkal, 2014), expression analysis of the above genes can be used as an alternative approach. In seeds, specific

tissues/cell layers can be collected using laser capture microdissection, which then can be used to quantify the tissue and developmental stage-specific gene expressions by quantitative PCR.

In this study, we also observed accumulation of auxin in split pericarps when treated with polar auxin transport inhibitor NPA, irrespective of the place of NPA treatment (section 3.7).

Further in general, a short-term growth reduction was also observed in those NPA-treated pericarps but there was no effect in the long-term growth assays (section 3.8). This NPA-induced growth inhibition can be due to the accumulation of auxins to a supraoptimal level in the pericarp tissues. Comparison of auxin levels in NPA treated and non-treated fruits will reveal whether the NPA treatment has a significant effect on auxin accumulation in the pericarp tissues.

Furthermore, an expression analysis of selected genes such as *PsGH3*, which regulate the auxin conjugation, will be helpful to understand the mechanisms how plants mitigate the long-term effects of NPA in developing pericarps. We also observed a tendency of an inhibitory effect of NPA on 4-Cl-IAA and GA₃ induced pericarp growth (Appendix C). However, the 4-Cl-IAA- and GA₃-induced (controls) pericarp growth was markedly lower than that observed previously in our lab. Therefore, it would be useful to repeat this experiment before making any conclusion.

Reference

- Abel S, Theologis A** (2010) Odyssey of auxin. *Cold Spring Harb Perspect Biol.* doi: 10.1101/cshperspect.a004572
- Allen JRF, Baker DA** (1980) Free tryptophan and indole-3-acetic acid levels in the leaves and vascular pathways of *Ricinus communis* L. *Planta* **148**: 69–74
- Allen JRF, Greenway AM, Baker DA** (1979) Determinations of indole-3-acetic acid in xylem sap of *Ricinus communis* L. using mass fragmentography. *Planta* **144**: 299–303
- Aloni R** (2010) The induction of vascular tissues by auxin. In PJ Davies, ed, *Plant Hormones: Biosynthesis, Signal Transduction, Action*, Third ed. Springer Netherlands, Dordrecht, pp 485–518
- Atif RM, Patat-Ochatt EM, Svabova L, Ondrej V, Klenoticova H, Jacas L, Griga M, Ochatt SJ** (2013) Gene transfer in legumes. In Luttge U, Beyschlag W, Francic D, Cushman J, eds, *Prog. Bot.* Springer Berlin, Heidelberg, Germany, pp 37–100
- Baker DA** (2000) Long-distance vascular transport of endogenous hormones in plants and their role in source:sink regulation. *Isr J Plant Sci* **48**: 199–203
- Bennett MJ, Marchant A, Green HG, May ST, Ward SP, Millner PA, Walker AR, Schulz B, Feldmann KA** (1996) Arabidopsis *AUX1* gene: A permease-like regulator of root gravitropism. *Science* **273**: 948–950
- Berry T, Bewley JD** (1991) Seeds of tomato (*Lycopersicon esculentum* Mill.) which develop in a fully hydrated environment in the fruit switch from a developmental to a germinative mode without a requirement for desiccation. *Planta* **186**: 27–34
- Blakeslee JJ, Bandyopadhyay A, Lee OR, Mravec J, Titapiwatanakun B, Sauer M, Makam SN, Cheng Y, Bouchard R, Adamec J, et al** (2007) Interactions among PIN-FORMED and P-Glycoprotein auxin transporters in *Arabidopsis*. *Plant Cell* **19**: 131-147
- Blakeslee JJ, Peer WA, Murphy AS** (2005) Auxin transport. *Curr Opin Plant Biol* **8**: 494–500
- Borkovec V, Didehvar F, Baker DA** (1994) The biosynthesis and translocation of ¹⁴C-IAA in

- Ricinus communis*. Plant Growth Regul **15**: 137–141
- Brown KM** (1997) Ethylene and abscission. Physiol Plant **100**: 567–576
- Brunoud G, Wells DM, Oliva M, Larrieu A, Mirabet V, Burrow AH, Beeckman T, Kepinski S, Traas J, Bennett MJ, et al** (2012) A novel sensor to map auxin response and distribution at high spatio-temporal resolution. Nature **482**: 103–106
- Cambridge AP, Morris DA** (1996) Transfer of exogenous auxin from the phloem to the polar auxin transport pathway in pea (*Pisum sativum* L.). Planta **199**: 583–588
- Carrier DJ, Bakar NTA, Swarup R, Callaghan R, Napier RM, Bennett MJ, Kerr ID** (2008) The binding of auxin to the Arabidopsis auxin influx transporter AUX1. Plant Physiol **148**: 529–535
- Ceccato L, Masiero S, Roy DS, Bencivenga S, Roig-Villanova I, Ditengou FA, Palme K, Simon R, Colombo L** (2013) Maternal control of PIN1 is required for female gametophyte development in Arabidopsis. PLoS One **8**: e66148
- Chapman EJ, Estelle M** (2009) Mechanism of auxin-regulated gene expression in plants. Annu Rev Genet **47**:265-286
- Chauvaux N, Child R, John K, Ulvskov P, Borkhardt B, Prinsen E, Van Onckelen HA** (1997) The role of auxin in cell separation in the dehiscence zone of oilseed rape pods. J Exp Bot **48**: 1423–1429
- Chawla R, DeMason DA** (2004) Molecular expression of *PsPIN1*, a putative auxin efflux carrier gene from pea (*Pisum sativum* L.). Plant Growth Regul **44**: 1–14
- Chen D, Zhao J** (2008) Free IAA in stigmas and styles during pollen germination and pollen tube growth of *Nicotiana tabacum*. Physiol Plant **134**: 202–215
- Chen R, Hilson P, Sedbrook J, Rosen E, Caspar T, Masson PH** (1998) The *Arabidopsis thaliana* *AGRAVITROPIC 1* gene encodes a component of the polar-auxin-transport efflux carrier. Proc Natl Acad Sci **95**: 15112–15117
- Cleland RE** (1995) Auxin and cell elongation. In PJ Davies, ed, Plant Hormones: Physiology, Biochemistry and Molecular Biology. Springer Netherlands, Dordrecht, pp 214–227

- Cobb AH, Reade JPH** (2010) Auxin-type herbicides. *Herbic. Plant Physiol.*, Second ed. Wiley-Blackwell, pp 133-156
- Cooper DC** (1938) Embryology of *Pisum sativum*. *Bot Gaz* **100**: 123–132
- Costantini E, Landi L, Silvestroni O, Pandolfini T, Spena A, Mezzetti B** (2007) Auxin synthesis-encoding transgene enhances grape fecundity. *Plant Physiol* **143**: 1689–1694
- Cui W, Wang X, Lee J-Y** (2015) Drop-and-see: A simple, real-time, and noninvasive technique for assaying plasmodesmal permeability. . *In* M Heinlein, ed, *Plasmodesmata: Methods and Protocols*. Springer New York, New York, NY, pp 149–156
- Davies PJ** (2010) The plant hormones: Their nature, occurrence, and functions. *In* PJ Davies, ed, *Plant Hormones: Biosynthesis, Signal Transduction, Action*. Springer Netherlands, Dordrecht, pp 1–15
- DeMason DA, Polowick PL** (2009) Patterns of DR5:: GUS expression in organs of pea (*Pisum sativum*). *Int J Plant Sci* **170**: 1–11
- Do-Thanh CL, Vargas JJ, Thomas JW, Armel GR, Best MD** (2016) Design, synthesis, and evaluation of novel auxin mimic herbicides. *J Agric Food Chem* **64**: 3533–3537
- Dorcey E, Urbez C, Blázquez MA, Carbonell J, Perez-Amador MA** (2009) Fertilization-dependent auxin response in ovules triggers fruit development through the modulation of gibberellin metabolism in Arabidopsis. *Plant J* **58**: 318–332
- Dražeta L, Lang A, Cappellini C, Hall AJ, Volz RK, Jameson PE** (2004) Vessel differentiation in the pedicel of apple and the effects of auxin transport inhibition. *Physiol Plant* **120**: 162–170
- Eeuwens CJ, Schwabe WW** (1975) Seed and pod wall development in *Pisum sativum*, L. in relation to extracted and applied hormones. *J Exp Bot* **26**: 1–14
- Else MA, Stankiewicz-Davies AP, Crisp CM, Atkinson CJ** (2004) The role of polar auxin transport through pedicels of *Prunus avium* L. in relation to fruit development and retention. *J Exp Bot* **55**: 2099–2109
- Ernstsen A, Sandberg G** (1986) Identification of 4-chloroindole-3-acetic acid and indole-3-

- aldehyde in seeds of *Pinus sylvestris*. *Physiol Plant* **68**: 511–518
- Ferro N, Bredow T, Jacobsen H-J, Reinard T** (2010) Route to novel auxin: auxin chemical space toward biological correlation carriers. *Chem Rev* **110**: 4690–4708
- Figueiredo DD, Batista RA, Roszak PJ, Hennig L, Köhler C** (2016) Auxin production in the endosperm drives seed coat development in *Arabidopsis*. *Elife* **5**: e20542
- Friml J, Vieten A, Sauer M, Weijers D, Schwarz H, Hamann T, Offringa R, Jürgens G** (2003) Efflux-dependent auxin gradients establish the apical–basal axis of *Arabidopsis*. *Nature* **426**: 147
- Gälweiler L, Guan C, Müller A, Wisman E, Mendgen K, Yephremov A, Palme K** (1998) Regulation of polar auxin transport by AtPIN1 in *Arabidopsis* vascular tissue. *Science* **282**: 2226–2229
- Garcia-Luis A, Oliveira MEM, Bordon Y, Siqueira DL, Tominaga S, Guardiola JL** (2002) Dry matter accumulation in citrus fruit is not limited by transport capacity of the pedicel. *Ann Bot* **90**: 755–764
- Geldner N, Friml J, Stierhof Y-D, Jürgens G, Palme K** (2001) Auxin transport inhibitors block PIN1 cycling and vesicle trafficking. *Nature* **413**: 425–428
- Gianfagna T** (1995) Natural and synthetic growth regulators and their use in horticultural and agronomic crops. In PJ Davies, ed, *Plant Hormones: Physiology, Biochemistry and Molecular biology*. Springer Netherlands, Dordrecht, pp 751–773
- Glazinska P, Wojciechowski W, Kulasek M, Glinkowski W, Marciniak K, Klajn N, Kesy J, Kopcewicz J** (2017) *De novo* transcriptome profiling of flowers, flower pedicels and pods of *Lupinus luteus* (Yellow Lupine) reveals complex expression changes during organ abscission. *Front Plant Sci* **8**: 641
- Goetz M, Hooper LC, Johnson SD, Rodrigues JCM, Vivian-Smith A, Koltunow AM** (2007) Expression of aberrant forms of *AUXIN RESPONSE FACTOR8* stimulates parthenocarpy in *Arabidopsis* and Tomato. *Plant Physiol* **145**: 351–366
- Grossmann K** (2007) Auxin herbicide action: lifting the veil step by step. *Plant Signal Behav* **2**:

421–423

- Grossmann K** (2010) Auxin herbicides: current status of mechanism and mode of action. *Pest Manag Sci* **66**: 113–120
- Gustafson FG** (1936) Inducement of fruit development by growth-promoting chemicals. *Proc Natl Acad Sci* **22**: 628–636
- Gustafson FG** (1942) Parthenocarpy: Natural and artificial. *Bot Rev* **8**: 599–654
- Hamamoto H, Shishido Y, Furuya S, Yasuba K** (1998) Growth and development of tomato fruit as affected by 2, 3, 5-Triiodobenzoic acid (TIBA) applied to the peduncle. *J Japanese Soc Hortic Sci* **67**: 210–212
- Hoad G V** (1995) Transport of hormones in the phloem of higher plants. *Plant Growth Regul* **16**: 173–182
- Homan DN** (1964) Auxin transport in the physiology of fruit development. *Plant Physiol* **39**: 982–986
- van Huizen R, Ozga JA, Reinecke DM** (1997) Seed and hormonal regulation of *gibberellin 20-oxidase* expression in pea pericarp. *Plant Physiol* **115**: 123 LP-128
- van Huizen R, Ozga JA, Reinecke DM, Twitchin B, Mander LN** (1995) Seed and 4-chloroindole-3-acetic acid regulation of gibberellin metabolism in pea pericarp. *Plant Physiol* **109**: 1213 LP-1217
- Hull GA, Devic M** (1995) The β -Glucuronidase (*gus*) reporter gene system gene fusions; spectrometric, fluorometric, and histochemical detection. *In* H Jones, ed, *Plant Gene Transfer and Expression Protocols*. Springer New York, Totowa, NJ, pp 125–141
- Ito Y, Nakano T** (2015) Development and regulation of pedicel abscission in tomato. *Front Plant Sci.* **6**: 442
- Jayasinghe CPA** (2017) Characterization of auxin receptors and auxin-ethylene interaction during pea fruit development. PhD Thesis. University of Alberta
- Jefferson RA** (1987) Assaying chimeric genes in plants: the *GUS* gene fusion system. *Plant Mol Biol Report* **5**: 387–405

- Johnstone MMG, Reinecke DM, Ozga JA** (2005) The auxins IAA and 4-Cl-IAA differentially modify gibberellin action via ethylene response in developing pea fruit. *J Plant Growth Regul* **24**: 214–225
- Katekar GF, Geissler AE** (1980) Auxin transport inhibitors. *Plant Physiol* **66**: 1190 LP-1195
- Kim IS, Okubo H, Fujieda K** (1992) Endogenous levels of IAA in relation to parthenocarp in cucumber (*Cucumis sativus* L.). *Sci Hortic (Amsterdam)* **52**: 1–8
- Kramer EM, Bennett MJ** (2006) Auxin transport: a field in flux. *Trends Plant Sci* **11**: 382–386
- Křeček P, Skůpa P, Libus J, Naramoto S, Tejos R, Friml J, Zažímalová E** (2009) The PIN-FORMED (PIN) protein family of auxin transporters. *Genome Biol* **10**: 249
- Kumar R, Khurana A, Sharma AK** (2014) Role of plant hormones and their interplay in development and ripening of fleshy fruits. *J Exp Bot* **65**: 4561–4575
- Kumar R, Tyagi AK, Sharma AK** (2011) Genome-wide analysis of auxin response factor (ARF) gene family from tomato and analysis of their role in flower and fruit development. *Mol Genet Genomics* **285**: 245-260
- Lam HK, McAdam, Scott AM, McAdam EL, Ross JJ** (2015) Evidence that chlorinated auxin is restricted to the Fabaceae but not to the Fabeae. *Plant Physiol* **168**: 798-803
- Larsson E, Vivian-Smith A, Offringa R, Sundberg E** (2017) Auxin homeostasis in arabidopsis ovules is anther-dependent at maturation and changes dynamically upon fertilization. *Front Plant Sci* **8**: 1735
- Lemaire-Chamley M, Petit J, Garcia V, Just D, Baldet P, Germain V, Fagard M, Mouassite M, Cheniclet C, Rothan C** (2005) Changes in transcriptional profiles are associated with early fruit tissue specialization in tomato. *Plant Physiol* **139**: 750-769
- Liao C-Y, Smet W, Brunoud G, Yoshida S, Vernoux T, Weijers D** (2015) Reporters for sensitive and quantitative measurement of auxin response. *Nat Methods* **12**: 207–210
- Ligerot Y, de Saint Germain A, Waldie T, Troadec C, Citerne S, Kadakia N, Pillot J-P, Prigge M, Aubert G, Bendahmane A, et al** (2017) The pea branching *RMS2* gene encodes the *PsAFB4/5* auxin receptor and is involved in an auxin-strigolactone regulation loop.

- Ljung K, Bhalerao RP, Sandberg G** (2001) Sites and homeostatic control of auxin biosynthesis in *Arabidopsis* during vegetative growth. *Plant J* **28**: 465–474
- Lomax TL, Mehlhorn RJ, Briggs WR** (1985) Active auxin uptake by zucchini membrane vesicles: quantitation using ESR volume and delta pH determinations. *Proc Natl Acad Sci* **82**: 6541–6545
- Lomax TL, Muday GK, Rubery PH** (1995) Auxin transport. *In* PJ Davies, ed, *Plant Hormones: Physiology, Biochemistry and Molecular Biology*. Springer Netherlands, Dordrecht, pp 509–530
- Luschnig C** (2001) Auxin transport: Why plants like to think BIG. *Curr Biol* **11**: R831–R833
- Luschnig C, Gaxiola RA, Grisafi P, Fink GR** (1998) EIR1, a root-specific protein involved in auxin transport, is required for gravitropism in *Arabidopsis thaliana*. *Genes Dev* **12**: 2175–2187
- Ma C, Meir S, Xiao L, Tong J, Liu Q, Reid MS, Jiang C-Z** (2015) A KNOTTED1-LIKE HOMEODOMAIN protein regulates abscission in tomato by modulating the auxin pathway. *Plant Physiol* **167**: 844–853
- Magnus V, Ozga JA, Reinecke DM, Pierson GL, Larue TA, Cohen JD, Brenner ML** (1997) 4-chloroindole-3-acetic and indole-3-acetic acids in *Pisum sativum*. *Phytochemistry* **46**: 675–681
- Martinoia E, Klein M, Geisler M, Bovet L, Forestier C, Kolukisaoglu U, Muller-Rober B, Schulz B** (2002) Multifunctionality of plant ABC transporters—more than just detoxifiers. *Planta* **214**: 345–355
- McAtee P, Karim S, Schaffer R, David K** (2013) A dynamic interplay between phytohormones is required for fruit development, maturation, and ripening. *Front Plant Sci* **4**: 79
- Meir S, Philosoph-Hadas S, Sundaresan S, Selvaraj KSV, Burd S, Ophir R, Kochanek B, Reid MS, Jiang C-Z, Lers A** (2010) Microarray analysis of the abscission-related transcriptome in the tomato flower abscission zone in response to auxin depletion. *Plant*

Physiol **154**: 1929–1956

Meir S, Sundaresan S, Riov J, Agarwal I, Philosoph-Hadas S (2015) Role of auxin depletion in abscission control. *Stewart Postharvest Rev* **11**: 1–15

Michniewicz M, Brewer PB, Friml J (2007) Polar auxin transport and asymmetric auxin distribution. *Arabidopsis Book* **5**: e0108

Mir R, Aranda LZ, Biaocchi T, Luo A, Sylvester AW, Rasmussen CG (2017) A DII domain-based auxin reporter uncovers low auxin signaling during telophase and early G1. *Plant Physiol* **173**: 863–871

Morris DA (2000) Transmembrane auxin carrier systems—dynamic regulators of polar auxin transport. *Plant Growth Regul* **32**: 161–172

Morris DA, Friml J, Zažímalová E (2010) The transport of auxins. *In* PJ Davies, ed, *Plant Hormones: Biosynthesis, Signal Transduction, Action*. Springer Netherlands, Dordrecht, pp 451–484

Morris DA, Rubery PH, Jarman J, Sabater M (1991) Effects of inhibitors of protein synthesis on transmembrane auxin transport in *Cucurbita pepo* L. hypocotyl segments. *J Exp Bot* **42**: 773–783

Morris DA, Thomas AG (1978) A microautoradiographic study of auxin transport in the stem of intact pea seedlings (*Pisum sativum* L.). *J Exp Bot* **29**: 147–157

Muday GK, DeLong A (2001) Polar auxin transport: controlling where and how much. *Trends Plant Sci* **6**: 535–542

Muday GK, Murphy AS (2002) An emerging model of auxin transport regulation. *Plant Cell* **14**: 293–299

Müller A, Guan C, Gälweiler L, Tänzler P, Huijser P, Marchant A, Parry G, Bennett M, Wisman E, Palme K (1998) *AtPIN2* defines a locus of *Arabidopsis* for root gravitropism control. *EMBO J* **17**: 6903–6911

Müntz K, Rudolph A, Schlesier G, Silhengst P (1978) The function of the pericarp in fruits of crop legumes. *Die Kult* **26**: 37–67

- Nadeau CD** (2009) Hormone metabolism and action in developing pea fruit. MSc Thesis.
University of Alberta
- Ngo P, Ozga JA, Reinecke DM** (2002) Specificity of auxin regulation of *gibberellin 20-oxidase* gene expression in pea pericarp. *Plant Mol Biol* **49**: 439–448
- Nishio S, Moriguchi R, Ikeda H, Takahashi H, Fujii N, Guilfoyle TJ, Kanahama K, Kanayama Y** (2010) Expression analysis of the auxin efflux carrier family in tomato fruit development. *Planta* **232**: 755-764
- Noh B, Murphy AS, Spalding EP** (2001) *Multidrug resistance*-like genes of arabidopsis required for auxin transport and auxin-mediated development. *Plant Cell* **13**: 2441–2454
- Oberholster SD, Peterson CM, Dute RR** (1991) Pedicel abscission of soybean: cytological and ultrastructural changes induced by auxin and ethephon. *Can J Bot* **69**: 2177–2186
- Obroucheva N V** (2014) Hormonal regulation during plant fruit development. *Russ J Dev Biol* **45**: 11–21
- Okada K, Ueda J, Komaki MK, Bell CJ, Shimura Y** (1991) Requirement of the auxin polar transport system in early stages of *Arabidopsis* floral bud formation. *Plant Cell* **3**: 677–684
- Ostrowski M, Mierek-Adamska A, Porowińska D, Goc A, Jakubowska A** (2016) Cloning and biochemical characterization of indole-3-acetic acid-amino acid synthetase PsGH3 from pea. *Plant Physiol Biochem* **107**: 9–20
- Ozga JA, Brenner ML, Reinecke DM** (1992) Seed effects on gibberellin metabolism in pea pericarp. *Plant Physiol* **100**: 88–94
- Ozga JA, van Huizen R, Reinecke DM** (2002) Hormone and seed-specific regulation of pea fruit growth. *Plant Physiol* **128**: 1379–1389
- Ozga JA, Reinecke DM** (1999) Interaction of 4-chloroindole-3-acetic acid and gibberellins in early pea fruit development. *Plant Growth Regul* **27**: 33–38
- Ozga JA, Reinecke DM** (2003) Hormonal interactions in fruit development. *J Plant Growth Regul* **22**: 73–81
- Ozga JA, Reinecke DM, Ayele BT, Ngo P, Nadeau C, Wickramarathna AD** (2009)

- Developmental and hormonal regulation of gibberellin biosynthesis and catabolism in pea fruit. *Plant Physiol* **150**: 448–462
- Ozga JA, Yu J, Reinecke DM** (2003) Pollination-, development-, and auxin-specific regulation of Gibberellin 3 β -hydroxylase gene expression in pea fruit and seeds. *Plant Physiol* **131**: 1137–1146
- Palme K, Gälweiler L** (1999) PIN-pointing the molecular basis of auxin transport. *Curr Opin Plant Biol* **2**: 375–381
- Pattison RJ, Catalá C** (2012) Evaluating auxin distribution in tomato (*Solanum lycopersicum*) through an analysis of the *PIN* and *AUX/LAX* gene families. *Plant J* **70**: 585–598
- Pattison RJ, Csukasi F, Zheng Y, Fei Z, van der Knaap E, Catalá C** (2015) Comprehensive tissue-specific transcriptome analysis reveals distinct regulatory programs during early tomato fruit development. *Plant Physiol* **168**: 1684 -1701
- Petrášek J, Friml J** (2009) Auxin transport routes in plant development. *Development* **136**: 2675 LP-2688
- Petrášek J, Mravec J, Bouchard R, Blakeslee JJ, Abas M, Seifertová D, Wiśniewska J, Tadele Z, Kubeš M, Čovanová M, et al** (2006) PIN proteins perform a rate-limiting function in cellular auxin efflux. *Science* (80-) **312**: 914 -918
- Rashotte AM, Brady SR, Reed RC, Ante SJ, Muday GK** (2000) Basipetal auxin transport is required for gravitropism in roots of arabidopsis. *Plant Physiol* **122**: 481–490
- Raven JA** (1975) Transport of indoleacetic acid in plant cells in relation to pH and electrical potential gradients, and its significance for polar IAA transport. *New Phytol* **74**: 163–172
- Reinecke DM** (1999) 4-Chloroindole-3-acetic acid and plant growth. *Plant Growth Regul* **27**: 3–13
- Reinecke DM, Ozga JA, Magnus V** (1995) Effect of halogen substitution of indole-3-acetic acid on biological activity in pea fruit. *Phytochemistry* **40**: 1361–1366
- Rubery PH** (1978) Hydrogen ion dependence of carrier-mediated auxin uptake by suspension-cultured crown gall cells. *Planta* **142**: 203–206

- Rubery PH, Sheldrake AR** (1974) Carrier-mediated auxin transport. *Planta* **118**: 101–121
- Sastry K, Muir RM** (1965) Transport of indoleacetic acid in pedicels of tomato and its relation to fruit growth. *Bot Gaz* **126**: 13–19
- Schlicht M, Ludwig-Müller J, Burbach C, Volkmann D, Baluska F** (2013) Indole-3-butyric acid induces lateral root formation via peroxisome-derived indole-3-acetic acid and nitric oxide. *New Phytol* **200**: 473–482
- Serrani JC, Carrera E, Ruiz-Rivero O, Gallego-Giraldo L, Peres LEP, García-Martínez JL** (2010) Inhibition of auxin transport from the ovary or from the apical shoot induces parthenocarpic fruit-set in tomato mediated by gibberellins. *Plant Physiol* **153**: 851–862
- Serrani JC, Ruiz-Rivero O, Fos M, García-Martínez JL** (2008) Auxin-induced fruit-set in tomato is mediated in part by gibberellins. *Plant J* **56**: 922–934
- Simon S, Petrášek J** (2011) Why plants need more than one type of auxin. *Plant Sci* **180**: 454–460
- Smýkal P** (2014) Pea (*Pisum sativum* L.) in biology prior and after Mendel's discovery. *Czech J Genet Plant Breed* **50**: 52–64
- Sorefan K, Girin T, Liljegren SJ, Ljung K, Robles P, Galván-Ampudia CS, Offringa R, Friml J, Yanofsky MF, Østergaard L** (2009) A regulated auxin minimum is required for seed dispersal in *Arabidopsis*. *Nature* **459**: 583
- Sugawara S, Mashiguchi K, Tanaka K, Hishiyama S, Sakai T, Hanada K, Kinoshita-Tsujimura K, Yu H, Dai X, Takebayashi Y, et al** (2015) Distinct characteristics of indole-3-acetic acid and phenylacetic acid, two common auxins in plants. *Plant Cell Physiol* **56**: 1641–1654
- Sundberg E, Østergaard L** (2009) Distinct and dynamic auxin activities during reproductive development. *Cold Spring Harb Perspect Biol* **1**: a001628
- Sutcliffe JF, Pate JS** (1977) *The physiology of the garden pea*. Academic Press, London
- Terasaka K, Blakeslee JJ, Titapiwatanakun B, Peer WA, Bandyopadhyay A, Makam SN, Lee OR, Richards EL, Murphy AS, Sato F, et al** (2005) PGP4, an ATP binding cassette

- P-Glycoprotein, catalyzes auxin transport in *Arabidopsis thaliana* roots. *Plant Cell* **17**: 2922 LP-2939
- Thimann K V** (1952) Plant growth hormones. In KV Thimann, ed, *The Action of Hormones in Plants and Invertebrates*. Academic Press, pp 1–76
- Thomson K-S, Hertel R, Müller S, Tavares JE** (1973) 1-N-naphthylphthalamic acid and 2, 3, 5-triiodobenzoic acid. *Planta* **109**: 337–352
- Titapiwatanakun B, Murphy AS** (2009) Post-transcriptional regulation of auxin transport proteins: cellular trafficking, protein phosphorylation, protein maturation, ubiquitination, and membrane composition. *J Exp Bot* **60**: 1093–1107
- Tivendale ND, Davidson SE, Davies NW, Smith JA, Dalmais M, Bendahmane AI, Quittenden LJ, Sutton L, Bala RK, Le Signor C, et al** (2012) Biosynthesis of the halogenated auxin, 4-chloroindole-3-acetic acid. *Plant Physiol* **159**: 1055 LP-1063
- Tranbarger TJ, Tucker ML, Roberts JA, Meir S** (2017) Plant organ abscission: from models to crops. *Front Plant Sci* **8**: 196
- Truernit E** (2014) Phloem imaging. *J Exp Bot* **65**: 1681–1688
- Ulmasov T, Liu Z-B, Hagen G, Guilfoyle TJ** (1995) Composite structure of auxin response elements. *Plant Cell* **7**: 1611–1623
- Ulmasov T, Murfett J, Hagen G, Guilfoyle TJ** (1997) Aux/IAA proteins repress expression of reporter genes containing natural and highly active synthetic auxin response elements. *Plant Cell* **9**: 1963-1971
- Vernoux T, Brunoud G, Farcot E, Morin V, Van den Daele H, Legrand J, Oliva M, Das P, Larrieu A, Wells D** (2011) The auxin signalling network translates dynamic input into robust patterning at the shoot apex. *Mol Syst Biol* **7**: 508
- Vieten A, Sauer M, Brewer PB, Friml J** (2007) Molecular and cellular aspects of auxin-transport-mediated development. *Trends Plant Sci* **12**: 160–168
- Wang H, Jones B, Li Z, Frasse P, Delalande C, Regad F, Chaabouni S, Latche A, Pech JC, Bouzayen M** (2005) The tomato *Aux/IAA* transcription factor *IAA9* is involved in fruit

development and leaf morphogenesis. *Plant Cell* **17**: 2676-2692

Wang R, Estelle M (2014) Diversity and specificity: auxin perception and signaling through the TIR1/AFB pathway. *Curr Opin Plant Biol* **21**: 51–58

Went FW (1926) On growth-accelerating substances in the coleoptile of *Avena sativa*. *Proc. Kon. Ned. Akad. Wet* **30**: 10-19

Went FW, Thimann K V (1937) *Phytohormones* MacMillan, New York, New York, USA

Wolters H, Jürgens G (2009) Survival of the flexible: hormonal growth control and adaptation in plant development. *Nat Rev Genet* **10**: 305-317

Yamamoto M, Yamamoto KT (1998) Differential effects of 1-naphthaleneacetic acid, indole-3-acetic acid and 2,4-dichlorophenoxyacetic acid on the gravitropic response of roots in an auxin-resistant mutant of *Arabidopsis*, *aux1*. *Plant Cell Physiol* **39**: 660–664

Yang Y, Hammes UZ, Taylor CG, Schachtman DP, Nielsen E (2006) High-affinity auxin transport by the AUX1 influx carrier protein. *Curr Biol* **16**: 1123–1127

Yin Z, Robert M, Agnieszka Z, Hans Somme R, Wojciech P, Stefan M (2006) The *DefH9-iaaM*-containing construct efficiently induces parthenocarpy in cucumber. *Cell Mol Biol Lett* **11**: 279

Appendix A

Supporting micrographs

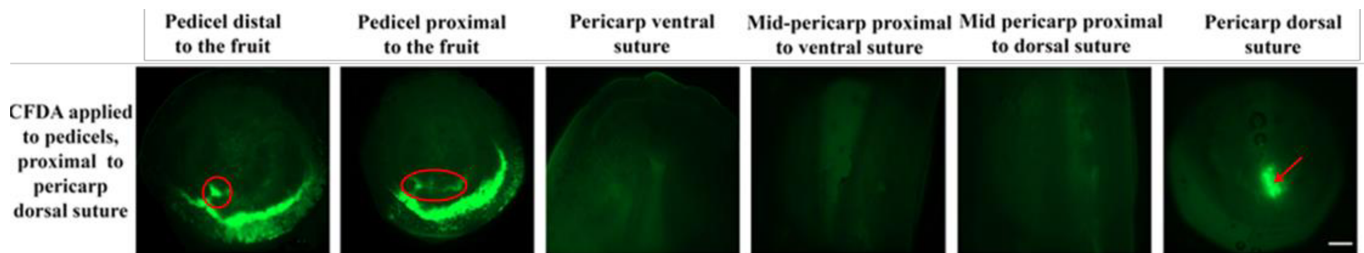


Figure A1. Representative micrographs of 5 (6)-carboxyfluorescein diacetate (CFDA) fluorescence (green color) patterns in the pedicels and pericarps of 4-6 DAA pea inflorescences. CFDA green fluorescence observed in the pericarp dorsal suture and pedicel tissues 4 hr after the application of CFDA to the pedicles proximal to the pericarp dorsal suture. In the pedicel, CFDA green fluorescence was observed mainly in the cortical tissue, with a small amount observed in the vasculature of the pedicel (circled in red). Scale bar = 200 μm .

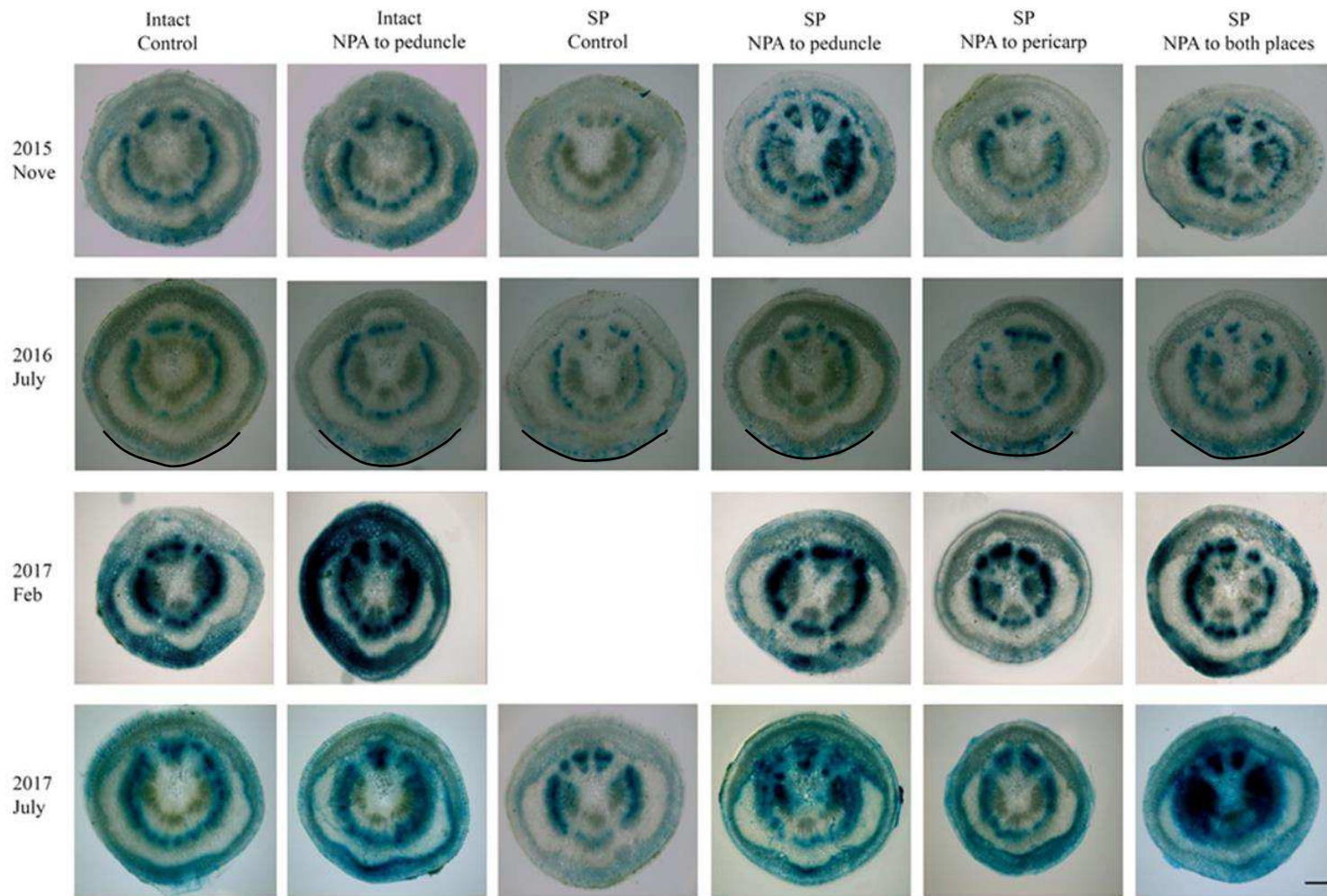


Figure A2. Representative micrographs of pedicel cross-sections showing GUS staining in the cortical region, with more prominent GUS staining usually occurring in the cortical region proximal to the pericarp dorsal suture attachment site (the region marked with a line in the tiles from July 2016). Scale bar = 200 μ m.

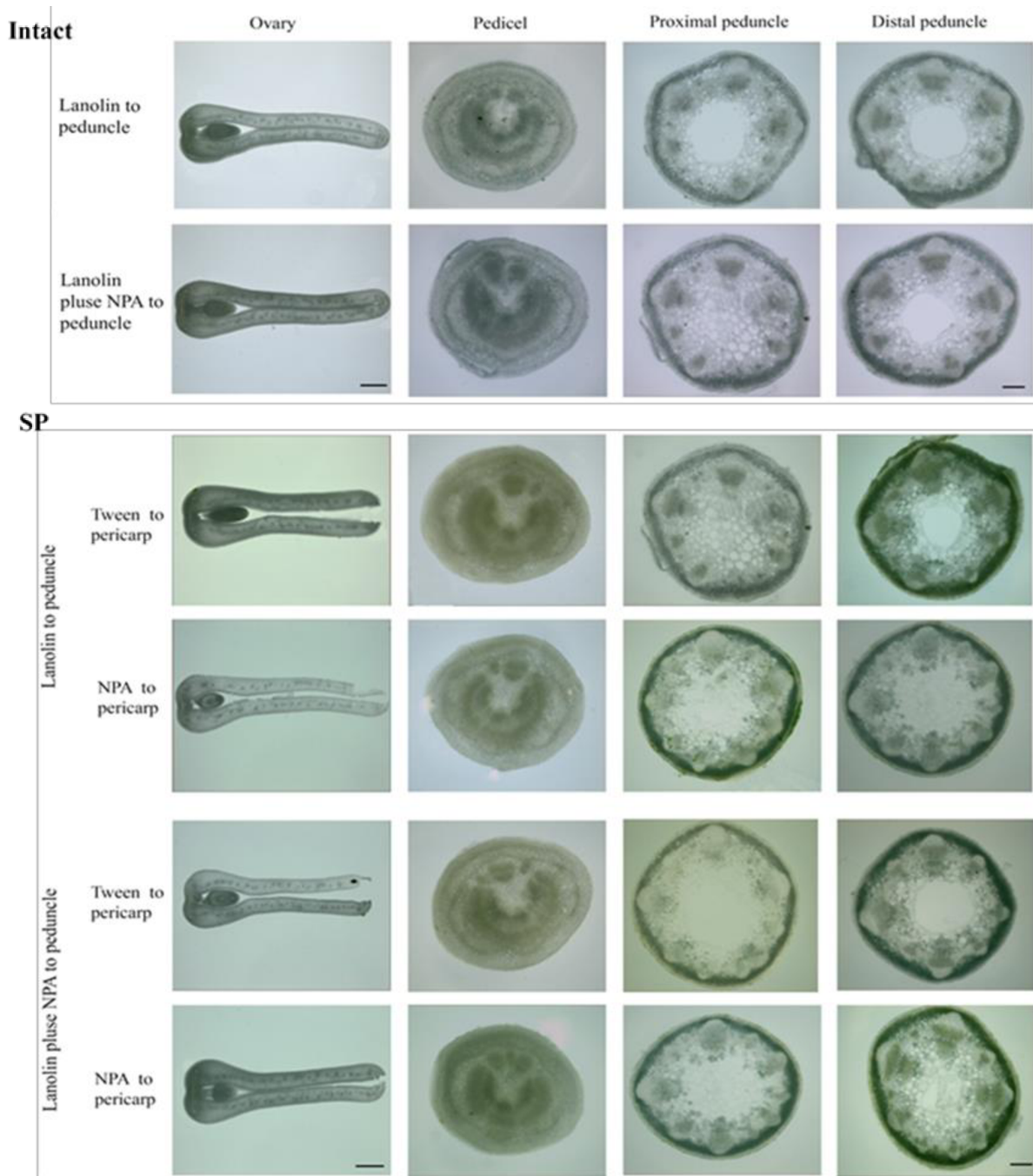


Figure A3. Representative micrographs showing GUS staining patterns in the ovaries of 4 DAA fruits, and the attached pedicel, and proximal and distal peduncle tissues from WT pea plants. The peduncle and/or inner pericarp wall were treated with NPA or control paste/solutions at 2 DAA, and fresh tissue cross-sections were taken from the mid-region of each tissue type at 4 DAA for GUS staining. Ovary scale bar =1000 μ m; pedicel and peduncle scale bar = 200 μ m.

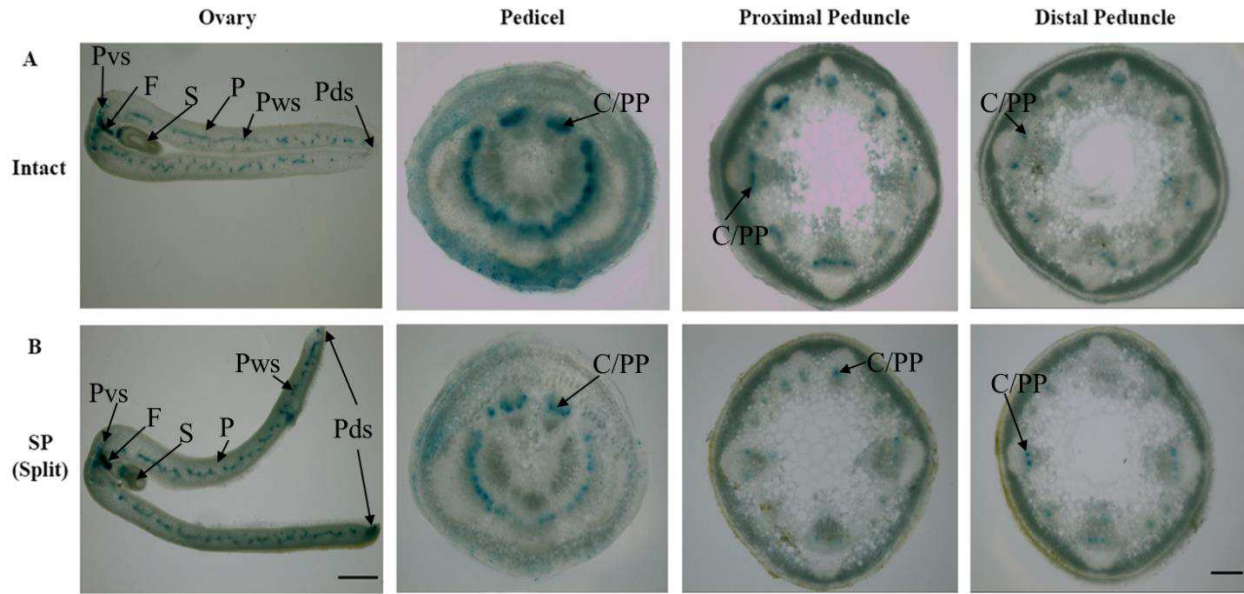


Figure A4. The effect of pericarp splitting on the GUS staining patterns observed in pea fruit and attachment tissues of DR5::GUS expressing pea plants. Representative micrographs of the GUS staining patterns observed in cross-sections of intact (A) and split (B) ovaries (pericarp + seeds) of 4 DAA fruits and the attached pedicel, and proximal and distal peduncle tissues. C/PP, cambium/primary phloem; F, funiculus; P, pericarp; Pds, pericarp dorsal suture; Pvs, pericarp ventral suture; Pws, pericarp wall vasculature; Ph, phloem; S, seed; X, xylem. A and B scale bar = 1000 μ m; C-G scale bar = 200 μ m

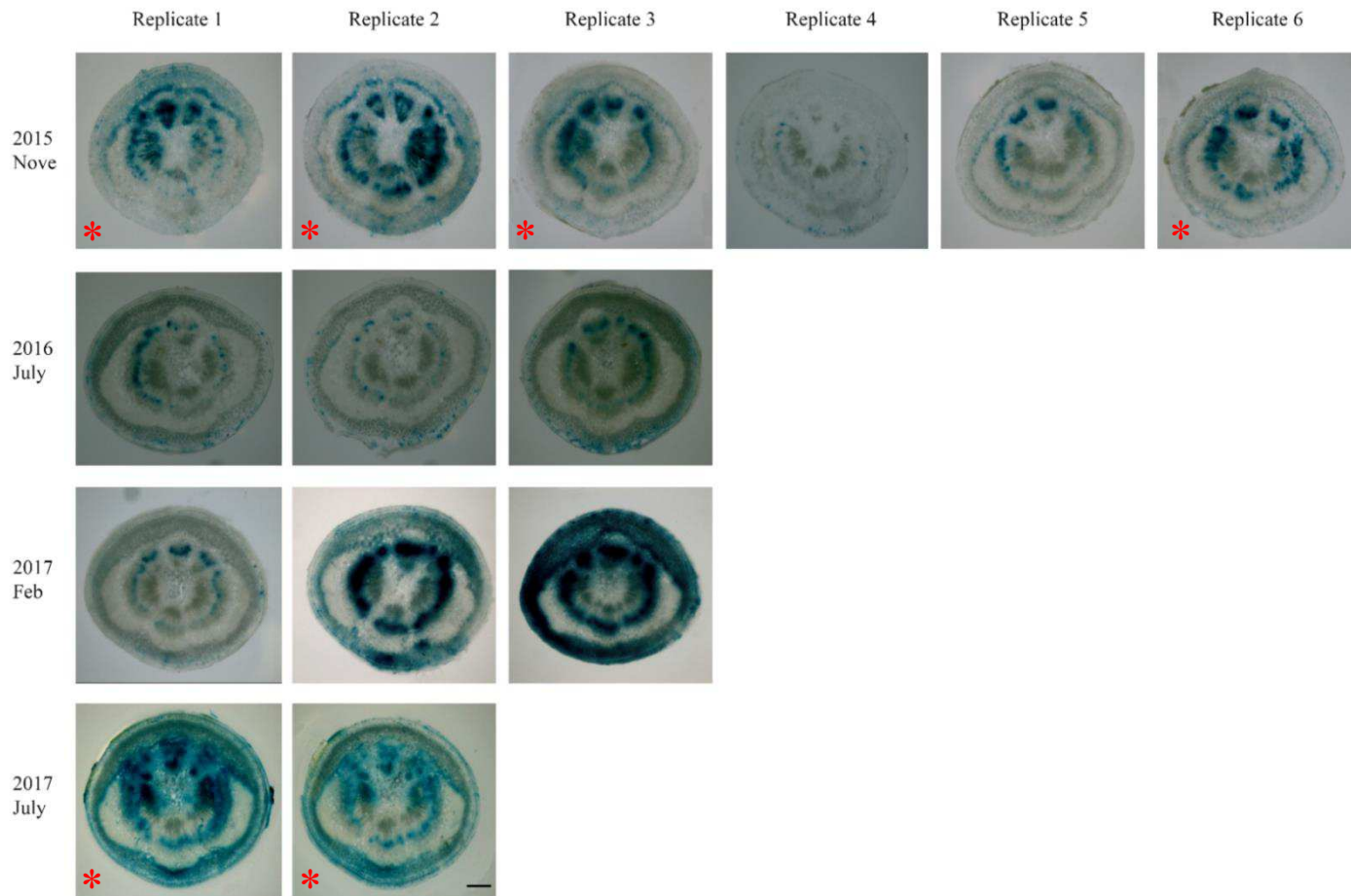


Figure A5. Representative micrographs of pedicel cross-sections showing GUS staining in the primary xylem and the cambium/primary phloem as a result of NPA application to the peduncles of split pericarps (marked with an asterisk). Six out of fourteen pedicel replicates across four independent experiments showed this pattern. Scale bar = 200 μ m.

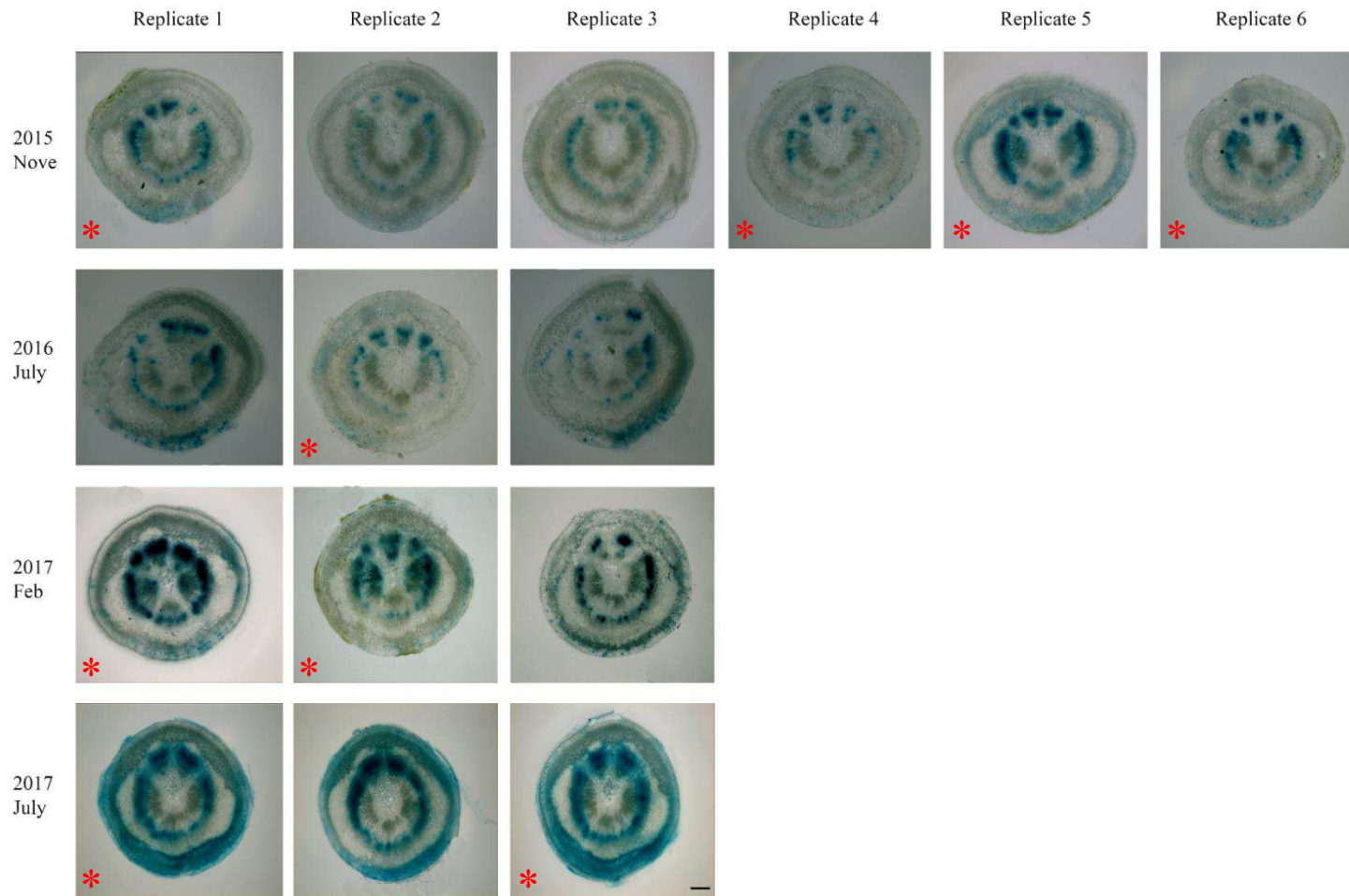


Figure A6. Representative micrographs of pedicel cross-sections showing GUS staining in the primary xylem and the cambium/ primary phloem as result of NPA application to the inner pericarp wall of split pericarps (marked with an asterisk). Nine out of fifteen pedicel replicates across four independent experiments showed this pattern. scale bar = 200 μ m.

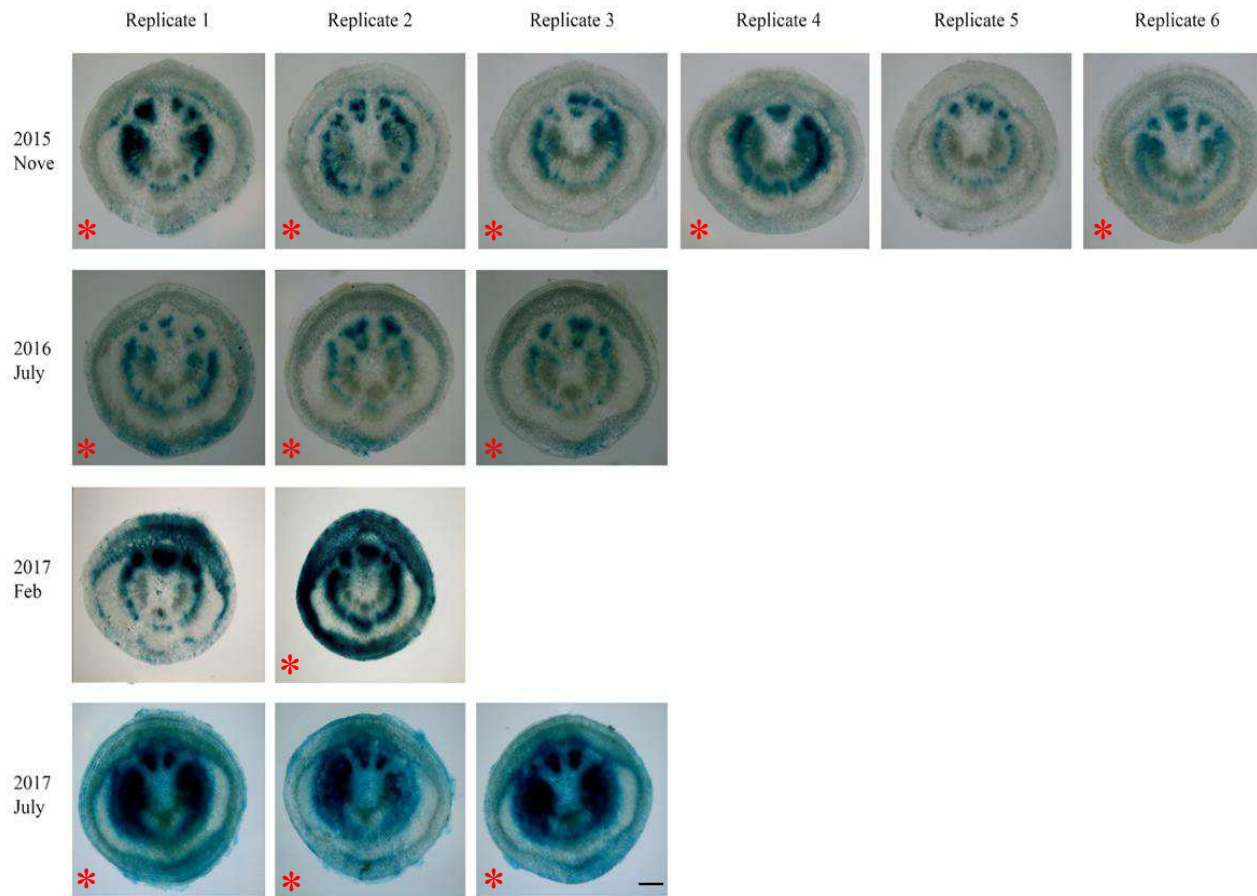


Figure A7. Representative micrographs of pedicel cross-sections showing GUS staining in the primary xylem and the cambium/primary phloem as a result of NPA application to both peduncle and inner pericarp wall of split pericarps (marked with an asterisk). Twelve out of fourteen pedicel replicates across four independent experiments showed this pattern. scale bar = 200 μm .

Appendix B

GUS micrographs from individual experiments

- Figure B1** Representative micrographs showing the GUS staining patterns in intact ovaries from three individual experiments. A and B in 2015 Nov experiment represents the cross-sections taken from the two halves of the pericarp; A-cross-sections taken from the pericarp half proximal to the pedicel and B- cross-sections taken from the pericarp half distal to the pedicel. Scale bar = 1000 μm .
- Figure B2** Representative micrographs showing the GUS staining patterns in pedicels attached to intact ovaries from four individual experiments. A and B in 2015 Nov experiment represents the cross-sections taken from the two halves of the pedicels; A-cross-sections taken from the pedicel half proximal to the pericarp and B- cross-sections taken from the pedicel half distal to the pericarp. Scale bar = 200 μm .
- Figure B3** Representative micrographs showing the GUS staining patterns in proximal peduncles attached to the intact ovaries from four individual experiments. A and B in 2015 Nov experiment represents the cross-sections taken from the two halves of the proximal peduncle; A-cross-sections taken from the peduncle half proximal to the pedicel and B-cross-sections taken from the peduncle half distal to the pedicel. Scale bar = 200 μm .
- Figure B4** Representative micrographs showing the GUS staining patterns in distal peduncles attached to the intact ovaries from four individual experiments. A and B in 2015 Nov experiment represents the cross-sections taken from the two halves of the distal peduncle; A-cross-sections taken from the peduncle half proximal to the pedicel and B-cross-sections taken from the peduncle half distal to the pedicel. Scale bar = 200 μm .
- Figure B5** Representative micrographs showing the GUS staining patterns in intact ovaries treated with NPA to the peduncle from four individual experiments. A and B in 2015 Nov experiment represents the cross-sections taken from the two halves of the pericarp; A-cross-sections taken from the pericarp half proximal to the pedicel and B- cross-sections taken from the pericarp half distal to the pedicel. Scale bar = 1000 μm .
- Figure B6** Representative micrographs showing the GUS staining patterns in pedicels attached to the intact ovaries treated with NPA to the peduncle from four individual experiments. A and B in 2015 Nov experiment represents the cross-sections taken from the two

halves of the pedicels; A-cross-sections taken from the pedicel half proximal to the pericarp and B- cross-sections taken from the pedicel half distal to the pericarp. Scale bar = 200 μm .

Figure B7 Representative micrographs showing the GUS staining patterns in proximal peduncles attached to intact ovaries treated with NPA to the peduncle from four individual experiments. A and B in 2015 Nov experiment represents the cross-sections taken from the two halves of the proximal peduncle; A-cross-sections taken from the peduncle half proximal to the pedicel and B- cross-sections taken from the peduncle half distal to the pedicel. Scale bar = 200 μm .

Figure B8 Representative micrographs showing the GUS staining patterns in distal peduncles attached to the intact ovaries treated with NPA to the peduncle from four individual experiments. A and B in 2015 Nov experiment represents the cross-sections taken from the two halves of the distal peduncle; A-cross-sections taken from the peduncle half proximal to the pedicel and B- cross-sections taken from the peduncle half distal to the pedicel. Scale bar = 200 μm .

Figure B9 Representative micrographs showing the GUS staining patterns in split pericarps from three individual experiments. A and B in 2015 Nov experiment represents the cross-sections taken from the two halves of the pericarp; A-cross-sections taken from the pericarp half proximal to the pedicel and B- cross-sections taken from the pericarp half distal to the pedicel. Scale bar = 1000 μm .

Figure B10 Representative micrographs showing the GUS staining patterns in pedicels attached to split pericarps from three individual experiments. A and B in 2015 Nov experiment represents the cross-sections taken from the two halves of the pedicels; A-cross-sections taken from the pedicel half proximal to the pericarp and B- cross-sections taken from the pedicel half distal to the pericarp. Scale bar = 200 μm .

Figure B11 Representative micrographs showing the GUS staining patterns in proximal peduncles attached to split pericarps from three individual experiments. A and B in 2015 Nov experiment represents the cross-sections taken from the two halves of the proximal peduncle; A-cross-sections taken from the peduncle half proximal to the pedicel and B-cross-sections taken from the peduncle half distal to the pedicel. Scale bar = 200 μm .

Figure B12 Representative micrographs showing the GUS staining patterns in distal peduncles attached to split pericarps from three individual experiments. A and B in 2015 Nov experiment represents the cross-sections taken from the two halves of the distal

peduncle; A-cross-sections taken from the peduncle half proximal to the pedicel and B-cross-sections taken from the peduncle half distal to the pedicel. Scale bar = 200 μm .

Figure B13 Representative micrographs showing the GUS staining patterns in split pericarps treated with NPA to the peduncle from four individual experiments. A and B in 2015 Nov experiment represents the cross-sections taken from the two halves of the pericarp; A-cross-sections taken from the pericarp half proximal to the pedicel and B-cross-sections taken from the pericarp half distal to the pedicel. Scale bar = 1000 μm .

Figure B14 Representative micrographs showing the GUS staining patterns in pedicels attached to the split pericarps treated with NPA to the peduncle from four individual experiments. A and B in 2015 Nov experiment represents the cross-sections taken from the two halves of the pedicels; A-cross-sections taken from the pedicel half proximal to the pericarp and B-cross-sections taken from the pedicel half distal to the pericarp. Scale bar = 200 μm .

Figure B15 Representative micrographs showing the GUS staining patterns in proximal peduncles attached to the split pericarps treated with NPA to the peduncle from four individual experiments. A and B in 2015 Nov experiment represents the cross-sections taken from the two halves of the proximal peduncle; A-cross-sections taken from the peduncle half proximal to the pedicel and B-cross-sections taken from the peduncle half distal to the pedicel. Scale bar = 200 μm .

Figure B16 Representative micrographs showing the GUS staining patterns in distal peduncles attached to the split pericarps treated with NPA to the peduncle from four individual experiments. A and B in 2015 Nov experiment represents the cross-sections taken from the two halves of the distal peduncle; A-cross-sections taken from the peduncle half proximal to the pedicel and B-cross-sections taken from the peduncle half distal to the pedicel. Scale bar = 200 μm .

Figure B17 Representative micrographs showing the GUS staining patterns in split pericarps treated with NPA to the inner pericarp wall from four individual experiments. A and B in 2015 Nov experiment represents the cross-sections taken from the two halves of the pericarp; A-cross-sections taken from the pericarp half proximal to the pedicel and B-cross-sections taken from the pericarp half distal to the pedicel. Scale bar = 1000 μm .

Figure B18 Representative micrographs showing the GUS staining patterns in pedicels attached to the split pericarps treated with NPA to the inner pericarp wall from four individual experiments. A and B in 2015 Nov experiment represents the cross-sections taken from the two halves of the pedicels; A-cross-sections taken from the pedicel half proximal to

the pericarp and B- cross-sections taken from the pedicel half distal to the pericarp. Scale bar = 200 μ m.

Figure B19 Representative micrographs showing the GUS staining patterns in proximal peduncles attached to the split pericarps treated with NPA to the inner pericarp wall from four individual experiments. A and B in 2015 Nov experiment represents the cross-sections taken from the two halves of the proximal peduncle; A-cross-sections taken from the peduncle half proximal to the pedicel and B- cross-sections taken from the peduncle half distal to the pedicel. Scale bar = 200 μ m.

Figure B20 Representative micrographs showing the GUS staining patterns in distal peduncles attached to the split pericarps treated with NPA to the inner pericarp wall from four individual experiments. A and B in 2015 Nov experiment represents the cross-sections taken from the two halves of the distal peduncle; A-cross-sections taken from the peduncle half proximal to the pedicel and B- cross-sections taken from the peduncle half distal to the pedicel. Scale bar = 200 μ m.

Figure B21 Representative micrographs showing the GUS staining patterns in split pericarps treated with NPA to both peduncle and inner pericarp wall from four individual experiments. A and B in 2015 Nov experiment represents the cross-sections taken from the two halves of the pericarp; A-cross-sections taken from the pericarp half proximal to the pedicel and B- cross-sections taken from the pericarp half distal to the pedicel. Scale bar = 1000 μ m.

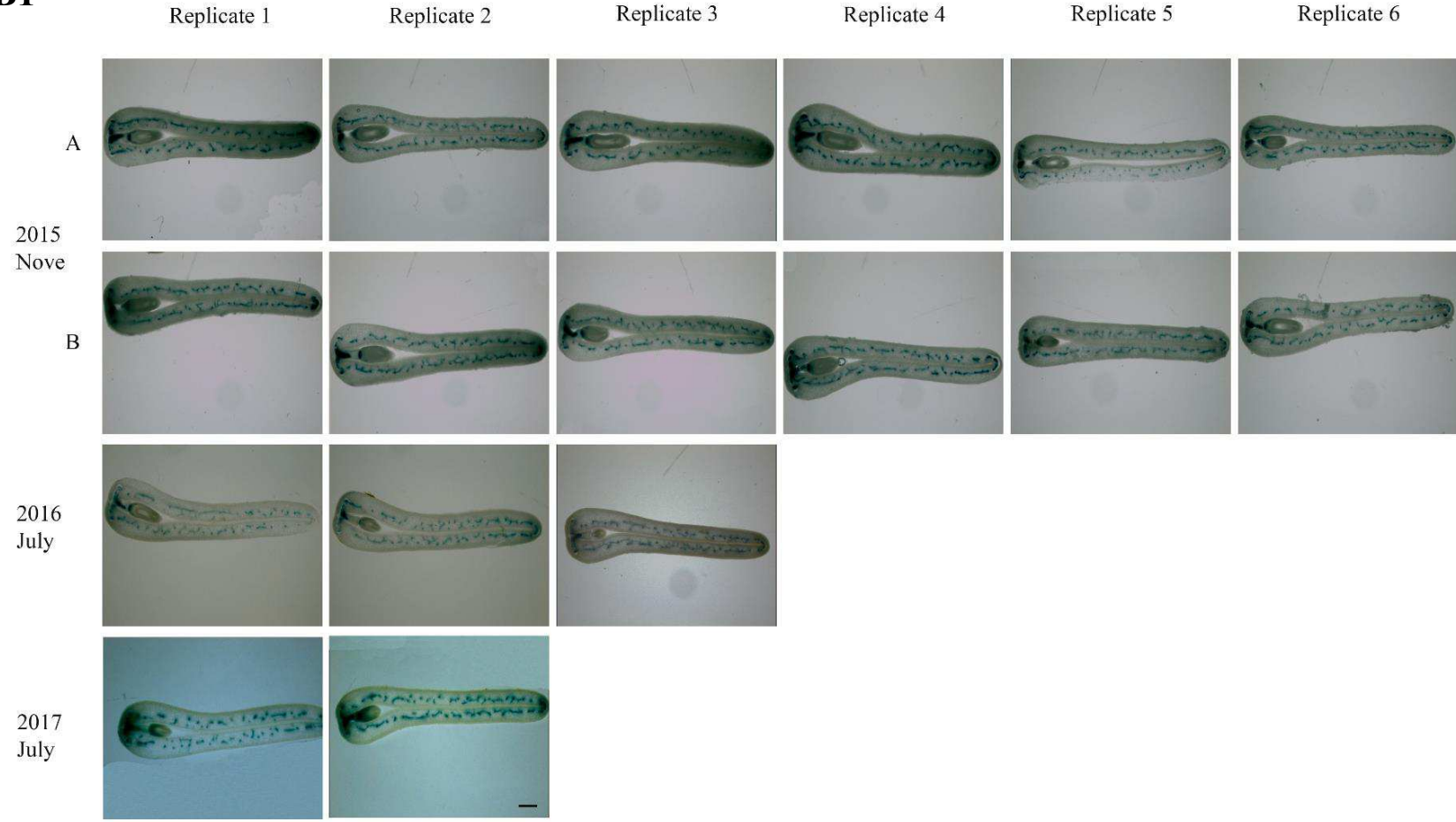
Figure B22 Representative micrographs showing the GUS staining patterns in pedicels attached to the split pericarps treated with NPA to both peduncle and inner pericarp wall from four individual experiments. A and B in 2015 Nov experiment represents the cross-sections taken from the two halves of the pedicels; A-cross-sections taken from the pedicel half proximal to the pericarp and B- cross-sections taken from the pedicel half distal to the pericarp. Scale bar = 200 μ m.

Figure B23 Representative micrographs showing the GUS staining patterns in proximal peduncles attached to the split pericarps treated with NPA to both peduncle and inner pericarp wall from four individual experiments. A and B in 2015 Nov experiment represents the cross-sections taken from the two halves of the proximal peduncle; A-cross-sections taken from the peduncle half proximal to the pedicel and B- cross-sections taken from the peduncle half distal to the pedicel. Scale bar = 200 μ m.

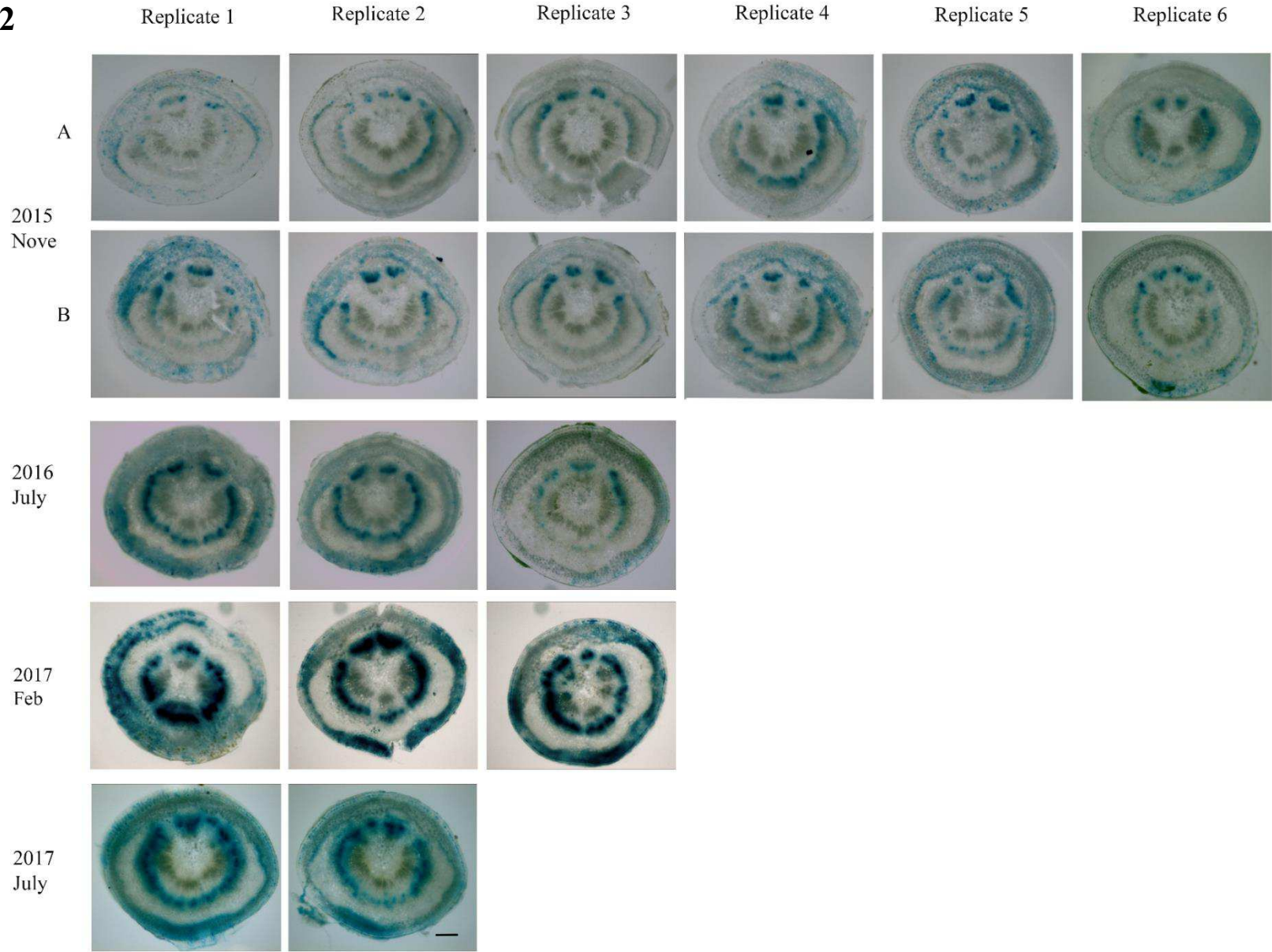
Figure B24 Representative micrographs showing the GUS staining patterns in distal peduncles attached to the split pericarps treated with NPA to both peduncle and inner pericarp

wall from four individual experiments. A and B in 2015 Nov experiment represents the cross-sections taken from the two halves of the distal peduncle; A-cross-sections taken from the peduncle half proximal to the pedicel and B- cross-sections taken from the peduncle half distal to the pedicel. Scale bar = 200 μm .

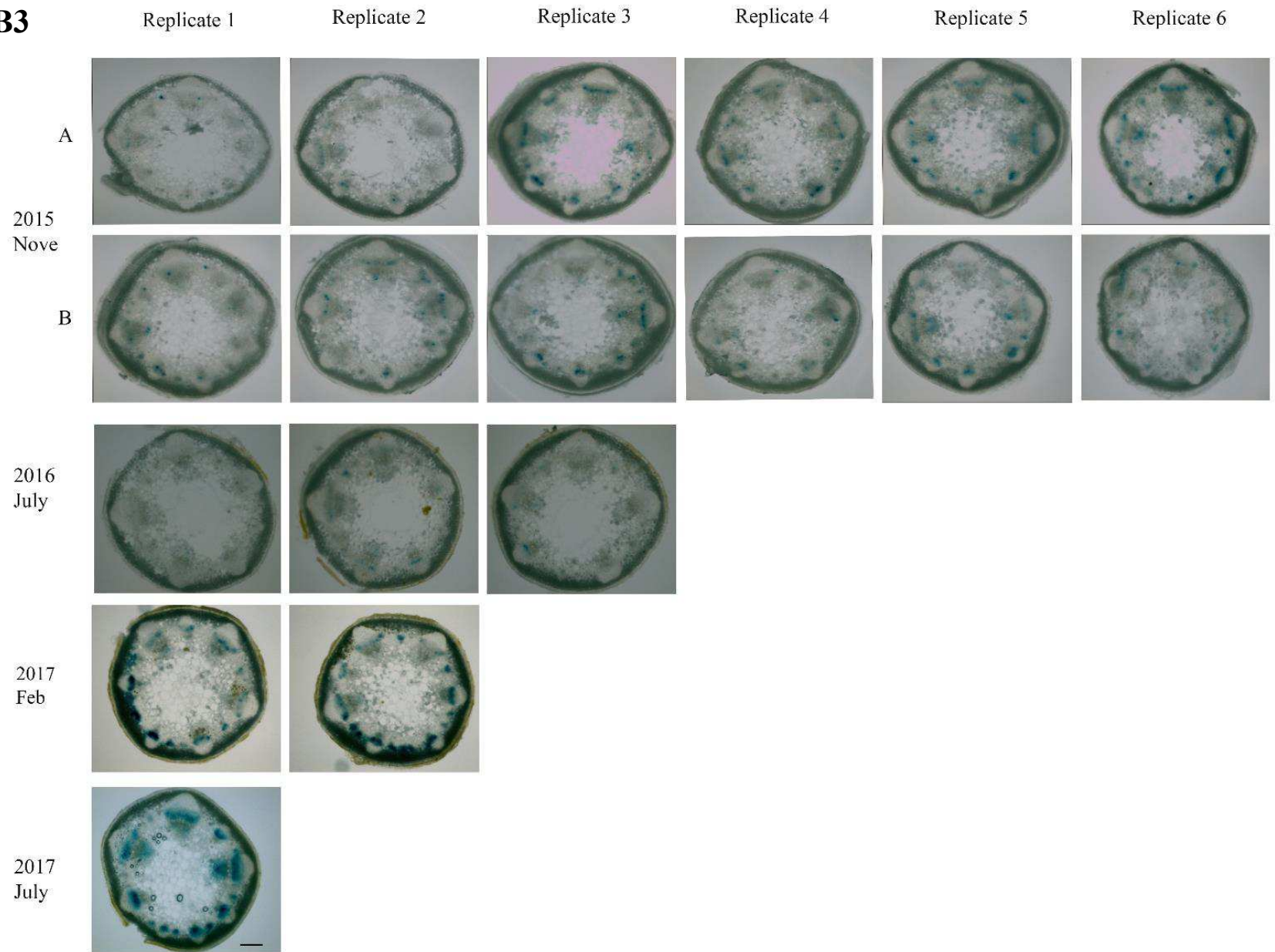
B1



B2



B3



B4

Replicate 1

Replicate 2

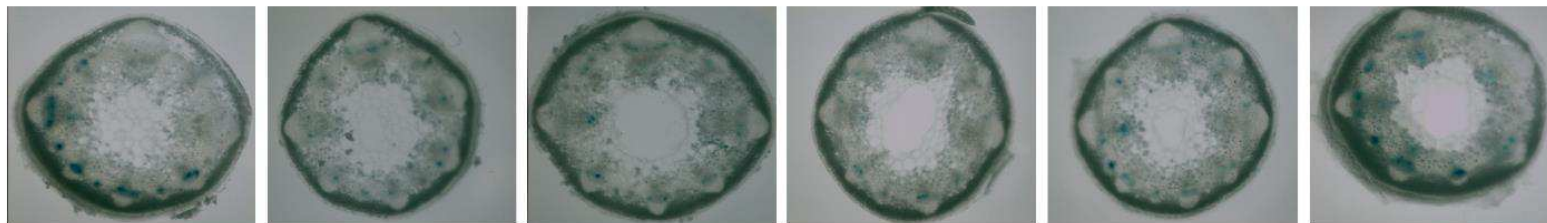
Replicate 3

Replicate 4

Replicate 5

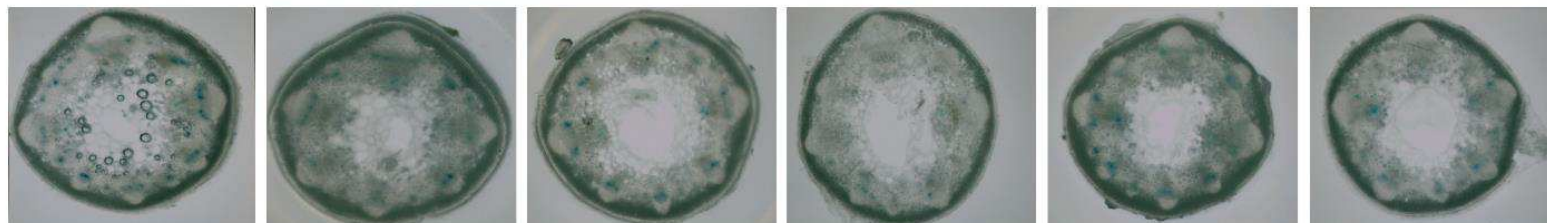
Replicate 6

A

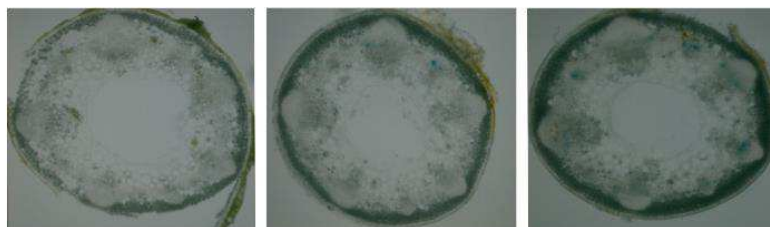


2015
Nove

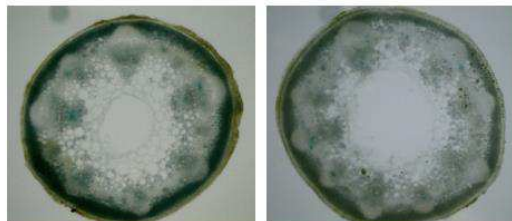
B



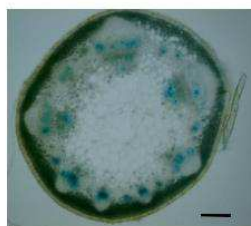
2016
July



2017
Feb



2017
July



B5

Replicate 1

Replicate 2

Replicate 3

Replicate 4

Replicate 5

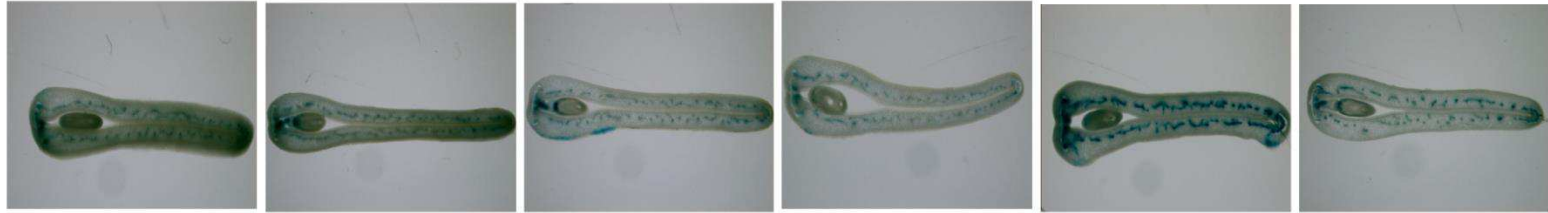
Replicate 6

A

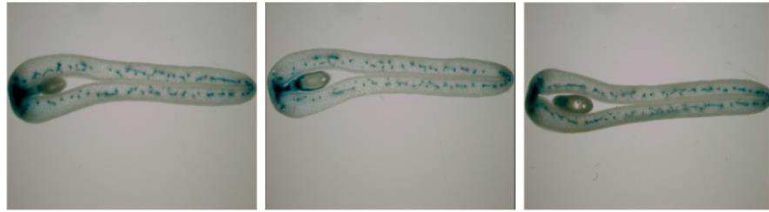


2015
Nove

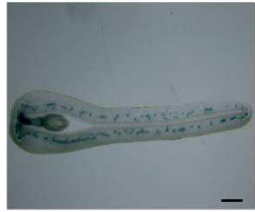
B



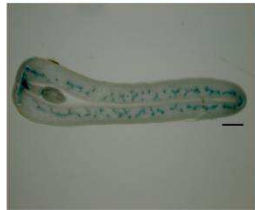
2016
July



2017
Feb



2017
July



B6

Replicate 1

Replicate 2

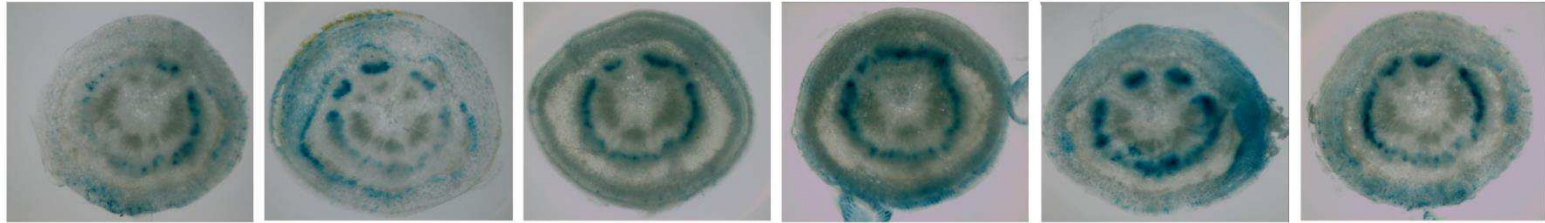
Replicate 3

Replicate 4

Replicate 5

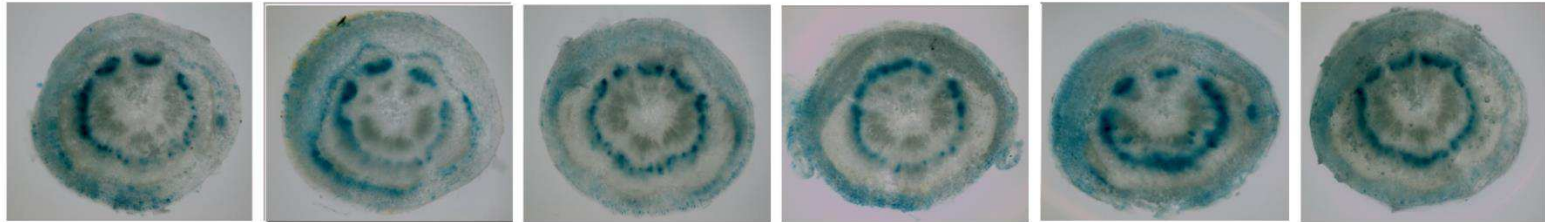
Replicate 6

A



2015
Nove

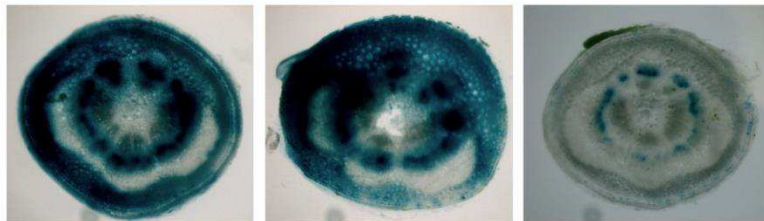
B



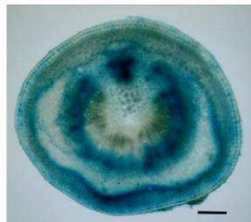
2016
July



2017
Feb



2017
July



B7

Replicate 1

Replicate 2

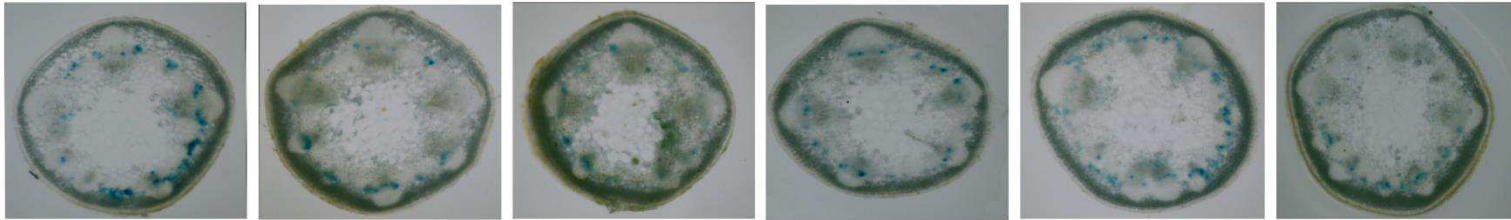
Replicate 3

Replicate 4

Replicate 5

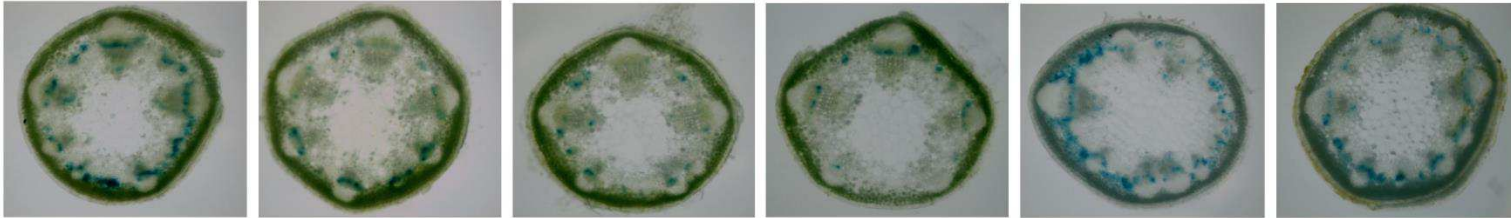
Replicate 6

A

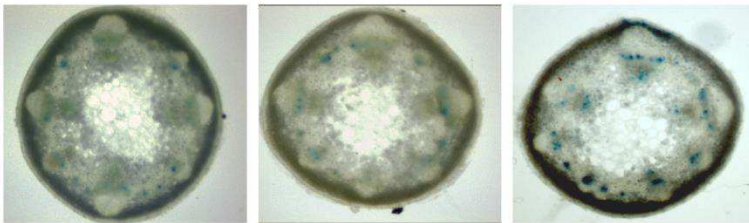


2015
Nove

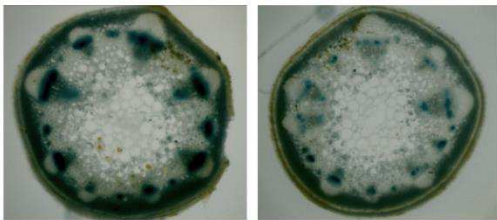
B



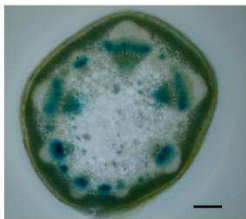
2016
July



2017
Feb



2017
July



B8

Replicate 1

Replicate 2

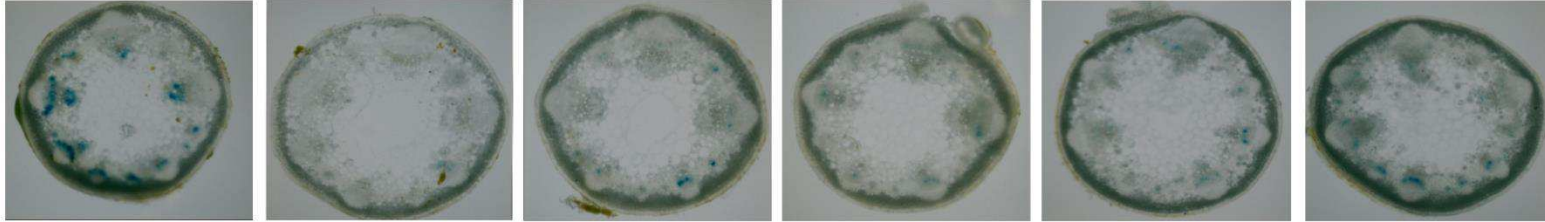
Replicate 3

Replicate 4

Replicate 5

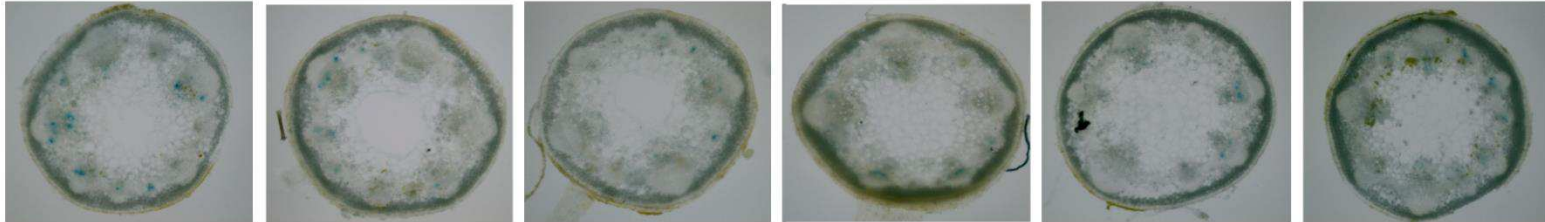
Replicate 6

A

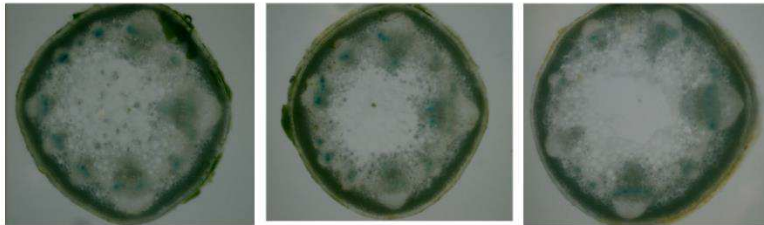


2015
Nove

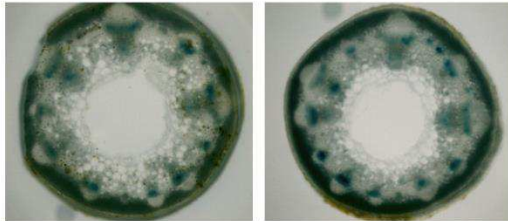
B



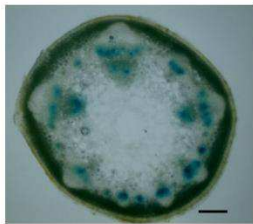
2016
July



2017
Feb



2017
July



B9

Replicate 1

Replicate 2

Replicate 3

Replicate 4

Replicate 5

Replicate 6

A

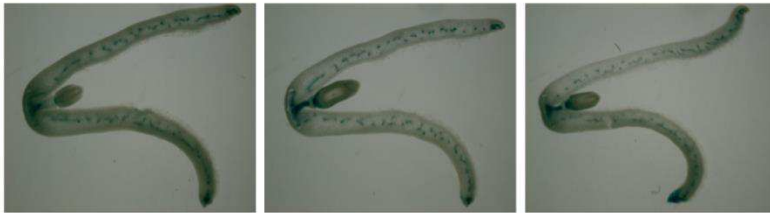


2015
Nove

B



2016
July



2017
Feb



B10

Replicate 1

Replicate 2

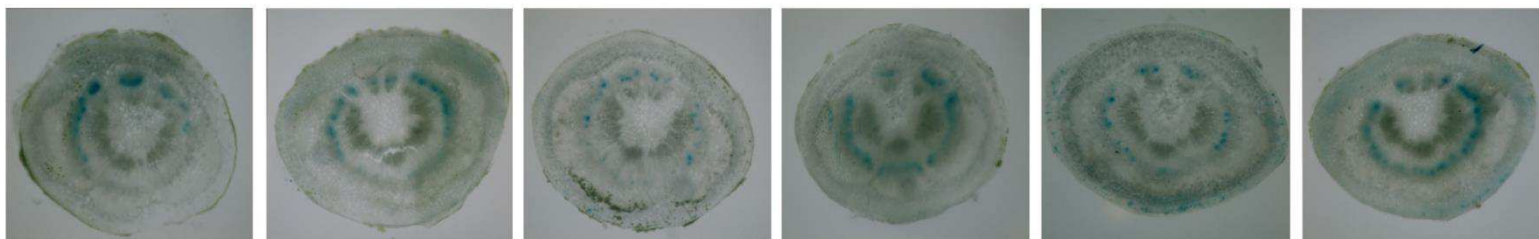
Replicate 3

Replicate 4

Replicate 5

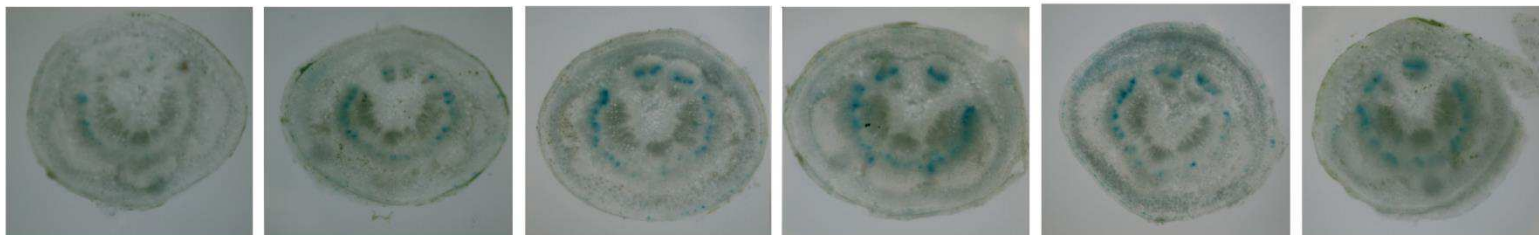
Replicate 6

A



2015
Nove

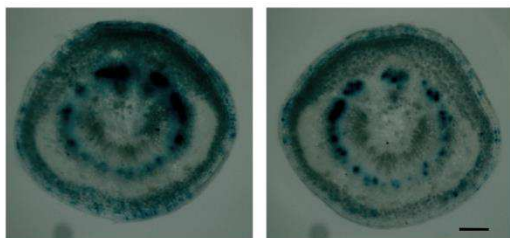
B



2016
July



2017
Feb



B11

Replicate 1

Replicate 2

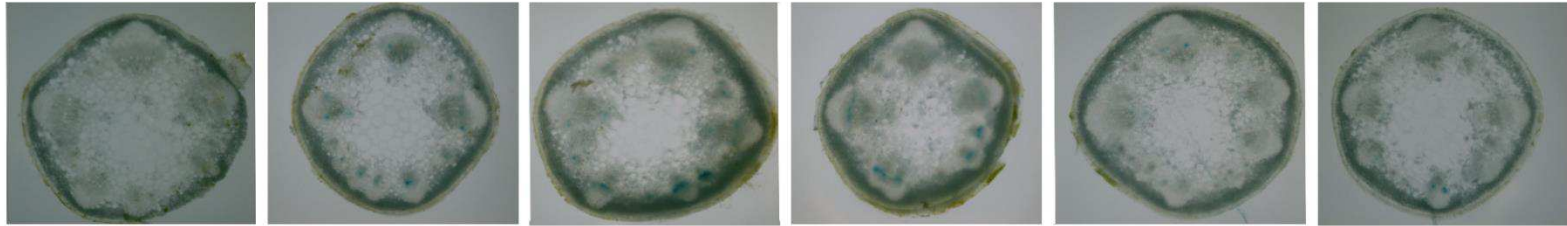
Replicate 3

Replicate 4

Replicate 5

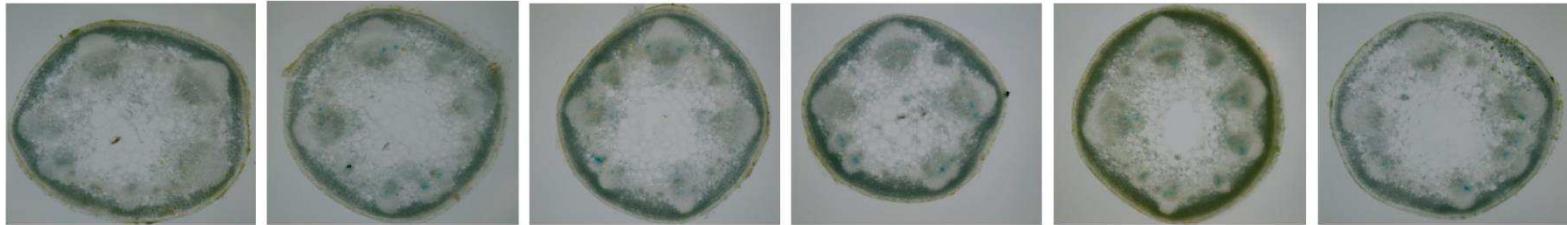
Replicate 6

A



2015
Nov

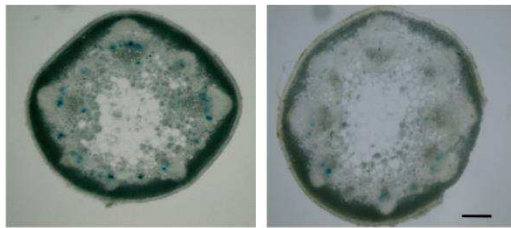
B



2016
July



2017
Feb



B12

Replicate 1

Replicate 2

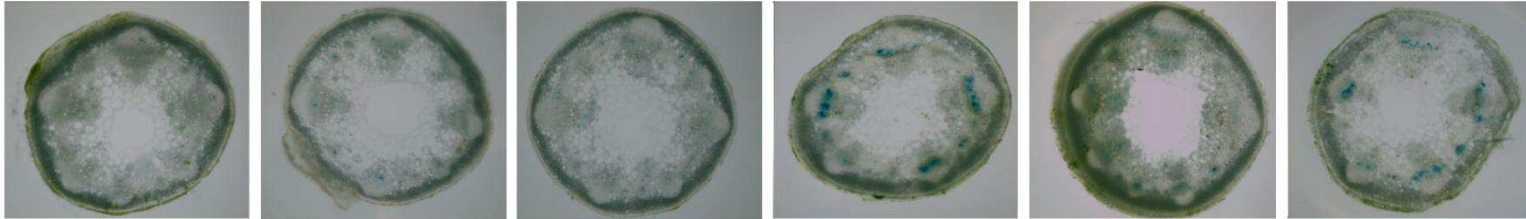
Replicate 3

Replicate 4

Replicate 5

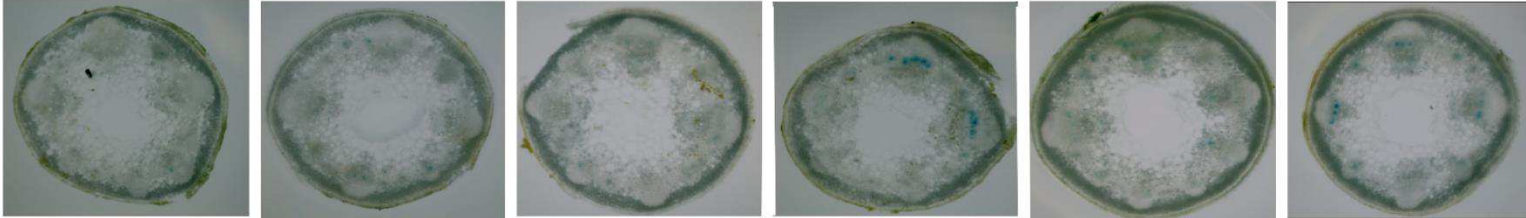
Replicate 6

A



2015
Nove

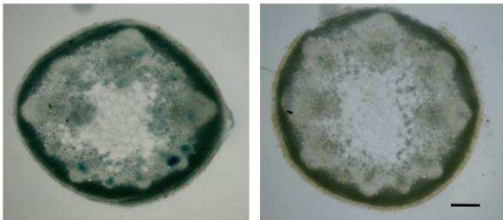
B



2016
July



2017
Feb



B13

Replicate 1

Replicate 2

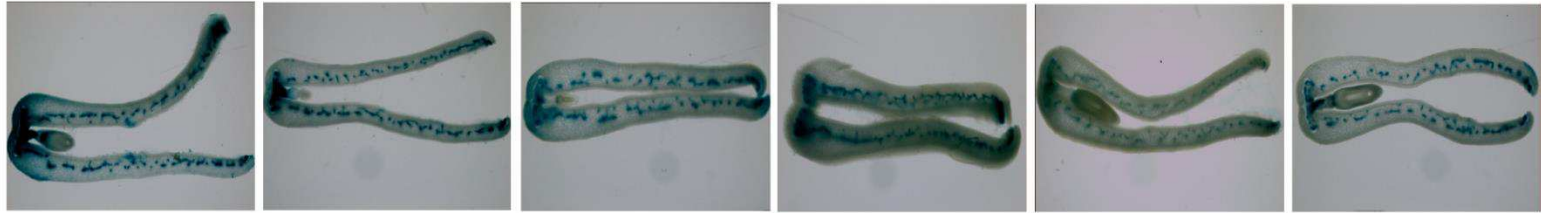
Replicate 3

Replicate 4

Replicate 5

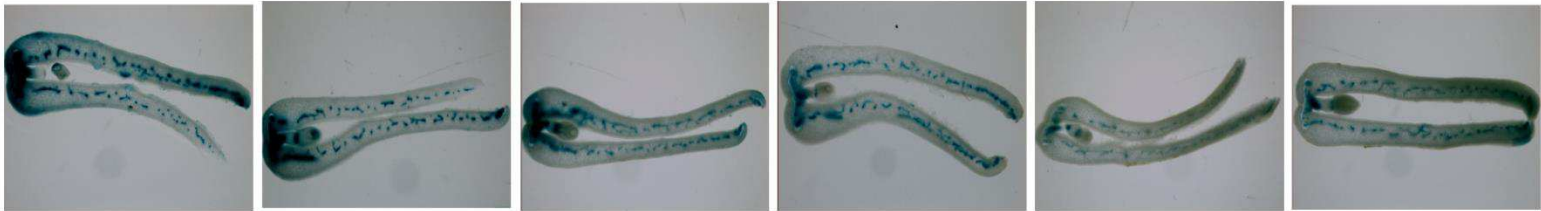
Replicate 6

A



2015
Nove

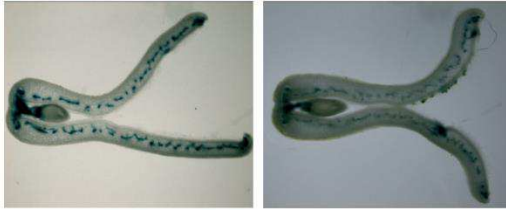
B



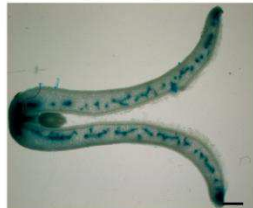
2016
July



2017
Feb



2017
July



B14

Replicate 1

Replicate 2

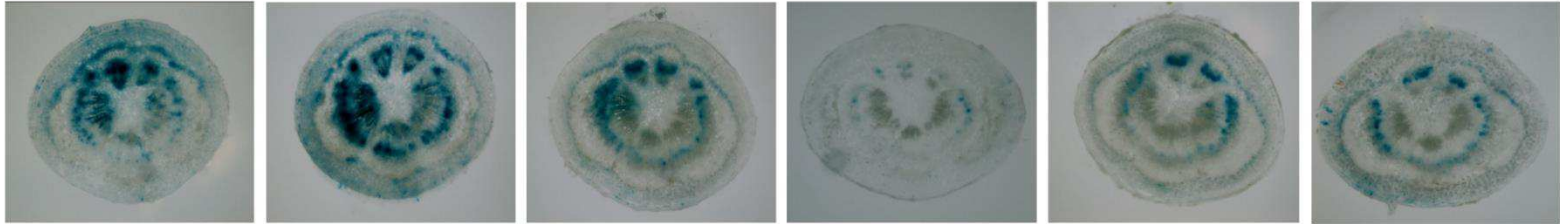
Replicate 3

Replicate 4

Replicate 5

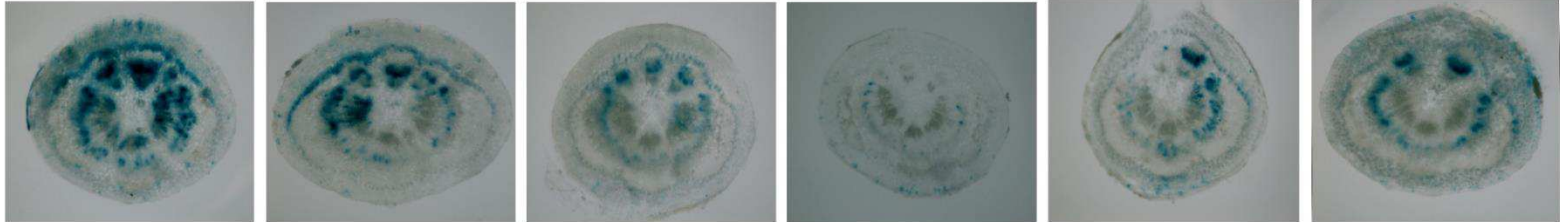
Replicate 6

A

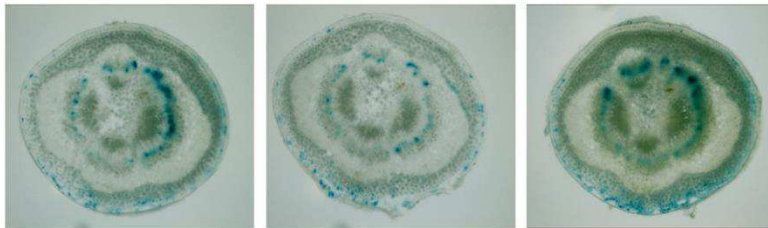


2015
Nove

B



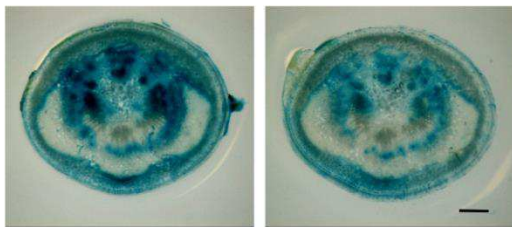
2016
July



2017
Feb



2017
July



B15

Replicate 1

Replicate 2

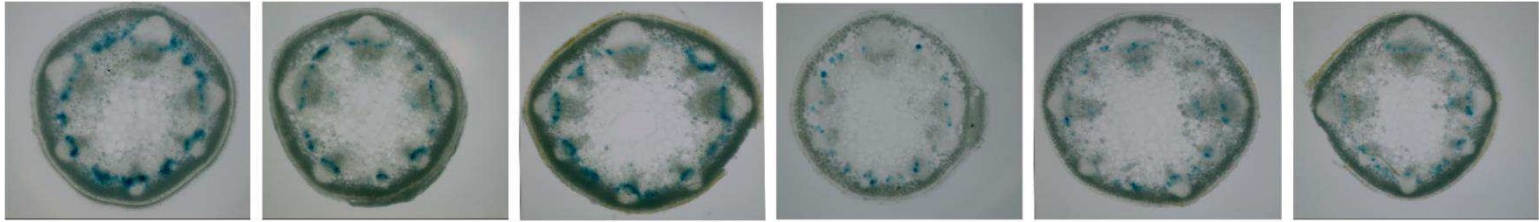
Replicate 3

Replicate 4

Replicate 5

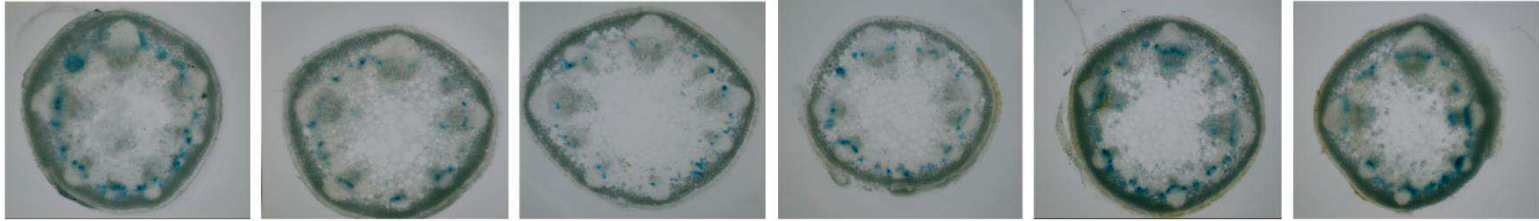
Replicate 6

A

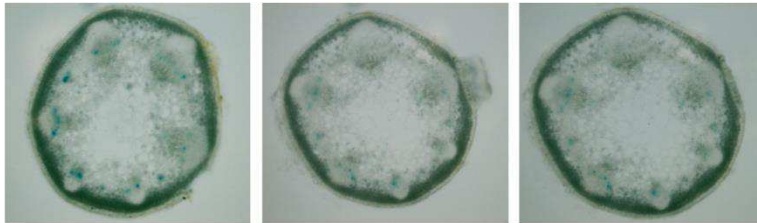


2015
Nove

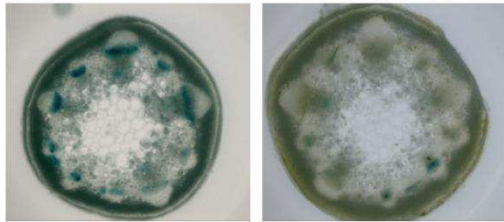
B



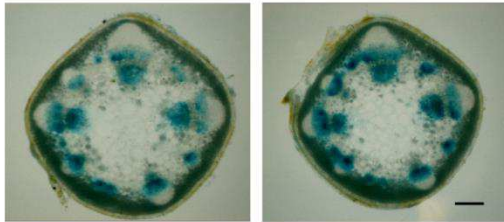
2016
July



2017
Feb



2017
July



B16

Replicate 1

Replicate 2

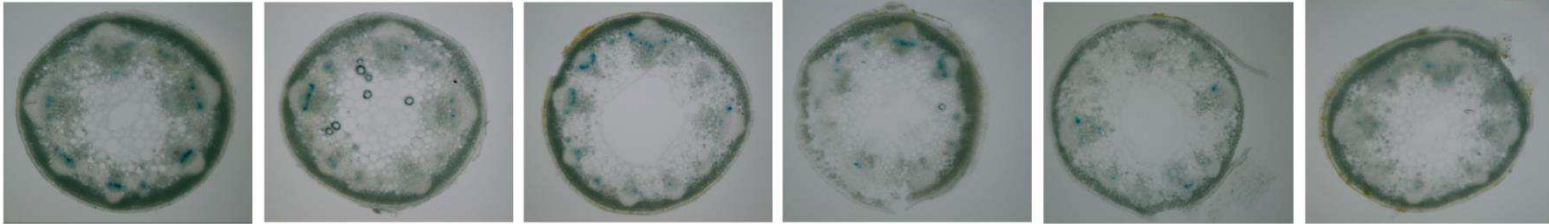
Replicate 3

Replicate 4

Replicate 5

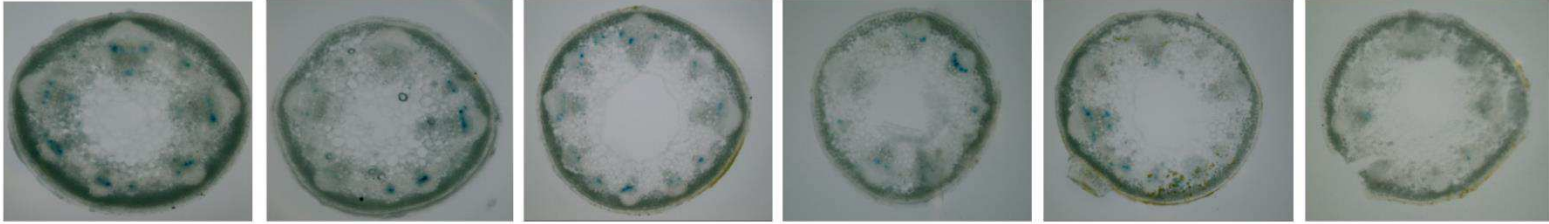
Replicate 6

A

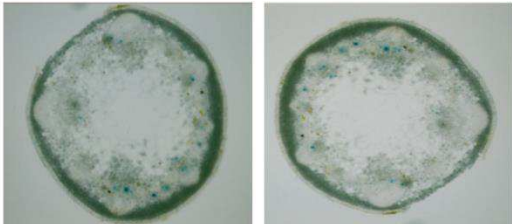


2015
Nove

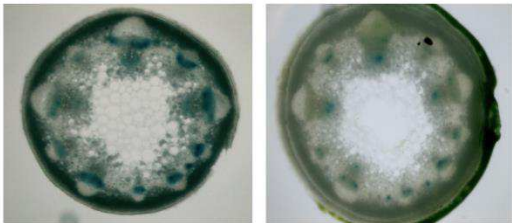
B



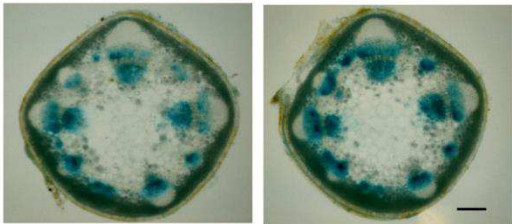
2016
July



2017
Feb



2017
July



B17

Replicate 1

Replicate 2

Replicate 3

Replicate 4

Replicate 5

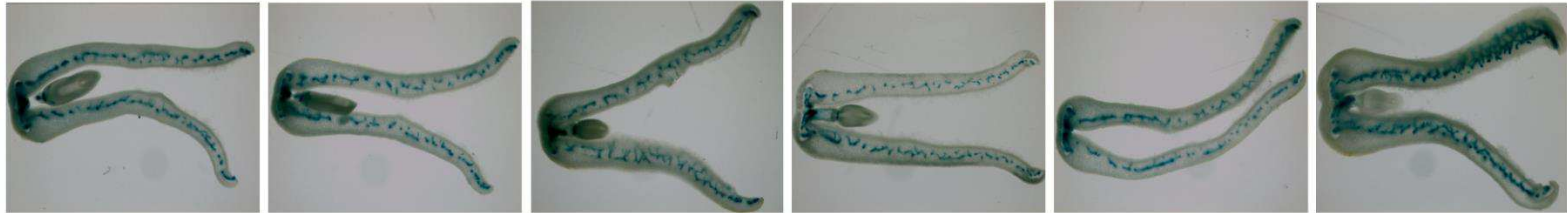
Replicate 6

A

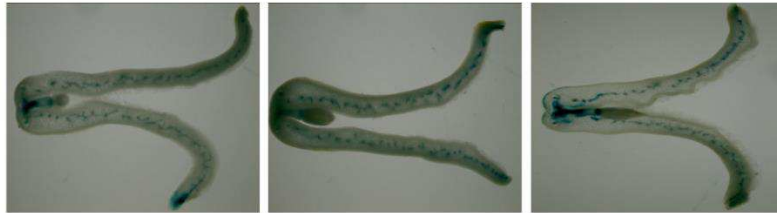


2015
Nove

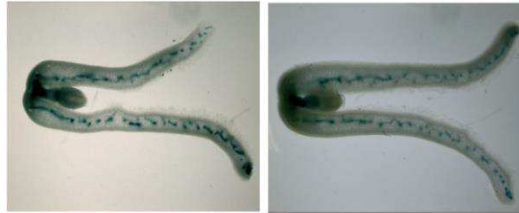
B



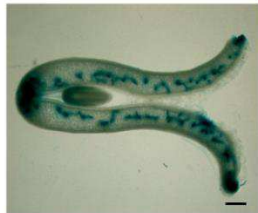
2016
July



2017
Feb



2017
July



B18

Replicate 1

Replicate 2

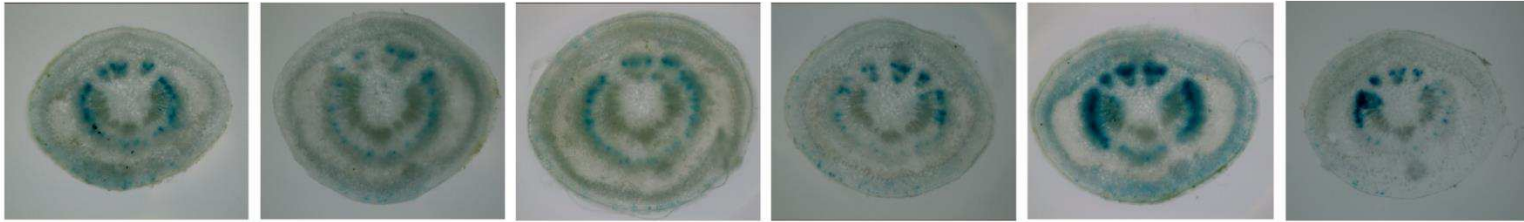
Replicate 3

Replicate 4

Replicate 5

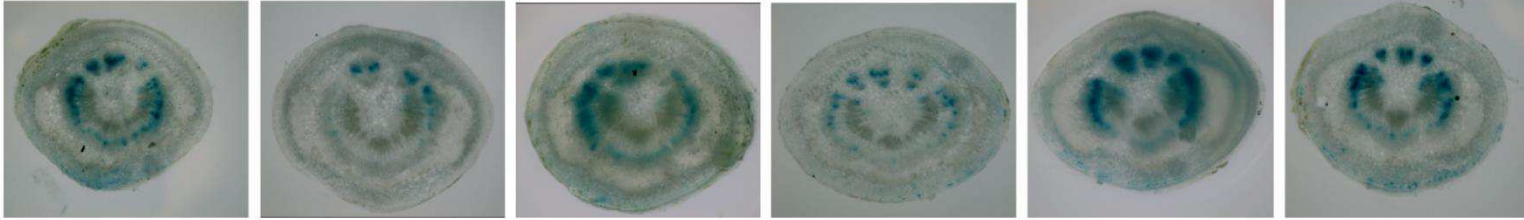
Replicate 6

A

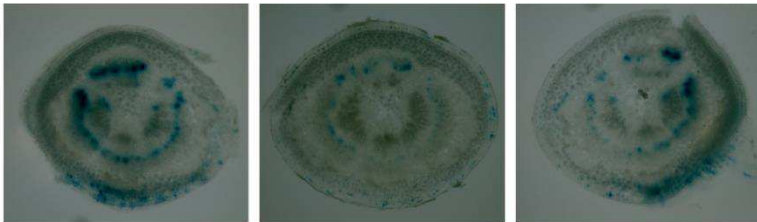


2015
Nove

B



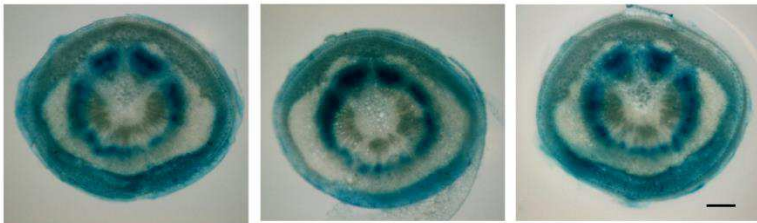
2016
July



2017
Feb



2017
July



B19

Replicate 1

Replicate 2

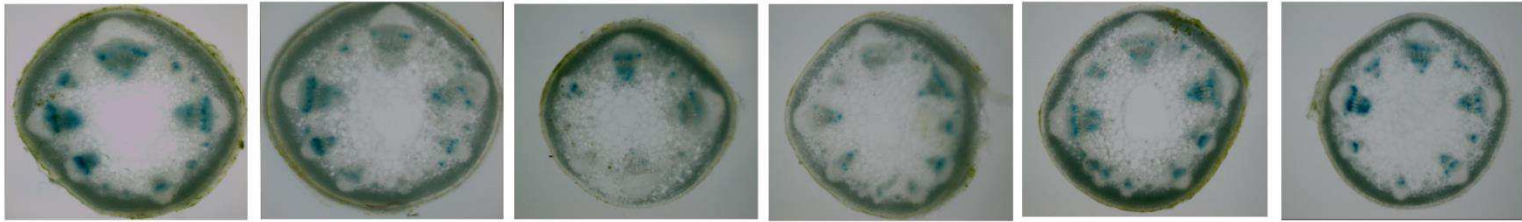
Replicate 3

Replicate 4

Replicate 5

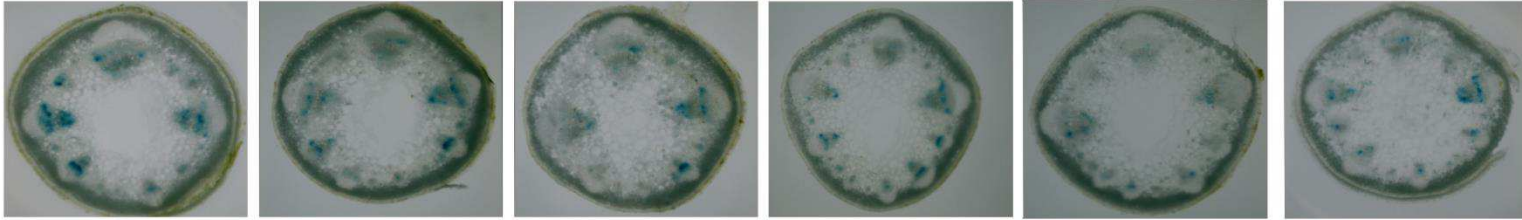
Replicate 6

A

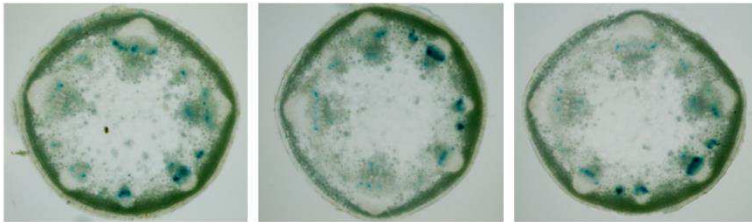


2015
Nove

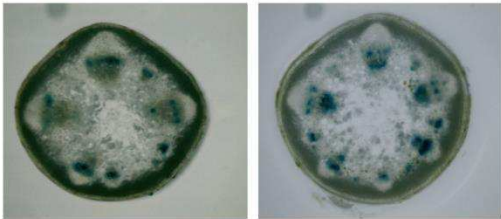
B



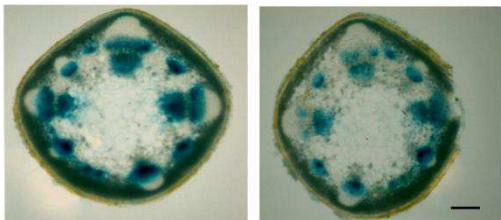
2016
July



2017
Feb



2017
July



B20

Replicate 1

Replicate 2

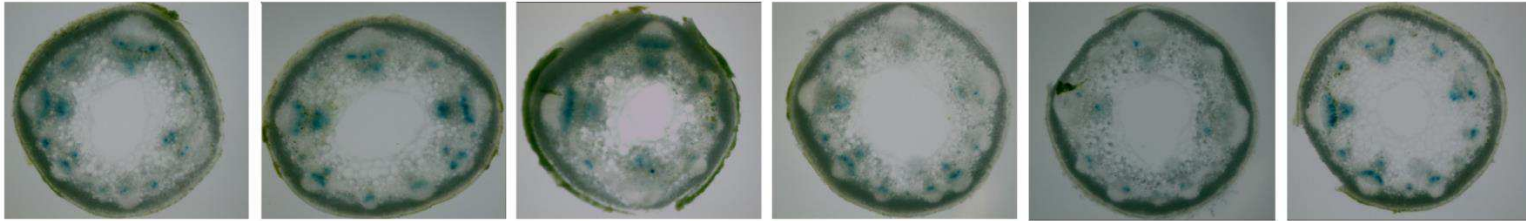
Replicate 3

Replicate 4

Replicate 5

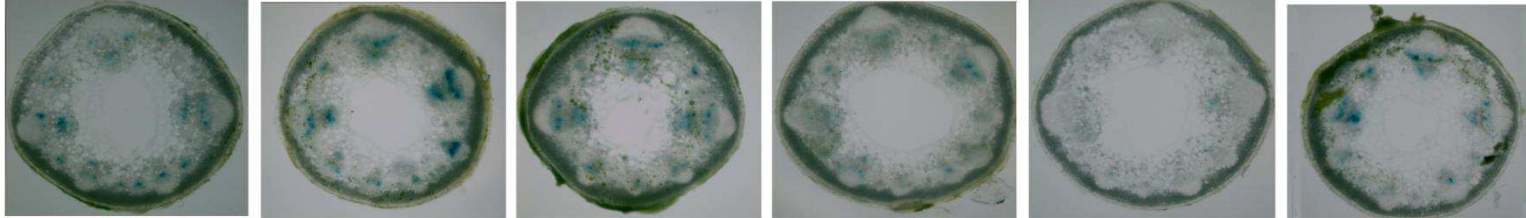
Replicate 6

A

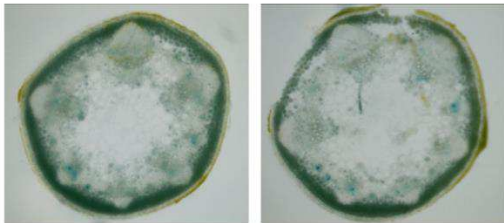


2015
Nove

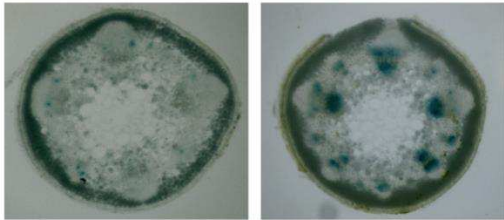
B



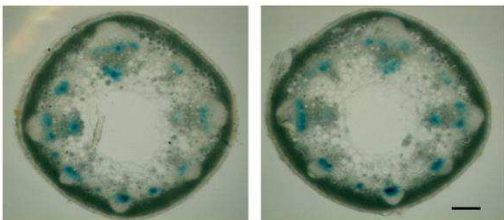
2016
July



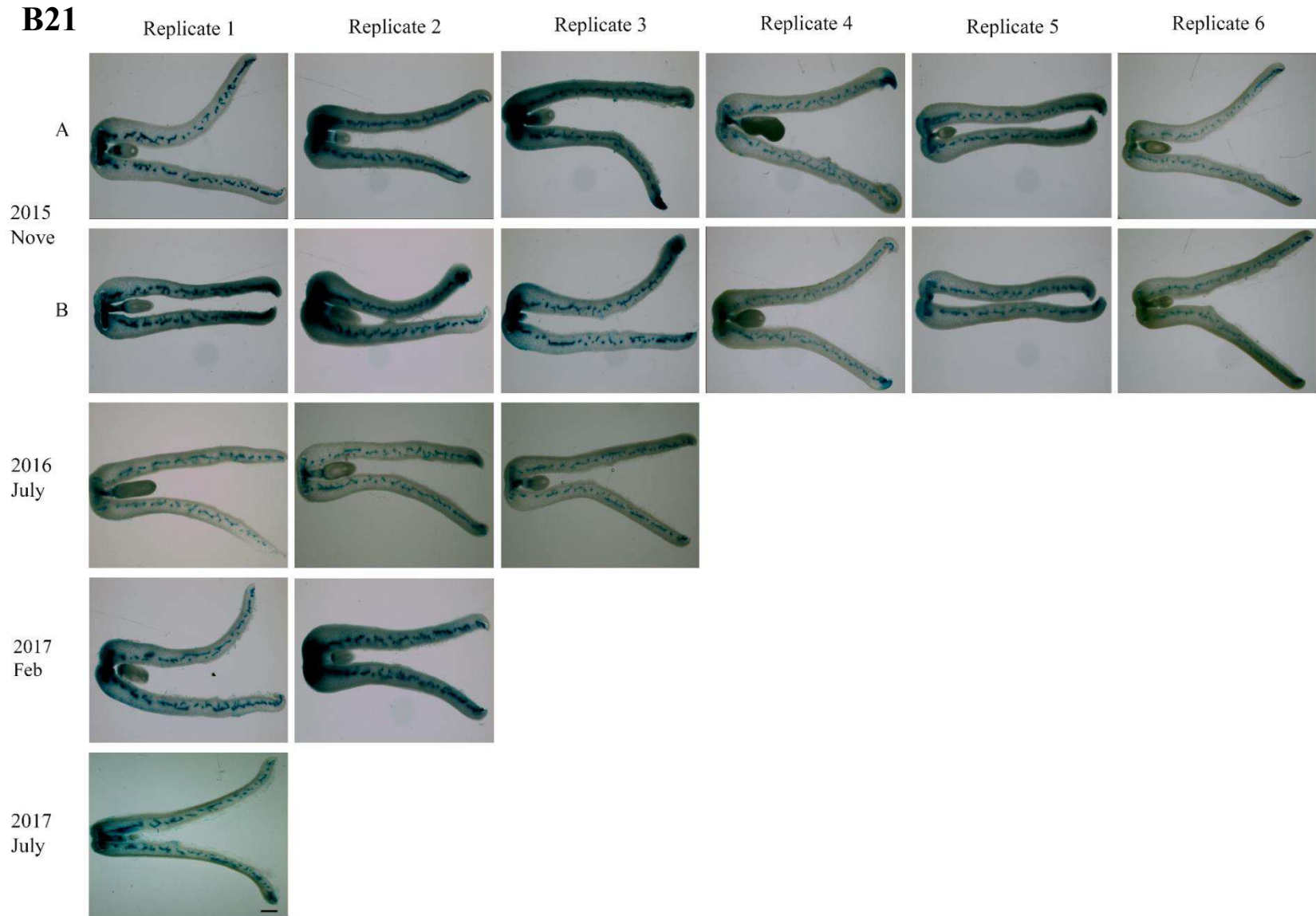
2017
Feb



2017
July



B21



B22

Replicate 1

Replicate 2

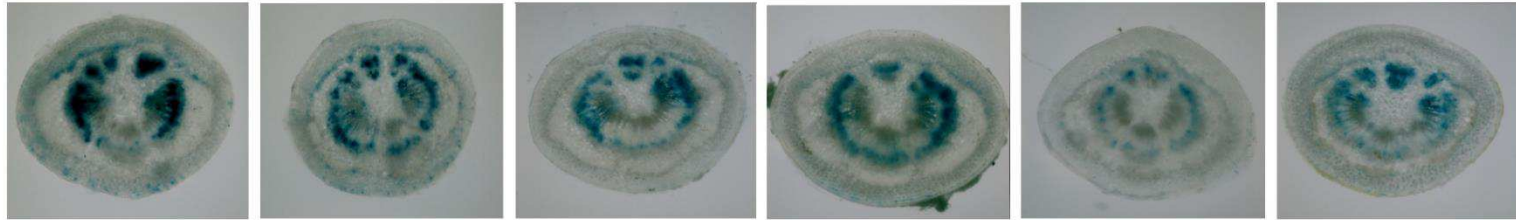
Replicate 3

Replicate 4

Replicate 5

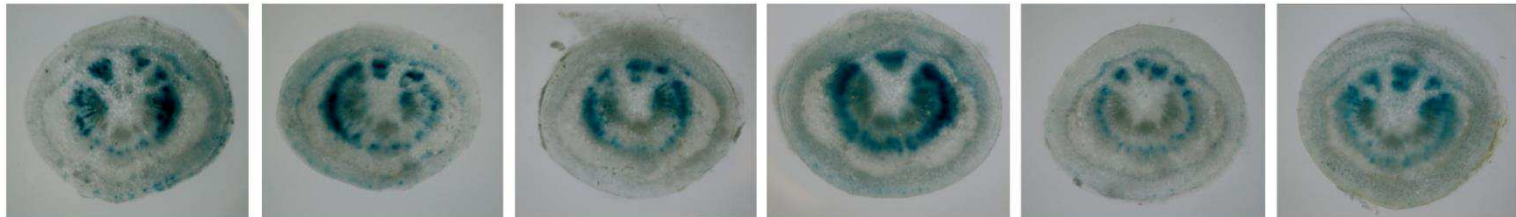
Replicate 6

A

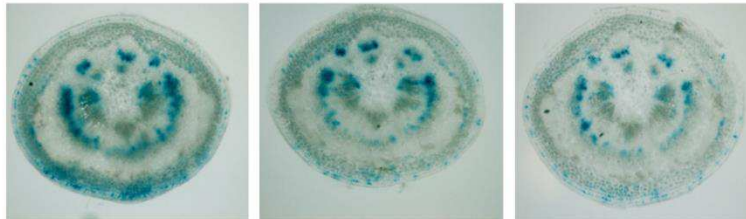


2015
Nove

B



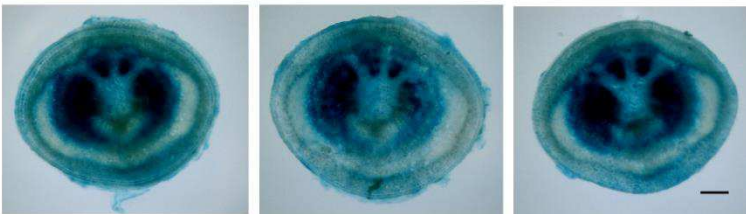
2016
July



2017
Feb



2017
July



B23

Replicate 1

Replicate 2

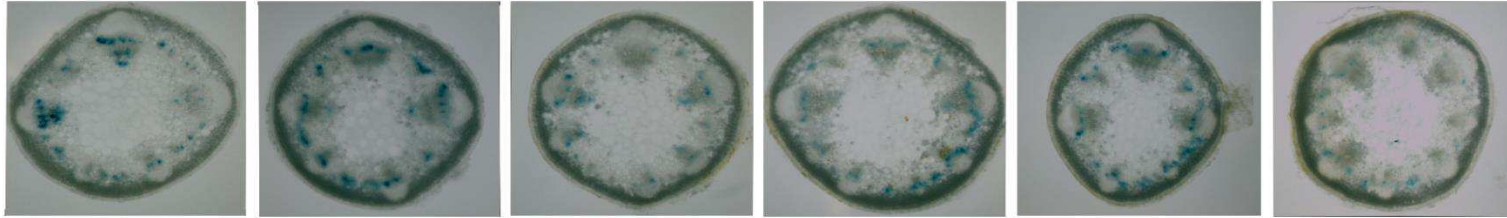
Replicate 3

Replicate 4

Replicate 5

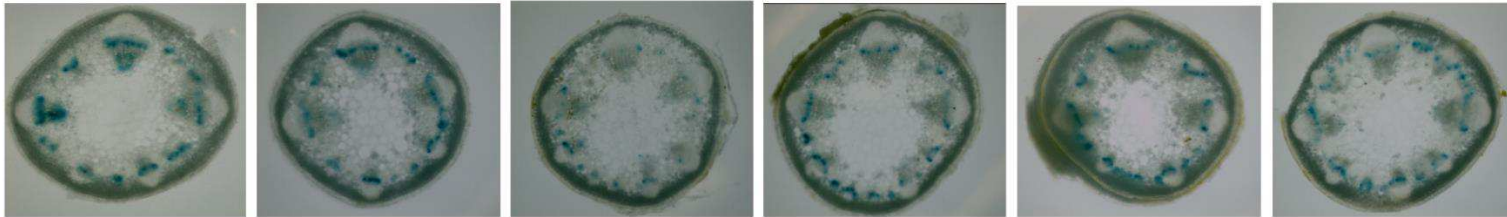
Replicate 6

A

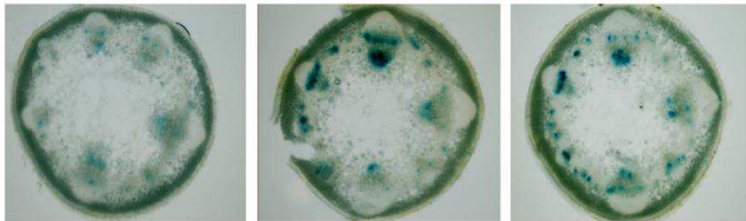


2015
Nove

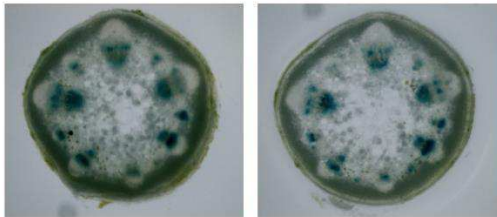
B



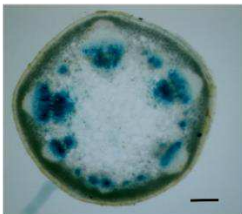
2016
July



2017
Feb



2017
July



B24

Replicate 1

Replicate 2

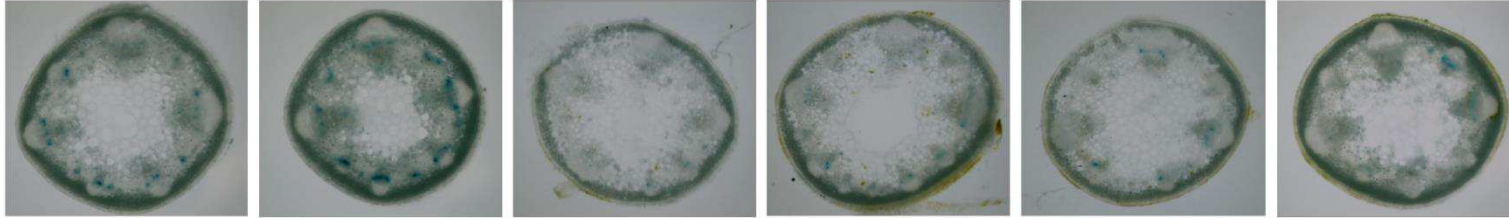
Replicate 3

Replicate 4

Replicate 5

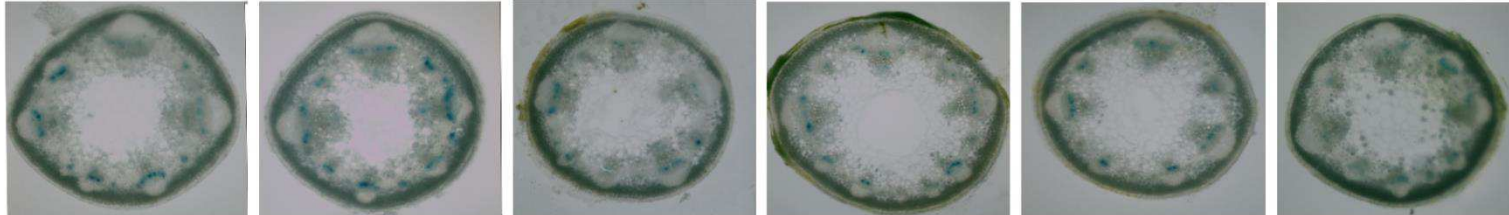
Replicate 6

A

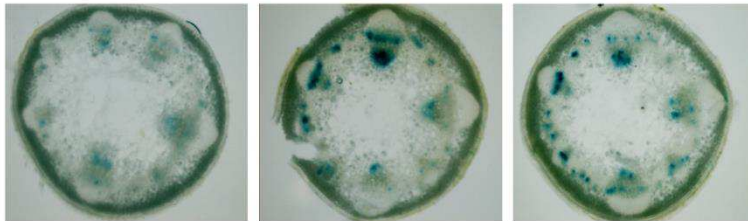


2015
Nove

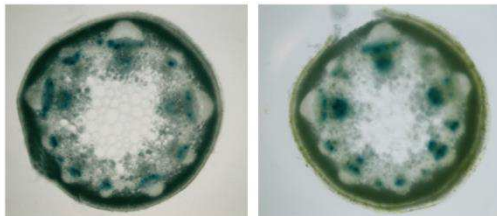
B



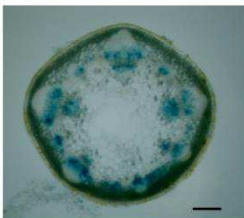
2016
July



2017
Feb



2017
July



Appendix C

EFFECT OF NPA ON IAA-, 4-CL-IAA-, OR GA₃-INDUCED DESEEDED PERICARP GROWTH

C.1 INTRODUCTION

Application of 4-Cl-IAA and GAs, naturally occurring hormones in pea fruits, can restore the deseeded pericarp growth by mimicking the presence of seeds (Eeuwens and Schwabe, 1975; Ozga and Reinecke, 1999; Ozga et al., 2002; Ozga et al., 2009). In contrast, the other naturally occurring auxin IAA is unable to rescue the deseeded pericarp growth (Reinecke et al., 1995). Moreover, both seeds and 4-Cl-IAA can regulate GA biosynthesis and catabolism in pea pericarps by regulating the corresponding gene transcript abundance (expression) in the pericarps (Ozga et al., 1992; Ozga et al., 2009), suggesting auxin (4-Cl-IAA) is a seed-derived signal that controls the bioactive GA levels in the pea pericarps. The bioactive GA (GA₁) is important for the pericarp growth (Ozga et al., 2009).

Auxin in plants can be transported either by non-directional phloem pathway or cell-to-cell, directional-polar pathway (Morris et al., 2010). Recent studies have shown the possibility of involvement of polar auxin transport (PAT) in fruit set and subsequent stages of fruit development in tomato (Serrani et al., 2010; Pattison and Catalá, 2012). NPA is a synthetic PAT inhibitor, which acts together with auxin efflux carriers to inhibit auxin transport (Muday and DeLong, 2001). Application of NPA together with IAA or GAs can alter the individual effect of hormonal activity on tomato fruit development (Serrani et al., 2010). The simultaneous application of NPA with GA₃ and IAA enhanced the individual growth induction effect of these two hormones, suggesting the ability of NPA to block auxin transport and lead to a build-up of auxin (IAA), which enhanced the auxin effect on growth (Serrani et al., 2010). Here, the effect of NPA pre-treatment on auxin and gibberellin induced deseeded pea pericarp growth was tested.

C. 2 MATERIALS AND METHODS

Pea plants (*Pisum sativum* L. cv. I₃ (Alaska-type)) were grown under growth chamber conditions, as previously described in section 2.1.2 of this thesis. One fruit per plant at the 3-5th flowering node was used for this experiment. Two days after anthesis (DAA) fruits were split down the dorsal suture and deseeded. NPA (30 μ L; 10 μ M in 0.1% aqueous Tween 80) or 0.1% aqueous Tween 80 was applied to the inner wall of pericarps immediately after splitting and deseeding. Twelve hours after the surgical manipulation, pericarps were treated daily with IAA, 4-Cl-IAA or GA₃ (50 μ M in 0.1% aqueous Tween 80), or 4-Cl-IAA plus IAA (50 μ M each in 0.1% aqueous Tween 80) for 5 days (30 μ L for the first 2 days and 40 μ L the remaining 3 days). Pericarps along with the pedicels were harvested two days after final hormonal treatment (9 DAA). The pericarp length and width, pedicel and peduncle length and diameter were measured at each day. Pericarp and pedicel weight were measured at the date of harvesting.

C. 3 RESULTS AND DISCUSSION

Pre-treatment of NPA to deseeded pericarps reduced the growth promoting effect of 4-Cl-IAA and GA₃ on pericarp growth. (Fig. C1). These data suggest that blocking of auxin transport

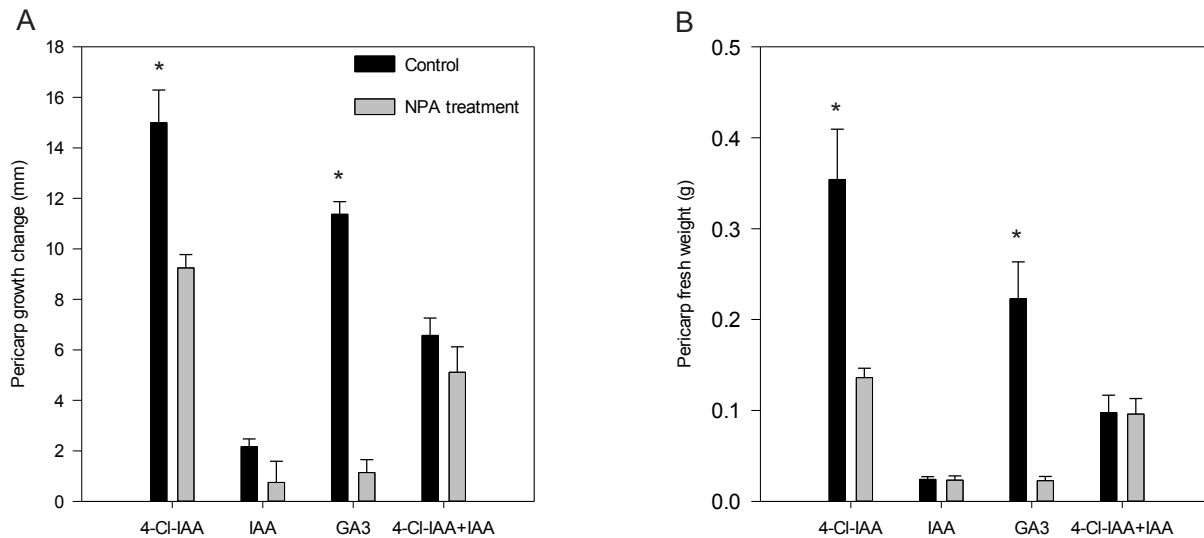


Figure C1. Effect of NPA pre-treatment on auxin and gibberellin-induced deseeded pericarp growth. Pericarps were split and deseeded at 2 DAA. NPA or control solution was applied to the

inner pericarp wall of deseeded pericarps immediately after surgical manipulation, and hormone treatments were applied 12h later. The pericarp growth change (A) and the fresh weight (B) was measured at 9 DAA (7 days after initial treatment). Data are means \pm SE, n= 7 to 9. Asterisks denote significantly different treatment means at $P < 0.05$.

within the pericarp tissue, inhibits growth promoting effects of 4-Cl-IAA or GA₃ on pericarp growth. It seems that NPA application is blocking the IAA, the non-growth stimulating auxin in pea, transport over the 4-Cl-IAA. However, this experiment needs to be repeated before any conclusion on the effect of NPA on auxin and gibberellin-induced deseeded pericarp growth can be made, as the 4-Cl-IAA- and GA₃-induced pericarp growth was markedly lower in my experiment than that observed in many experiments carried out in the Ozga lab including data reported by Johnstone et al. (2005)